INVESTIGATION OF FEAR AND MEN PATHWAY HOMOLOGS IN MULTINUCLEATE CELLS

Inauguraldissertation

zur
Erlangung der Würde eines Doktors der Philosophie
vorgelegt der
Philosophisch-Naturwissenschaftlichen Fakultät
der Universität Basel

von

Mark Robert Finlayson

aus Hasle bei Burgdorf, Bern

Basel, 2011

Genehmigt von der Philosophisch-Naturwissenschaftlichen Fakultät
auf Antrag von

Prof. Dr. Peter Philippsen
Prof. Dr. Anne Spang

Basel, den 22. Juni, 2010

Prof. Dr. Eberrhard Parlow

TABLE OF CONTENTS

Table of contents

SUMMARY

Summary

The cell cycle is a sequence of events enabling a cell to replicate and proliferate. Common landmark events in most eukaryotic cell cycles are duplication of the DNA, mitosis, and cell separation. The cell cycle lays the basis for development in multicellular organisms, and is of course important for cell or tissue renewal. Disregulation of the cell cycle can lead to uncontrolled growth and tumor formation.

Mitosis, or nuclear division, is tightly regulated to ensure proper segregation of nuclei to daughter cells. In budding yeast (*S. cerevisiae*), the timing of mitosis is coupled to cytokinesis by the action of the FEAR and MEN regulatory networks, which mediate exit from mitosis by activation of the phosphatase *Sc*Cdc14.

In this thesis, we investigate the function of homologs of these pathways in the filamentous fungus, *Ashbya gossypii*. This organism provides a unique cellular setting to study these matters, as it is a close relative of *S.cerevisiae* and shares most of the molecular machinery. However within its multinucleate hyphae, mitosis is uncoupled from cytokinesis, and cytokinesis is not followed by cell separation, thus leading to compartments containing 8-10 nuclei, separated by septa. We look into how exit from mitosis is affected in such a cellular environment where nuclei are free to divide without the spatial and temporal constraints as described in budding yeast, where each mitosis is followed by cytokinesis and cell separation.

In the first chapter, we study the core component of exit from mitosis signalling. We examinethe phosphatase *Ag*Cdc14 and discover that its regulation is very similar to *S. cerevisiae*, with the phosphatase being sequestered within the nucleolus throughout interphase, and released during anaphase. Furthermore, we find it to be an essential component in nuclear cycle progression in *A. gossypii,* with nuclei in null mutants failing to undergo mitosis.

In the second chapter, we look at MEN homologs in *A. gossypii* and present evidence that the kinase cascade function of the pathway is likely conserved. We however show MEN homologs to be non-essential and play no role in *Ag*Cdc14 regulation. On the other hand, we detect sporulation deficiencies in our mutants, which we could attribute to septation defects. More interestingly, we observe a partial mitotic arrest in MEN deficient cells. MEN homologs thus seem to have diverged from the primary role of their counter-parts in budding yeast.

The third chapter deals with homologs of the FEAR pathway. It had been previously suggested that, in primitive cells, the task of Cdc14 phosphatase regulation may be solely bestowed upon this network of genes. We find this to hold true for *A. gossypii*, where we report severe mitotic defects upon deletion of FEAR homologs, and in particular, disruption of control over *Ag*Cdc14 release.

We interpret the results as evidence for a simpler system regulating exit from mitosis in *A. gossypii* and lay out potential implications for the more complex system in *S. cerevisiae*.

Remarks

- In this thesis, homologous genes bearing the same common name in different organisms are discussed. To avoid confusion, all instances of genes, ORFs or proteins are written with a prefix indicating the species or class in mind. For example, *Ag*Cdc14 is the *Ashbya gossypii* ortholog of the *Sc*Cdc14 protein in *Saccharomyces cerevisiae* and the mammalian isoforms *m*Cdc14A and *m*Cdc14B (or *Mus musculus Mm*Cdc14A and *Mm*Cdc14B) .

- Due to an ancient genome duplication in the *S. cerevisiae* lineage, many genes in *A. gossypii* have two orthologs in *S. cerevisiae.* In these cases, the *A. gossypii* gene will be named after both homologs, starting with the one with the higher sequence similarity. For example, the lone ortholog of *Sc*Dbf2 and *Sc*Dbf20 in *A. gossypii* will appear in the text as *Ag*Dbf2/Dbf20. Genome duplication orthologs, correctly known as "ohnologs", will sometimes be referred to as "twin" genes.

- When speaking of developing mycelia, the "age" of *A. gossypii* cells refers to the time elapsed after introducing spores to nutrients. The first hypha emerges from a germ bubble after 6-7 hours.

- A larger, general introduction serving as a basis for all three chapters is provided at the beginning of this thesis. The smaller introductions at the start of each chapter are thought to provide some further, more specific information, relevant for the understanding of the discussed experiments.

- A comprehensive abbreviation list merged with a glossary of selected terms and definitions can be found at the back of the manuscript.

BACKGROUND

Background

Research on *Ashbya gossypii*: a short history

The filamentous ascomycete *Ashbya gossypii* was originally identified as a plant pathogen that caused fungal infections in a variaty of tropical or sub-tropical plants, such as cotton of the *Gossypium* genus or citrus fruit (Ashby and Nowell, 1926). The mode of infection relies on the aid of insects (of the heteroptera sub-order), which have been found to carry spores or mycelium on their mouthparts and provide for the physical damage required for succesful invasion (Frazer, 1944). Use of insecticide proved sufficient for erradicating widespread disease.

A. gossypii was later adopted by the food industry as a natural producer of vitamin B_2, or riboflavin (Stahmann *et al.,* 2000). This vitamin has found its way into many fortified food products, and research on biotechnological aspects of production is still ongoing (Sugimoto *et al,*. 2010). Currently, the world's largest chemical company, BASF, manufactures more than 1000 tons of the vitamin annually using *A. gossypii* cultures (corporate website, April 2010).

In the early 1990s, first steps in genetic manipulation of *A. gossypii* were undertaken (Wright and Philippsen, 1991). The high efficiency of homologous recombination in this organism was soon recognized (Steiner *et al.,* 1995) and has since spawned the development of a wide range of molecular tools adapted from *Saccharomyces cerevisiae* protocols and based on the integration of PCR-generated DNA fragments (Wendland *et al.,* 2000; Dunkler and Wendland, 2007; Kaufmann 2009).

Intriguing similarities with *S. cerevisiae* on the nucleic acid sequence level were discovered early on (Altmann-Jöhl and Philippsen, 1996; Prillinger *et al.,* 1997) and ultimately led to the sequencing of the entire *A. gossypii* genome (Dietrich *et al.,* 2004). Comprehensive comparative analysis revealed insights into the evolutionary history of both organisms, including evidence of a whole genome duplication event in *S. cerevisiae*.

Figure 1: Plant pathogen *Ashbya gossypii.* (A) *A. gossypii* mycelium on AFM (*A. gossypii* full medium) plate after three days of growth at 30°C. Image to scale (scale bar depicts 1 cm). (B) Cotton boll of *Gossypium hirsutum*.

The availablity of a fully annotated genome, combined with prior knowledge gained from decades of research on *S. cerevisiae,* paved the way for functional genomics in *A. gossypii*.

Special attention has been given to polar growth, cell septation and regulatory control as well as dynamics of nuclei, as these aspects of the life cycle show intriguing differences compared with *S. cerevisiae*. Lately, transcriptomics and proteomics approaches have been added to the growing repertoire of methods successfully applied in *A. gossypii* (manuscripts in preparation).

The life cycle of *A. gossypii*

A. gossypii has a genome very similar to that of the budding yeast *S. cerevisiae*, however this highly conserved genetic make-up functions within a completely different setting. *A. gossypii* is haploid and propagates by strictly filamentous growth, producing asexual spores in the older regions of mycelia (when nutrients run low), thought to contain one nucleus each. In the natural environment these spores are spread with the aid of insects. Germination from the mid-region of these needle-like spores occurs after a few hours of contact with nutrients in an isotropic fashion, leading to a germ-bubble (figure 2, A). Up to 3 rounds of nuclear division can occur within such a germ-bubble before sufficient polarization factors can be recruited and the switch to polarized growth is made. Two hyphal tips, 4-5 mm in diameter,

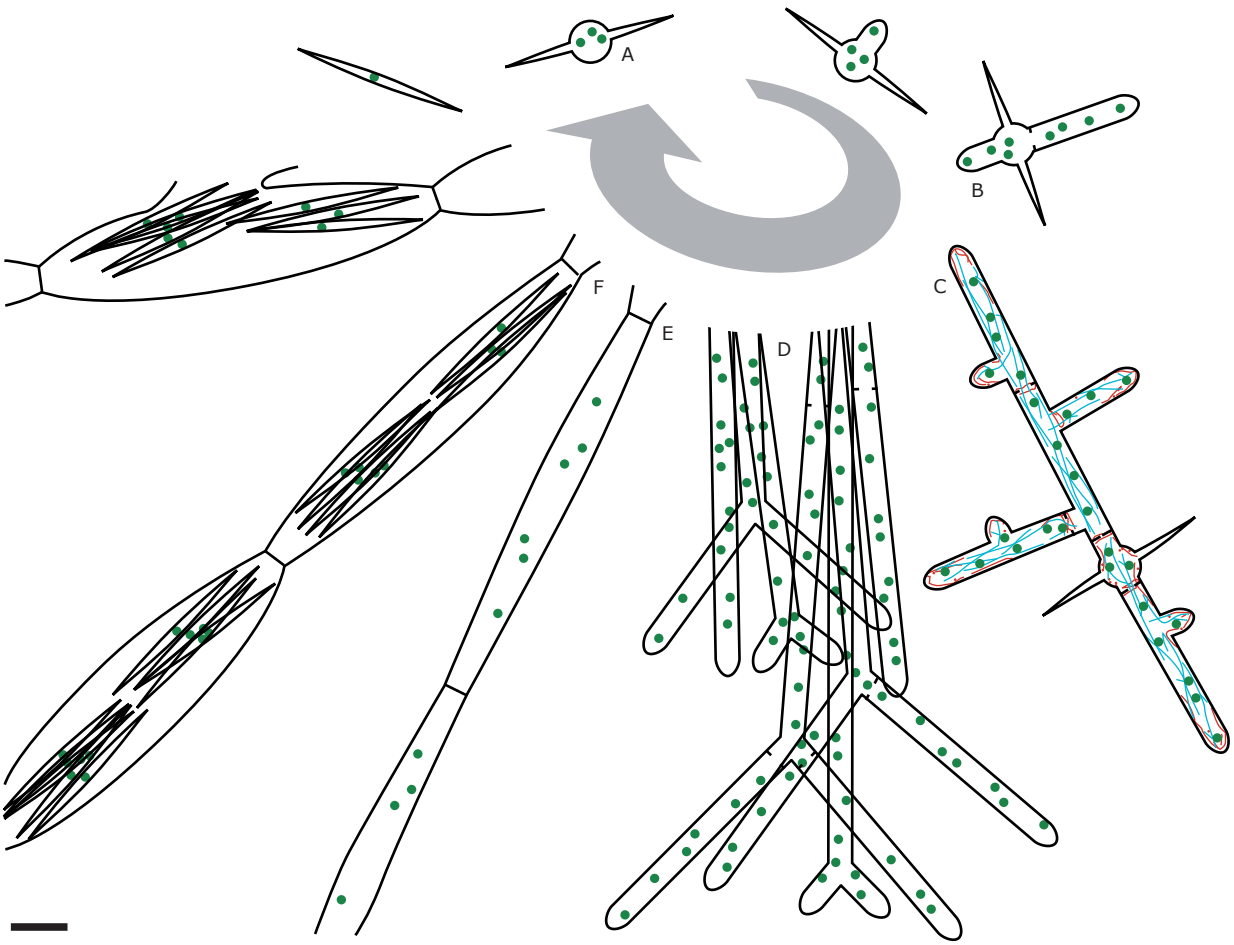

Figure 2: Life cycle of *A. gossypii*. (A) Germ bubble stage. Age: approx. 4-6 hours. Green dots represent nuclei. (B) Bipolar germling. Age: approx. 9-12 hours. (C) Young mycelium with lateral branches. Age: approx. 14-18 hours. Cytoskeleton also depicted in blue (cMT network, nucleated at SPBs) and red (actin cables and patches, mainly at hyphal tips and septation sites). (D) Hyphae of mature, fast-growing mycelium. Tip-splitting from the age of approx. 24 hours on. (E) Early stage sporangia. Can be seen in older/inner regions of approx. 2-3 day old myclia. (F) Mature sporangia. Occur in oldest regions of myclium after 3-4 days of growth on full medium plate. Scale bar depicts 10 μm.

emerge from opposite sides of the germ-bubble. Cells at this stage of development are known as bipolar germlings (figure 2, B). As the speed of the tip accelerates, new polarization sites are defined along the hyphae, leading to branches (figure 2, C). Septa are formed at these branching sites, but also along the hyphae, at an average distance of roughly 40 μm (Wendland and Philippsen, 2000; Kaufmann and Philippsen, 2009). As the mycelium matures, growing tips eventually reach the maximum speed of 3.5 μm/min after roughly 24 hours (Köhli *et al*., 2008). Already from the speed of 1.5 μm/min on, lateral distribution of growing tips is accomplished by tip-splitting (Knechtle *et al*., 2003; Schmitz *et al*., 2006; figure 2, D), rather than lateral branching. The average distance between septa is now approximately 70 μm. Within 2-3 days (depending on nutrient content of medium), hyphal compartments delimited by septa enter the next stage of the life cycle and start expanding to form sporangia (figure 2, E). It is within these bloated compartments that single nuclei are encompassed in rigid, needle-shaped, spores, measuring 25-35 μm in length (figure 2, F). Upon rupturing of the plasma membrane and cell wall due to mechanical stress or osmotic pressure, the spores are released and the cycle begins anew.

Nuclei and the nuclear division cycle in *A. gossypii*

One of the most striking differences between *A. gossypii* and *S. cerevisiae* concerns their growth morphology. *A. gossypii* has evolved extremely fast propagation on solid and in liquid nutrient sources. Maximum ratio of distance/surface is achieved by

tubular growth and septa are only laid down sparsely. This growth strategy, optimized for speed, provides a unique environment for the nuclei, which reside in a common cytoplasm. With basically the same set of genes as present in *S. cerevisiae* (Dietrich *et al*., 2004), nuclei in *A. gossypii* have adapted with/to these circumstances, and display behaviour unique to this species.

Movement of nuclei in growing *A. gossypii* hyphae can be broken down into at least three individually contributing components (Alberti-Segui *et al*., 2001; Lang *et al*., 2010a): 1) Passive, cytoplasmic flow, caused by the constant forward-directed streaming of cytoplasm towards the expanding tip and balanced by fluid uptake in posterior parts of the hyphae. 2) Short range cMT-dependent oscillation, the precise advantage of which is still unknown. 3) Long range cMT-dependent nuclear migration, including by-passing of other nuclei and sometimes passing through developing septa. All cMTs in *A. gossypii* are nucleated at the spindle pole bodies (SPB), which are the only MTOCs present in this species (Lang *et al*., 2010).

Mitosis in *A. gossypii* is not coupled to cytokinesis, which is why we speak of "nuclear division cycle", or simply "nuclear cycle", as opposed to "cell cycle". Mitoses in growing hyphae are asynchronous, with neighbouring nuclei in different nuclear division cycle stages. Asynchrony is possibly actively promoted by the cell, as nuclei synchronized with MT-depolymerizing compounds return to asynchronous division within two hours (Gladfelter *et al*., 2006).

Kinetics of mitosis seem to have adapted towards higher speed in *A. gossypii*. Anaphase in *A. gossypii* takes a maximum of 12 minutes and shows a constant spindle elongation speed throughout the entire duration (Alberti-Segui *et al*., 2001) and thus seems to be much quicker than in *S. cerevisiae*, where anaphase has been shown to be anywhere between 16 and 35 minutes and with clearly bi-phasic kinetics (Yeh *et al*., 1995; Straight *et al*., 1997; Kahana *et al*., 1995; Hoepfner D., referenced in Alberti-Segui *et al*., 2001; Movshovich *et al*., 2008; Zimniak *et al*., 2009). The high speed of mitosis in *A. gossypii* may serve to facilitate quicker adjustment of local nuclear density.

Spatial orientation of mitosis in *A. gossypii* is subject to less constraint than in *S. cerevisiae* (which has multiple mechanisms responsible for correct spindle positioning): Mitotic spindles can be established at virtually any angle relative to the growth axis (Alberti-Segui *et al.*, 2001; Lang *et al*., 2010b). As anaphase progresses, the mitotic spindle straightens out along the hyphal growth axis.

Some important differences in the regulation of the nuclear division cycle have been discovered, compared to *S. cerevisiae*. Cyclins in combination with a persistant Cdk also appear to be a driving force in *A. gossypii*, however their mode of function is of different nature. Of the five cyclin homologs (3 of which are essential: *Ag*Cln1/Cln2, *Ag*Clb1/Clb2 and *Ag*Clb5/Clb6), only *Ag*Clb5/Clb6 displays D-Box dependent oscillations of protein levels throughout the nuclear division cycle (Gladfelter *et al*., 2006b; Hungerbühler *et al*., 2007). The others all remain in at constant levels within the nucleus throughout all nuclear cycle stages, with *Ag*Cln1/Cln2 additionally localizing to the growing hyphal tip. It is proposed that alternating Cdk (*Ag*Cdc28) activity is primarily brought about by inhibitors, such as *Ag*Sic1, instead of recurring destruction and synthesis of cyclins. Nevertheless, the APC (of which all components are conserved) is needed for progression through the nuclear division cycle and is required for *Ag*Pds1 degradation at the onset of anaphase (Gladfelter *et al*., 2007). These findings likely reflect adaptations to the special requirements of individual nuclear regulation in a syncytium where exchange of factors between nuclei in different nuclear cycle stages is enabled.

As a further illustration of adaptation to filamentous growth concerning mitotic regulation, there is also evidence of increased mitotic activity in proximity to septa (Helfer *et al*., 2006). This would ensure that hyphae emanating from branches or forks (where septa are always observed) have sufficient nuclei to maintain growth.

GENERAL INTRODUCTION

Exit from mitosis in *S. cerevisiae*

The following is an attempt to condensate the body of work discussed in recent reviews (Queralt and Uhlmann, 2008; Rock and Amon, 2009; De Wulf *et al*., 2009). Statements, when not cited directly, will often stem from these reviews. The summarizing graph of the involved networks (figure 3) is a simplified representation based on various review figures (mainly Rock and Amon, 2009).

*Sc*Cdc14 phosphatase, a key regulator

Exit from mitosis is a term coined to describe the cell cycle transition that controls inactivation or disassembly of the cellular machinery used during mitosis (such as the mitotic spindle), and the completion of cytokinesis and chromosome decondensation. In budding yeast, these events are characterized/enabled by a transition from high to low *Sc*Clb2-Cdk activity. This decrease is brought about in multiple steps. Cdk down-regulation is first initiated by $APC^{ScCdc20}$ (an E3 ubiquitin ligase with *Sc*Cdc20 as a targeting co-factor), which becomes active at the metaphase to anaphase transition and serves to mark various targets, such as the mitotic cyclins, for destruction by protease complex. However, because $APC^{ScCdc20}$ itself is dependent on *Sc*Clb2-Cdk activity, it cannot be sufficient to fully inactivate the Cdk (Geymonat *et al*., 2002), as is required for successful mitotic exit.
Full reversal of Cdk activity is only achieved with the help of the phosphatase *Sc*Cdc14. Targets for dephosphorylation by *Sc*Cdc14 are *Sc*Cdh1 (a further APC co-factor involved in cyclin degradation), and *Sc*Sic1 (an inhibitor of Cdk). Dephosphorylated APC^{ScCdh1} and Sic1 together eliminate all mitotic Cdk activity, ultimately leading to mitotic exit. Other aspects of mitosis influenced by *Sc*Cdc14 include rDNA condensation (Sullivan *et al*. 2004) and segregation (Granot and Snyder, 1991), likely via RNA polymerase I inhibition (Clemente-Balnco *et al.,* 2009), spindle stabilization and spindle midzone assembly (review: Rock and Amon, 2009). *Sc*Cdc14 is also involved in multiple positive feedback loops (FEAR via securin: Holt *et al*., 2008; MEN via *Sc*Cdc15: Jaspersen *et al*., 2000), enhancing its own release kinetics and making the metaphase/anaphase transition more switch-like.

A two clutch system leading to Cdc14 release

Regulation of *Sc*Cdc14 itself is well understood in budding yeast and appears to be largely based on localization control. During interphase, prophase and metaphase, *Sc*Cdc14 is sequestered in a substructure of the nucleus called the nucleolus (the site of rRNA synthesis), where it is retained by association with its inhibitor, *Sc*Net1 (alternative name: *Sc*Cfi1; Visintin *et al*., 1999), which is part of the RENT complex (Shou *et al*., 1999). Release of *Sc*Cdc14 from this inhibition is mediated upon activation of separase (*Sc*Esp1) and onset of sister chromatid separation. As a result, *Sc*Cdc14 spreads throughout the entire nucleus and also into the cytoplasm. This nuclear export is crucial for the completion of cytokinesis (Bembenek *et al.,* 2005) The association with *Sc*Net1 appears to be largely controlled by phosphorylation status.

The FEAR (*Sc*Cdc14 early anaphase release) network

The first, transient wave of *Sc*Cdc14 release is triggered by components of the so-called FEAR network (Stegmeier *et al*., 2003). This loosely defined set of genes ultimately affects *Sc*Net1 binding to *Sc*Cdc14 in a number of ways. The core signalling pathway is initially sparked via the activation of *Sc*Zds1 and *Sc*Zds2 by *Sc*Esp1 at the very beginning of anaphase. *Sc*Zds1 and *Sc*Zds2 interact and downregulate the $PP2A^{ScCdc55}$ phosphatase. This may happen in a protein complex with *Sc*Esp1, and likely via induction of conformational changes or post-translational modifications and not by direct inhibition, as protein abundance of *Sc*Zds1 and *Sc*Zds2 is quite low (Queralt and Uhlmann, 2008). *Sc*Slk19 is also

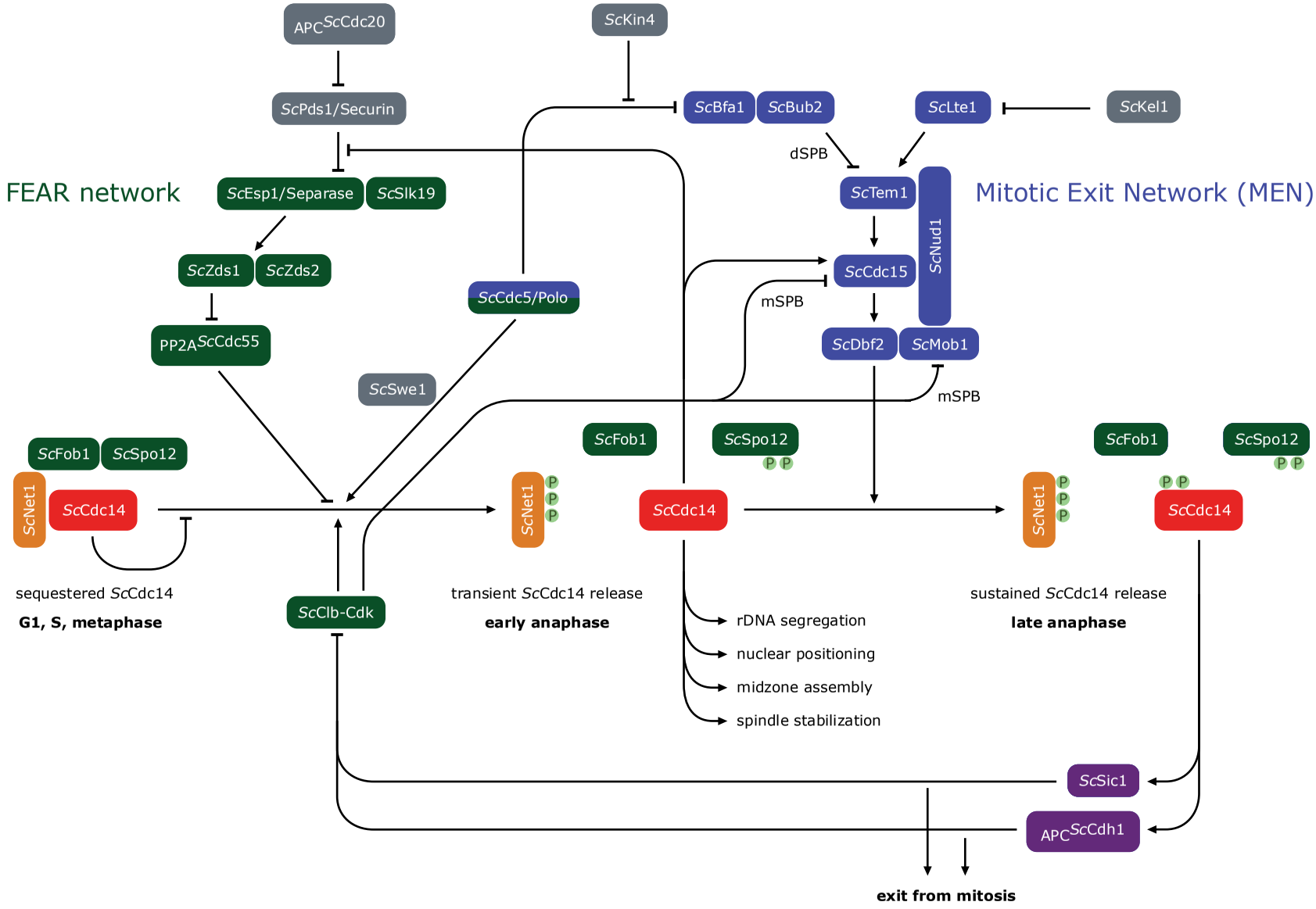

Figure 3: *Sc*Cdc14 regulation in *S. cerevisiae*. Simplified schematic scheme showing important or established interactions. *Sc*Cdc14 release from the nucleolus during early anaphase is mediated by the FEAR network and leads to a surge in *Sc*Cdc14 activity that coordinates certain anaphase events. *Sc*Cdc14 release from the nucleolus in late anaphase is mediated by the MEN and results in sustained *Sc*Cdc14 activity and, ultimately, exit from mitosis. dSPB: daughter-bound SPB. mSPB: mother-bound SPB. P: phosphate group.

believed to contribute to this step, most likely in a complex with *Sc*Esp1 (Sullivan and Uhlmann, 2003). Interestingly, *Sc*Slk19 is a target substrate of *Sc*Esp1 (Sullivan *et al*., 2001), however, proteolytic cleavage of *Sc*Slk19 by *Sc*Esp1 is not required for its role in the FEAR network (Stegmeier *et al*., 2002, Sullivan and Uhlmann, 2003). $PP2A^{ScCdc55}$ is a type 2A phosphatase, consisting of *Sc*Tpd3 as a scaffold, *Sc*Pph21 or *Sc*Pph22 as the catalytic subunit, and *Sc*Cdc55 as the specifity providing regulatory subunit. In metaphase, $PP2A^{Cdc55}$ prevents premature *Sc*Net1 phosphorylation and subsequent *Sc*Cdc14 activation. Its downregulation in anaphase leads to Cdk-dependent *Sc*Net1 phosphorylation and as such, *Sc*Cdc14 release (Queralt *et al.,* 2006). As hinted, the major part of *Sc*Net1 phosphorylation is thought to be contributed by *Sc*Clb2-Cdk (Azzam *et al*., 2004). Some evidence however has been collected that suggests a role within FEAR for the Polo kinase *Sc*Cdc5 in *Sc*Net1 phosphorylation, placing it downstream of, or in parallel to *Sc*Esp1 (Stegmeier *et al*., 2002; Visintin *et al*., 2003 and 2008). Other evidence points to the possibility that *Sc*Cdc5 acts via degradation of the Cdk inhibitor *Sc*Swe1 (Liang *et al.,* 2009). The precise role of *Sc*Cdc5 in mitotic exit remains subject to debate, the resolution of which is hindered by objections concerning the tightness of conditional mutants and more importantly, by *Sc*Cdc5's additional involvement in the MEN.

Two further members of the FEAR functional group are *Sc*Spo12 and *Sc*Fob1. *Sc*Fob1 is not only involved in nucleolar silencing (Huang and Moazed, 2003), but is also an inhibitory element of the FEAR network and is proposed to stabilize the *Sc*Cdc14–*Sc*Net1 interaction during anaphase (Stegmeier *et al.,* 2004). This action is thought to be antagonized by *Sc*Spo12 (Stegmeier *et al.,* 2004). *Sc*Spo12 itself appears to be controlled by phosphorylation status: Phosphorylated *Sc*Spo12 likely helps dissociate *Sc*Fob1 from the *Sc*Cdc14/*Sc*Net1 complex. The kinase thought to phosphorylate *Sc*Spo12 is the mitotic Cdk. The counter-acting phosphatase acting up until anaphase is believed to be *Sc*Cdc14, which is insofar interesting as that this would suggest phosphatase activity during sequestration in the nucleolus prior to anaphase (Tomson *et al.,* 2009).

*Sc*Cdc14 is only transiently released by FEAR and will return to the nucleolus in the absence of MEN activity. Importantly, early anaphase release of *Sc*Cdc14 is not essential for progression through the cell cycle in *S. cerevisiae*, but still crucial for certain aspects of chromosome separation such as spindle stabilization, as mentioned further up. In the absence of FEAR network function, cells undergoing anaphase show a loss of viability. These roles however probably require relatively little phosphatase activity (which may even be sufficiently provided by some ts-mutants at restrictive temperatures), and thus are less susceptible to deficiencies in *Sc*Cdc14 release or phosphatase activity.

The MEN (mitotic exit network)

Once *Sc*Cdc14 has been transiently released by FEAR, the MEN has the role of maintaining this release, allowing successful exit from mitosis. The core components of MEN resemble a Ras-like GTPase signal transduction cascade, with the G-Protein *Sc*Tem1 taking a central role. *Sc*Tem1 localizes to the cytoplasmic side (Pereira *et al.,* 2000) of the daughter cell bound SPB during anaphase (Bardin *et al*., 2000; summary provided in figure 4), together with its GTPase activating protein (GAP) complex *Sc*Bub2-*Sc*Bfa1 (Pereira *et al.,* 2000). The GAP complex serves as an interface for the regulatory input of the Polo-like kinase *Sc*Cdc5 on the MEN. *Sc*Cdc5 has been shown to phosphorylate *Sc*Bfa1, inhibiting activity of *Sc*Bub2-*Sc*Bfa1 and thus enhancing *Sc*Tem1 signalling (Hu *et al*., 2001). The importance of *Sc*Cdc5 in mitotic exit is underlined by the resequestration of *Sc*Cdc14 being heavily dependent on *Sc*Cdc5 degradation by APC^{ScCdh1} (Visintin *et al.,* 2008). *Sc*Kin4, a member of the proposed "spindle positioning checkpoint" (SPOC). Generally speaking, the wide-reaching branch of components upstream of *Sc*Tem1 identified as playing a role in monitoring spindle position. Literature often includes the MEN within SPOC (Lew and Burke, 2003), and vice-versa (Amon and Bardin, 2001). The boundaries are not really clearly defined, as would be expected when trying to define sub-sets of complex networks for the sake of simplification or the joy of inventing acronyms), inhibits the MEN activation by *Sc*Cdc5 (D'Aquino *et al*., 2005; Pereira and Schiebel, 2005) by phosphorylating *Sc*Bfa1 (Maekawa *et*

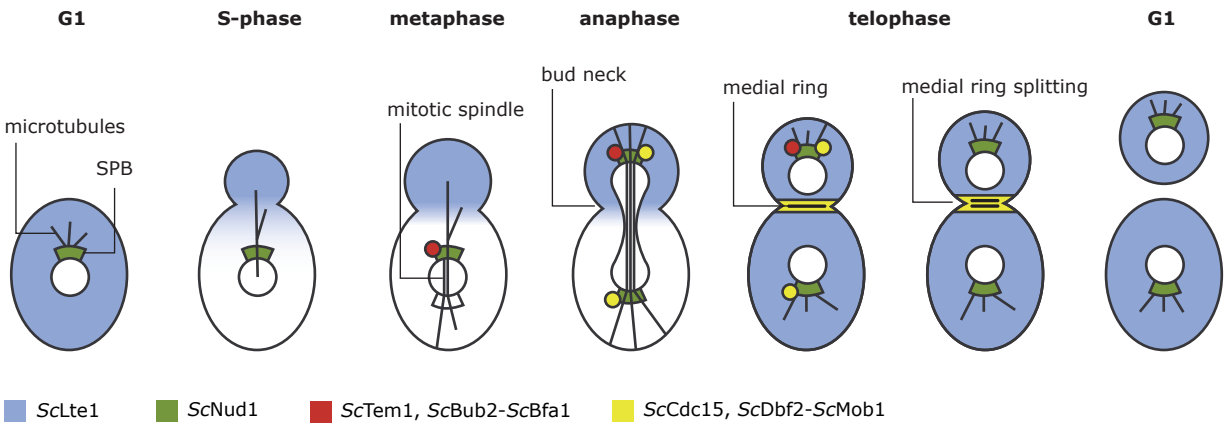

Figure 4: Localization of core MEN components in *S. cerevisiae*. Adapted from Bardin *et al*., 2001. *Sc*Lte1 is present throughout the entire cell during G1, and localizes to the bud during S phase and mitosis. *Sc*Nud1 acts as an anchor for MEN components at the SPB. As the mitotic spindle forms, *Sc*Tem1 and *Sc*Bub2–*Sc*Bfa1 localize to the dSPB. During anaphase, *Sc*Cdc15 and *Sc*Dbf2–*Sc*Mob1 are recruited to both SPBs (various conflicting data exists). During late telophase, *Sc*Cdc15, *Sc*Dbf2 and *Sc*Mob1 also localize to the site of cytokinesis.

al., 2007). This is one example of how the MEN integrates spatial monitoring of the dividing nucleus into the control of mitotic exit. A second example is the proposed function of *Sc*Lte1, a putative guanine nucleotide exchange factor (GEF) of *Sc*Tem1 (Shirayama *et al*., 1994a; Shirayama *et al*., 1994b). *Sc*Lte1, was long suggested to function as a sensory functional unit, due to its localization to the daughter bud cortex during anaphase (Bardin *et al*., 2000), and was thought to activate *Sc*Tem1, moving into the daughter bud on the daughter bound SPB upon correct elongation of the mitotic spindle. This however was often disputed, due to the lack of contribution to mitotic exit of *Sc*Lte1's GEF domain, among other reasons (Geymonat *et al*., 2002; Yoshida *et al*., 2003). It is also argued that *Sc*Tem1 has such high intrinsic guanine nucleotide exchange activity that no GEF would be required (Geymonat *et al*., 2002). Recently, additional evidence against the spatial switch model emerged showing that more likely, *Sc*Lte1 acts on mitotic exit by influencing the localization of *Sc*Bfa1 at the SPBs (Geymonat *et al*., 2009). Exactly how this might work remains subject to speculation, and other investigations have uncovered even more complexity than previously expected, spanning different aspects of the developing bud. An example of how further factors are intertwined into the pathway is the polarity factor *Sc*Kel1 (and *Sc*Kel2), which is localized to the bud cortex (Philips and Herskowitz, 1998). It was shown to be a negative regulator of MEN and bind *Sc*Tem1 and *Sc*Lte1 independently (Höfken and Schiebel, 2002). *Sc*Lte1 affects *Sc*Kel1 localization (Geymonat *et al*., 2009) and vice-versa (Seshan *et al*., 2002).

To further propagate the MEN signal, active *Sc*Tem1 interacts with the kinase *Sc*Cdc15 (Asakawa *et al*., 2001), which in turn activates the *Sc*Dbf2–*Sc*Mob1 kinase complex via phosphorylation of the kinase subunit *Sc*Dbf2 (Mah *et al*., 2001). These components all appear to localize to both SPBs during anaphase and telophase (summarized in review by Bardin and Amon, 2001), but have also been shown to localize to the site of cytokinesis (Yoshida and Toh-e, 2001). It has also been shown that *Sc*Dbf2-*Sc*Mob1 enters the nucleus during telophase (Stoepel *et al*., 2005). Tethering to the SPBs occurs on SPB component *Sc*Nud1 (Gruneberg *et al*., 2000). MEN components residing on the daughter cell-bound SPB (dSPB) are proposed to be mainly controlled by dSPB-localized *Sc*Bfa1-*Sc*Bub2. MEN components on the mSPB are negatively regulated by Cdk (König *et al*., 2010).

Although *Sc*Net1 was identified in a screen for *Sc*Dbf2 substrates (Mah *et al*., 2005), it is still unknown how the final kinase in the signalling cascade (*Sc*Dbf2) stimulates release of *Sc*Cdc14 from *Sc*Net1. Recently it was discovered that one function of the *Sc*Dbf2–*Sc*Mob1 complex is to phosphorylate *Sc*Cdc14 at sites adjacent to its nuclear localization sequence, thereby retaining *Sc*Cdc14 in the cytoplasm (Mohl *et al.,* 2009). Return of *Sc*Cdc14 to the nucleolus after mitotic exit in *S. cerevisiae* is at least in part mediated by

*Sc*Cdh1-mediated degradation of *Sc*Cdc5 (Visintin *et al*., 2008). In contrast to the viability of FEAR mutants, cells without functioning MEN signalling fail to exit mitosis.

To summarize, exit from mitosis is very complex and full of functional redundancy, collateral action and feedback loops. This complexity is required for the described two-clutch release of *Sc*Cdc14. Why the cells have evolved such a two-clutch system could have two reasons (Bosl and Li, 2005):

First, these complex networks may serve to provide circuitry loops to remove distortion and noise from signalling, leading to a fluctuation-free gradual release of *Sc*Cdc14. Feedback loops have been proven to be effective in achieving stable signals in biological networks (Becskei and Serrano, 2000). Feedback is also of utmost importance in providing uni-directionality in the cell cycle. It has been shown that degradation of cyclins is in fact intrinsically reversible, and that only via feedback systems can such transitions be rendered irreversible (Lopez-Aviles *et al*., 2009). This holds true for many instances of switch-like behaviour, however the abrupt events during mitosis rely particularly heavily on such mechanisms (Holt *et al*., 2008). Feedback loops may also generate oscillatory behaviour, providing a basis for cell-cycle dependent fluctuations of activity. Recently, an intrinsically oscillatory module controlling nucleolar release and resequestration of *Sc*Cdc14 was discovered, of which *Sc*Cdc15 (but not *Sc*Spo12) was shown to be a component (Lu and Cross, 2010). Frequency of these autonomous oscillations is thought to be fine-tuned by Cdk to occur once per cell cycle.

Second, the two-clutch regulation of *Sc*Cdc14 may have also developed to allow for MEN to play a role in spatial surveillance and monitoring of the position of the polarized mitotic spindle. As to how this additional level of control could have evolved, it has even been specifically suggested that “in a primitive cell, where the orientation of mitosis might be inconsequential, the FEAR network could represent the sole mechanism for Cdc14 release, and the MEN emerged later coevolving with oriented cell division. [..] It is possible that the original FEAR control of mitotic exit became less effective during the evolution process to allow additional control by the MEN.” (Bosl and Li, 2005).

AIM OF THESIS

Aim of thesis

Understanding of the regulation of exit from mitosis in *S. cerevisiae* has progressed far, and many interactions and functions have been clarified to date. The overall impression is that multiple signals from various parts of the cell converge in these overlapping regulatory networks, and a wide array of outputs is produced, affecting different aspects of M to G1 transition. How this complex network consisting of so many components could have evolved has often been discussed (Bosl and Li, 2005; Lu and Cross, 2010). With this body of work, we address this question and attempt to gain insight into the functions of these networks in *A. gossypii*.

Specifically speaking, we investigate the roles of the *A. gossypii* homologs of the genes involved in exit from mitosis. We set out to answer whether or not the phosphatase *Ag*Cdc14 plays a central role in this cell cycle stage transition, as it does in budding yeast. We also conduct experiments to determine the functions of the homologs of the upstream regulatory pathways, FEAR and MEN. Emphasis is placed on the requirement of these genes for successful mitosis and *Ag*Cdc14 release. This is analyzed by in vivo microscopy on cells harbouring a variety of fluorescent markers.

Generally speaking, we try to provide a snapshot of the evolution of this regulatory network within the *A. gossypii* lineage. The evolutionary distance between *A. gossypii* and *S. cerevisiae* is ideal for comparison: The species are close enough for entire functional groups of genes to be conserved, but distant enough to have developed fundamentally different survival strategies, using basically the same set of genes. We hope to find some answers to such questions as: Is *A. gossypii* a living example of an ancient, "primitive" cell? Why are the regulatory pathways in budding yeast so complex? Does the bulk of evolutionary pressure that formed this vast network stem from the need for spatial regulation and thus the integration of a wide range of inputs? Or does the complexity arise from the need for multiple feedback loops to dampen signal noise, create abruptness and irreversibility or to generate oscillatory behaviour? In the first case, one would expect the regulatory network to be less complex in a simpler setting without coordination between nuclear division cycles and cell separation, such as in *A. gossypii*.

CHAPTER I

Introduction

Due to our interest in the regulatory networks controlling exit from mitosis, a prior characterization of the central effector phosphatase *Ag*Cdc14 was needed. To be able to study localization patterns of *Ag*Cdc14, precise knowledge of the spatial organisation of *A. gossypii* nuclei was needed, but not sufficiently provided by prior studies. To further refine our understanding of the structure of nuclei, we selected two genes for localization studies: 1) *Ag*Nup49, to visualize the nuclear membrane, and give us an idea of total nuclear volume, and 2) *Ag*Nop1, a prominent marker known to be localized in the nucleolus. Both genes had been extensively applied as subnuclear markers in *S. cerevisiae* studies, and proved to be of great use.

*Sc*Nup49 is part of the so called *Sc*Nsp1 complex (Grandi *et al*., 1995), which is a component of the core nuclear pore complex (NPC) machinery. The *Sc*Nsp1 complex likely interacts directly with transport receptors (karyopherins) used to actively shuttle substrates larger than 40 kDa through the NPC. The complex may also help in adjusting the pore diameter (Melcak *et al*., 2007).

*Sc*Nop1 (known as fibrillarin in higher eukaryotes) is found in the nucleolus, as part of the small subunit processome complex, which is required for processing of pre-18S rRNA (Tollervey *et al*., 1991). It is also shown to be a component of the so-called RENT (regulator of nucleolar silencing and telophase exit) complex (Shou *et al*., 1999), together with other protein products such *Sc*Net1 or *Sc*Sir2. Like the acronym suggests, the RENT complex is important for *Sc*Cdc14 sequestration (Visintin *et al*., 1999), but also for other rDNA

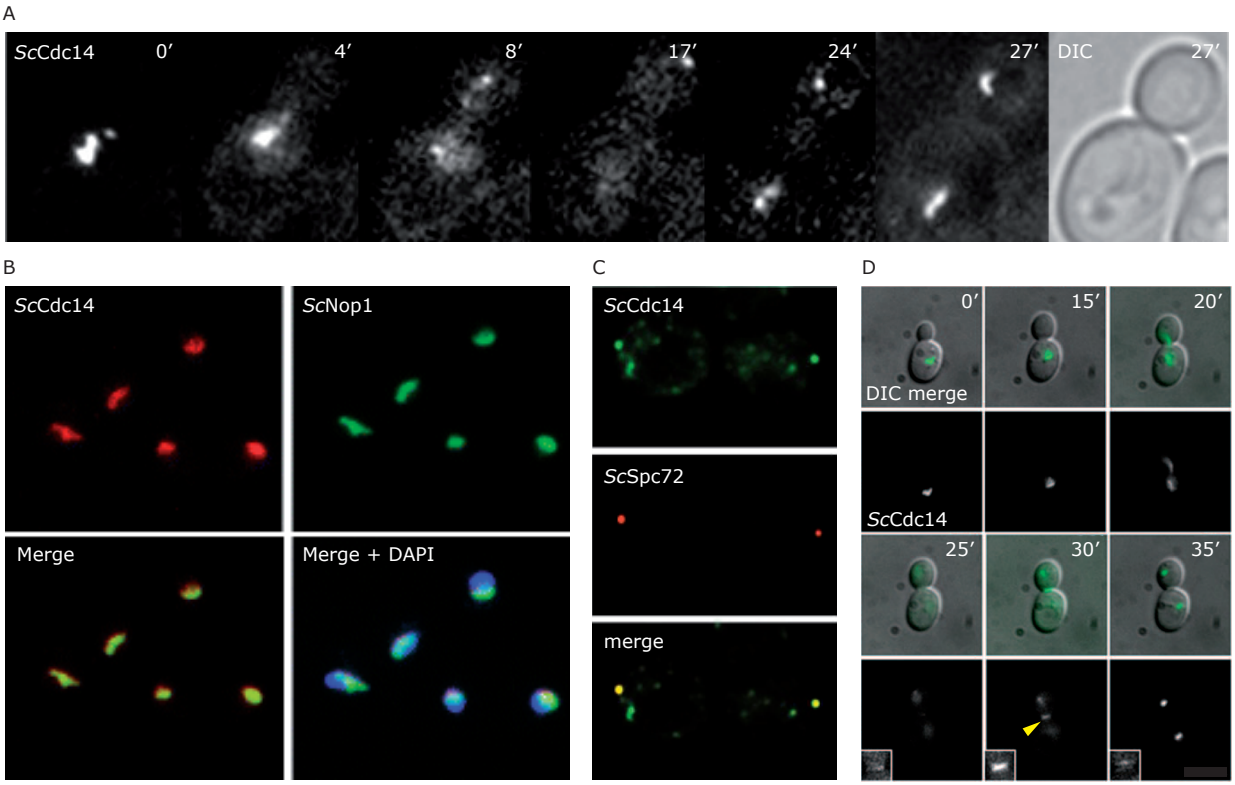

Figure 5: *Sc*Cdc14 localization in *S. cerevisiae*. (A) Release dynamics of *Sc*Cdc14 during mitosis (adapted from Yoshida *et al.* 2002). (B) *Sc*Cdc14 sequestered in nucleoli of interphase cells (adapted from Visintin *et al.* 1999). (C) *Sc*Cdc14 localizes to SPBs (adapted from Yoshida *et al.* 2002). (D) *Sc*Cdc14 localizes to bud neck (yellow arrowhead) (adapted from Bembenek *et al.* 2005).

related tasks, such as silencing (Straight *et al*., 1999). *Sc*Cdc14 activity is heavily dependent on its localization. Many known sites of action have been described in *S. cerevisiae* and we were interested in seeing whether localization patterns are conserved in *A. gossypii*. In budding yeast, *Sc*Cdc14 nucleolar sequestering and release into the nucleoplasm during anaphase can be monitored in vivo, using *Sc*Cdc14-GFP fusions (Figure 5, A). Sequestration in the nucleolus can be readily shown by *Sc*Nop1 co-localization (Figure 5, B). Using multiple fluorescent tags simultaneously, other, lesser pronounced localizations can be made out. For example, *Sc*Cdc14 apparently finds its way to the SPBs (Figure 5, C), with SPB signal strength peaking during anaphase. Also, *Sc*Cdc14 was shown to play a role at the bud neck in actomyosin ring contraction. The relocalization required for this task (Figure 5, D) is dependent on an NES motif. In *S. cerevisiae*, cells carrying a ts-allele of *Sc*CDC14 arrest in late anaphase with an elongated mitotic spindle when shifted to the restrictive temperature, (Pringle and Hartwell, 1981), due to failure in promoting exit from mitosis (Visintin *et al*., 1998).

In this chapter, experiments addressing the conservation of the functional group surrounding *Ag*Cdc14 in *A. gossypii* are discussed. This can be seen as a prerequisite for the investigation of the underlying regulatory pathways of this potentially pivotal phosphatase. Homologs of *Sc*Cdc14 in other organisms have been reported, and functional analysis has resulted in varying findings. The mammalian ortholog, *m*Cdc14A, is essential for cytokinesis (reviewed in Trautmann and McCollum, 2002), and the homolog in *S. pombe*, *Sp*Clp1 is non-essential, but crucial for cell fission. We performed knock-out and localization experiments on *Ag*Cdc14 to gain insight into its role within the unique environment of a cell that doesn't undergo cytokinesis. We hypothesized that the role of *Ag*Cdc14 would likely somehow reflect that of *Sc*Cdc14, at least concerning its involvement in nuclear division, due to the high degree of conservation between the species. However, given the decoupling of cell division from the cell cycle and asynchronicity of the nuclear cycle in this organism, we wondered whether this gene was essential at all.

Materials and Methods

Ashbya gossypii media and growth conditions

A. gossypii media and culturing are described in Ayad-Durieux *et al.*, 2000, and Wendland *et al.*, 2000.

A. gossypii transformation

A. gossypii transformation was performed as described in Wendland *et al.*, 2000.

Strain and plasmid construction

All plasmids and strains used in this study are listed in supplemental tables 5 and 6. DNA manipulations were carried out according to *Molecular Cloning* protocols (Sambrook, 2001) with *E. coli* DH5αF' as a host strain (Hanahan, 1983). PCR amplification was performed using standard methods and methods adapted from product decriptions with Taq DNA polymerase, using the Expand High Fidelity or the Expand Long Template PCR system (Roche Diagnostics). Oligonucleotides are listed in supplemental table 4 and were synthesized by Microsynth AG, CH-9436 Balgach. For recombination of plasmids and PCR products, both were co-transformed into the budding yeast host strain DY3 (*MATα his3Δ200 trp1Δ63 leu2Δ1 ura3-52Δ*) according to (Gietz *et al.*, 1995). Plasmids were isolated from yeast cells using the High Pure Plasmid Purification Kit (Roche Diagnostics) with a modified protocol as previously described (Schmitz *et al.*, 2006).

To construct pMF8, the *Ag*NOP1 locus was amplified by high fidelity PCR from genomic DNA using the primers NOP1SpeIup and NOP1BamHIdown. A BamHI/SpeI digest of the product was sticky-end ligated into a BamHI/SpeI digested pRS416 backbone, and verified first by enzyme digestion, then by sequencing of the cloned ORF.

pMF12 was constructed by homologous recombination in *S. cerevisiae* cells. pAGT211 was used as a template to generate an insertion cassette with homologous flanking regions using NOP1_F5 and NOP1_F2. The product was co-transformed into DY3 cells together with pMF8, and the resulting fusion plasmid was isolated and verified by enzyme digestion and sequencing of the mCherry moiety as well as the C-terminus of *Ag*NOP1.

To generate the *Ag*Nup49-GFP GFP-*Ag*Tub1 strain, the plasmid pNUP49-yEGFP (courtesy of Sandrine Grava) was transformed into a GFP-*Ag*Tub1 strain (courtesy of Claudia Lang).

*Ag*Nop1-Cherry *Ag*Cdc14-GFP was generated by transformation and genomic integration of a fragment produced by digestion of pMF12 with EcoRI and SpeI (and additionally DraI and BspHI to disrupt ARS dependent repication of the plasmid). Homokaryons were not functional, so imaging was conducted in heterokaryotic mycelium.

To generate *Ag*Nop1-Cherry *Ag*H4-GFP *Ag*Tub4-YFP, pMF12 was introduced into an *Ag*H4-GFP *Ag*Tub4-YFP background and maintained by constant selection. Genomic integration was not attempted, due to the non-functionality observed in *Ag*Nop1-Cherry *Ag*Cdc14-GFP homokaryons.

Deletion cassettes for homologous recombination as used for all gene deletions in this thesis were generated by PCR using either pAGT100 (NAT1 marker), pAGT120 (LEU2 marker) or pAGT140 (GEN3 marker) as templates, and oligonucleotide primer pairs with 50 bp homologous flanking sequences for integration. Deletion cassettes were additionally purified prior to transformation, mostly by ethanol precipitation, or via PCR product purification columns (Roche Diagnostics).

Transformation of *A. gossypii* first leads to heterokaryotic cells, which contain both of transformed and wild-type nuclei. Homokaryotic mycelia are obtained by isolating single spores which normally carry a single nucleus. Verification of all deletion strains was carried out by analytical PCR, using primer pairs designed to amplify 5' and 3' integration boundaries, as well as wild-type (non-integrated) corresponding regions as controls. Gel scans of verification reactions are provided at the end of the thesis.

For verification of fluorescent protein fusion transformants generated with plasmid digests,

verification PCR primers were designed to amplify 1) the fusion boundary, 2) a non-integrated region of the plasmid (to be able to rule out a propagation of undigested plasmid leading to resistance toward selective compound), 3) the corresponding N- or C-terminus of the wt allele, and 4) (if feasible) a product demonstrating integration of the selection marker into the genome. Latter is not always possible if the distance from the marker to the edge of the cloned genomic sequence is too large for amplification via PCR, as is the case on the pNup49-yEGFP plasmid.
Selective conditions were maintained with 200 µg/ml Geneticin/G418 Disulphate (ForMedium Ltd. for GEN3 marker), 50 µg/ml clonNAT (Werner BioAgents, for NAT1 marker) or ASC-Leucine (Michael Köhli, doctoral thesis, for LEU2 marker).

Fluorescence microscopy and image processing

For microscopy, an Axioplan2 microscope equipped with the objectives Plan-Apochromat 100x/1.40 NA Oil DIC and Plan-Apochromat 63x/1.40 NA Oil DIC (Carl Zeiss AG, Feldbach, Switzerland) and appropriate filters (Zeiss and Chroma Technology, Brattleboro, VT) was used. The light source for fluorescence microscopy was a Polychrome V monochromator (TILL Photonics GmbH, Gräfelfing, Germany). Images were acquired at room temperature using a cooled charge-coupled device camera CoolSNAP HQ (Photometrics, Tucson, AZ) with MetaMorph 6.2r5 software (Molecular Devices Corp., Downingtown, PA). For fluorescence images, multiple planes with a distance between 0.5 and 1 µm in the Z-axis were taken. Raw image processing was performed with MetaMorph 6.2r5 software. Z-stacks were optionally deconvolved with the built-in nearest neighbor algorithm and compressed by maximum or average projection with Stack Arithmetic and saved as 8-bit grayscale or RGB TIFF files. Further processing for thesis figures and all measurements were carried out with ImageJ (Wayne Rasband, National Institute of Health), using the 4D hypervolume viewer plugin. Channel overlays and cropping were performed with Photoshop CS2 (Adobe Systems, Mountain View, CA). For in vivo image acquisition, glass slides were prepared covered with 0.6 ml of ASC or ALF medium (ASC medium with low fuorescence YNB, Sunrise Scientific Products) supplemented with 1% agarose, upon which small pieces of mature mycelium from the border of A. gossypii colonies or young mycelia cultured in liquid medium were placed and left to recover for at least two hours. 30 µl of ASC or ALF was added to mycelium before cells were covered with a coverslip for image acquisition. Such slides are also referred to as time-lapse slides, or TL slides.

Bioinformatic analysis

Protein alignments were performed with sequences retrieved from the Ashbya Genome Database (AGD, Gattiker *et al.,* 2007) and the *Saccharomyces* Genome Database (SGD, Nash *et al*., 2007).
Cdk motifs were predicted using the Fuzzpro tool of the EMBOSS suite (Rice et al., 2000) and the search patterns [ST]-P-x-[KR] and [KR]-[ST]-P. Automatization to scan the entire genome was implemented using a custom PERL script written with Crimson Editor 5.70 (Ingyu Kang), running natively on a UNIX server hosting EMBOSS.
Domain predictions were run individually using InterProScan (Hunter et al., 2009) and combined with predictions delivered by SGD.
Orthologs of S. cerevisiae genes in other organisms than A. gossypii were determined using psiBLAST (www.ebi.ac.uk/Tools, Altschul et al., 1997).
Amino acid sequence identity calculations and graphical alignments were produced with the multiple sequence alignment tool of the Clone Manager 7 Suite (Scientific and Educational Software, Cary, NC), using progressive assembly with default parameters.
All oligonucleotide sequences were chosen with optimized annealing characteristics using the primer design tool of the Clone Manager 7 Suite (Scientific and Educational Software, Cary, NC).

Results

Compartments of the *A. gossypii* nucleus

In previous studies focussing on the *A. gossypii* nuclear cycle (Gladfelter *et al*., 2006; Helfer and Gladfelter 2006; Hungerbuehler *et al*., 2007; Gladfelter *et al*., 2007) a variety of components involved with or localizing to nuclei have been investigated. Nevertheless, our knowledge on the structure of the nuclei has remained somewhat basic, and due to the sub-nuclear phenomena dealt with in this work a more detailed picture of the *A. gossypii* nucleus was required.

To gain a better understanding on the dimensions and shape of the entire nucleus, we decided to localize the putative nuclear pore complex component *Ag*Nup49. The *A. gossypii* ORF shares 54% overall amino acid sequence identity with its predicted syntenic *S. cerevisiae* ortholog, including a region of 75% identity composed of the last 200 C-terminal residues (of 383 total amino acids). A C-terminal fusion of yEGFP to *Ag*Nup49 was introduced into a strain already harbouring GFP-*Ag*Tub1 (courtesy of Claudia Lang). GFP-*Ag*Tub1 was known to have an easily distuingishable signal and was included in this experiment in order to help identify mitotic nuclei.

*Ag*Nup49-yEGFP was shown to be unevenly distributed around the nuclear membrane (figure 6). No characteristic pattern or axis of symmetry could be made out in nuclei undergoing mitosis (figure 6, arrowhead). Measurements showed the mean projected area of the nuclear membrane to be $3.44 \pm 0.56\ \mu m^2$ (1 SD, N = 24) (this corresponds to diameters between 1.91 and 2.26 μm).

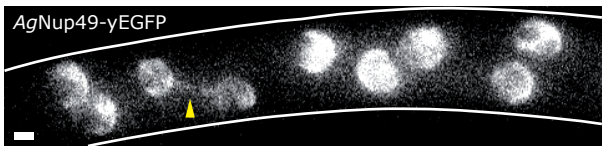

Figure 6: The nuclear envelope in *A. gossypii*. Localization of *Ag*Nup49-yEGFP and GFP-*Ag*Tub1 in mature, growing wild-type reference strain. Arrowhead indicates anaphase spindle. Maximum intensity projection of 5 planes with 1 μm Z-distance. Scale bar depicts 1 μm.

The sub-nuclear compartment most important to our studies due to it's role in exit from mitosis is the nucleolus. We visualized the RENT complex within this distinct region of the nucleus by constructing a C-terminal fusion of the putative RENT component *Ag*Nop1 (which is 93% identical with it's *S. cerevisiae* ortholog) with mCherry. This construct was introduced into a *Ag*H4-GFP *Ag*Tub4-YFP background in order to be able to determine the position of the nucleolus relative to the non-nucleolar DNA within the nucleus. Heterokaryotic mycelia still containing wt copies of *Ag*Nop1 were used for the experiments, as *Ag*Nop1-mCherry did not prove to be functional on its own.

Fluorescent imaging showed *Ag*Nop1-mCherry to occupy a distinct space within the nucleus, clearly distinguishable from that of *Ag*H4-GFP (figure 7). Mean areas occupied by the projections of these two markers were calculated to be $1.28 \pm 0.51\ \mu m^2$ (1 SD, N = 50) for *Ag*Nop1-mCherry and $2.04 \pm 0.60\ \mu m^2$ (1 SD, N = 50) for *Ag*H4-GFP. The size ratio is similar to that observed in *S. cerevisiae*. Also, the nucleolus trails behind the rest of the nucleus during anaphase and divides at a later stage than the nuclear DNA. This is also concurrent with what is known about *S. cerevisiae* nucleoli (Granot and Snyder, 1991).

The measurements done on *Ag*H4-GFP, *Ag*Nup49-yEGFP and *Ag*Nop1-mCherry are summarized as a basic scheme of a typical interphase nucleus (figure 8) in which mean size ratios were maintained graphically. As *Ag*Tub4YFP was also co-localized together with *Ag*Nop1-mCherry and *Ag*H4-GFP, its position in relation to the other components could also be included in the scheme. We observed that *Ag*Tub4-YFP was generally localized adjacent to *Ag*H4-GFP, but not necessarily opposite *Ag*Nop1-mCherry. In retrospective, we found that this basic model is accurately reflected in published EM images depicting nuclei, where the nucleolus is likely observable as a large and well defined electron-dense area physically separated from the SPBs (Lang *et al.,* 2010a, supplemental figure 1).

*Sc*Cdc14 functional group conserved in *A. gossypii*

*Sc*Cdc14 was found to be highly conserved in *A.*

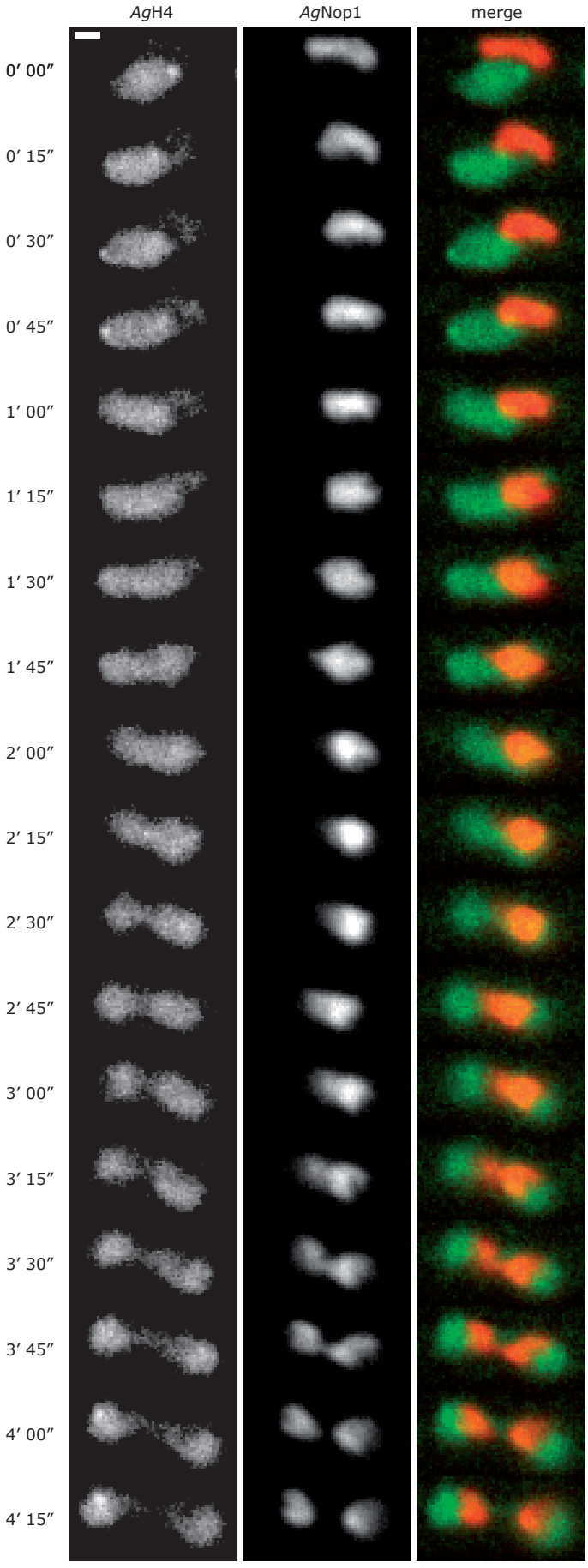

Figure 7: The nucleolus in *A. gossypii*. Subnuclear localization of *Ag*H4-GFP and *Ag*Nop1-mCherry throughout nuclear division in growing hyphae. Image cropped individually for each timepoint. Scale bar depicts 1 μm.

gossypii, with an amino acid identity value of 77% predicted. All important components known to be interact with or be directly downstream of *Sc*Cdc14 in *S. cerevisiae* were found to have orthologs in *A. gossypii*, with sequence identity on the amino acid level ranging from 19% to 77% (table 1). All genes were found in syntenic locations, providing compelling evidence that low homology ORFs such as *Ag*SIC1 are true orthologs. When checking for motifs identified in *S. cerevisiae* to be sites phosphorylated by the cyclin dependent kinase (Cdk), we found that these motifs are also common sequence features in *A. gossypii*. We interpret the presence of these motifs as a possible indication of cell cycle related function. Notable are the extra occurences of such motifs in *Ag*Net1/Tof2 and *Ag*Cdc14 (table 1). In a more detailed look at the amino acid sequences (figure 9) we identified regions of particularly strong homology and ran protein domain predictions on all genes. All predicted domains in *Sc*Cdc14 and *Sc*Cdh1 were also predicted for the *A. gossypii* orthologs. Both the NES motif and the C-terminal NLS motif identified in *Sc*Cdc14 were discovered to be at the same location within *Ag*Cdc14.

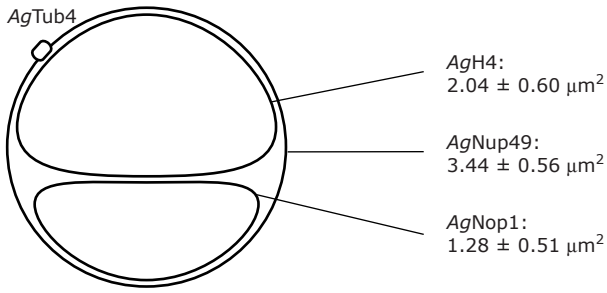

Figure 8: Nuclear compartments of *A. gossypii*. Overview providing size comparison of nuclear subcompartments. Area measurements were done using Z projections of growing hyphae. Size ratios are maintained in illustration.

In the case of Net1, where overall identity is only 33%, one highly conserved (67% ID) stretch was confined to the N-terminus, which has been shown to be responsible for *Sc*Cdc14 binding in *S. cerevisiae* (Traverso *et al.,* 2001).

*Ag*Cdc14 sequestration and release

Due to the high degree of conservation observed on the amino acid sequence level, we were interested to see to which extent functionality was conserved in *A. gossypii*. In order to study the behaviour of *Ag*Cdc14, a C-terminal GFP fusion was constructed (Katrin Hungerbühler, unpublished). *Ag*Nop1-mCherry was then additionally introduced into this strain to co-visualize the nucleolus. Time-lapse imaging series revealed different phases of *Ag*Cdc14-GFP localization during the nuclear division cycle (figure 10): During interphase, *Ag*Cdc14 is sequestered within the nucleolus. The *Ag*Cdc14-GFP signal was shown to be restricted to within the area of Nop1-mCherry, but also to have a granular localization pattern, seemingly composed of multiple foci (figure 10, 0' 00"). During mitosis, *Ag*Cdc14 is then progressively released from this confined space, and spreads to a total area of roughly 3.8 μm^2 (figure 10, 2' 30") which indicates localization throughout the entire nucleoplasm, according to the size estimates in figure BA. Coinciding with this release, *Ag*Cdc14 also localizes to two distinct foci (figure 10, 3' 00") which then migrate apart as mitosis progresses (figure 10, from 4' 15" on). After mitosis is complete, *Ag*Cdc14-GFP then relocalizes to the nucleoli (figure 10, 14' 30").

As *Sc*Cdc14 was described to localize to SPBs during anaphase in *S. cerevisiae* (Yoshida *et al.,*

	***A. gossypii* ortholog**				***S. cerevisiae* 1st homolog**					***S. cerevisiae* 2nd homolog**		
common	systematic	aa	Cdk	synt.	systematic	aa	ID	null mutant	Cdk	common	systematic	aa
*Sc*CDC14	AEL025W	537	1	Y	YFR028C	551	77%	lethal	0			
*Sc*CDH1	AFL007C	551	7	Y	YGL003C	567	77%	viable	7			
*Sc*NET1	AAL181C	1222	8	Y	YJL076W	1189	30%	double: viable	4	*Sc*TOF2	YKR010C	771
*Sc*SIC1	ABR240W	227	5	Y	YLR079W	285	19%	viable	5			
*Sc*SWI5	AGL197W	844	11	Y	YDR146C	710	33%	double: viable	10	*Sc*ACE2	YLR131C	770

Table 1: Homologs of *Sc*Cdc14 functional group. aa: length in amino acids. Cdk: predicted number of Cdk phosphorylation motifs.

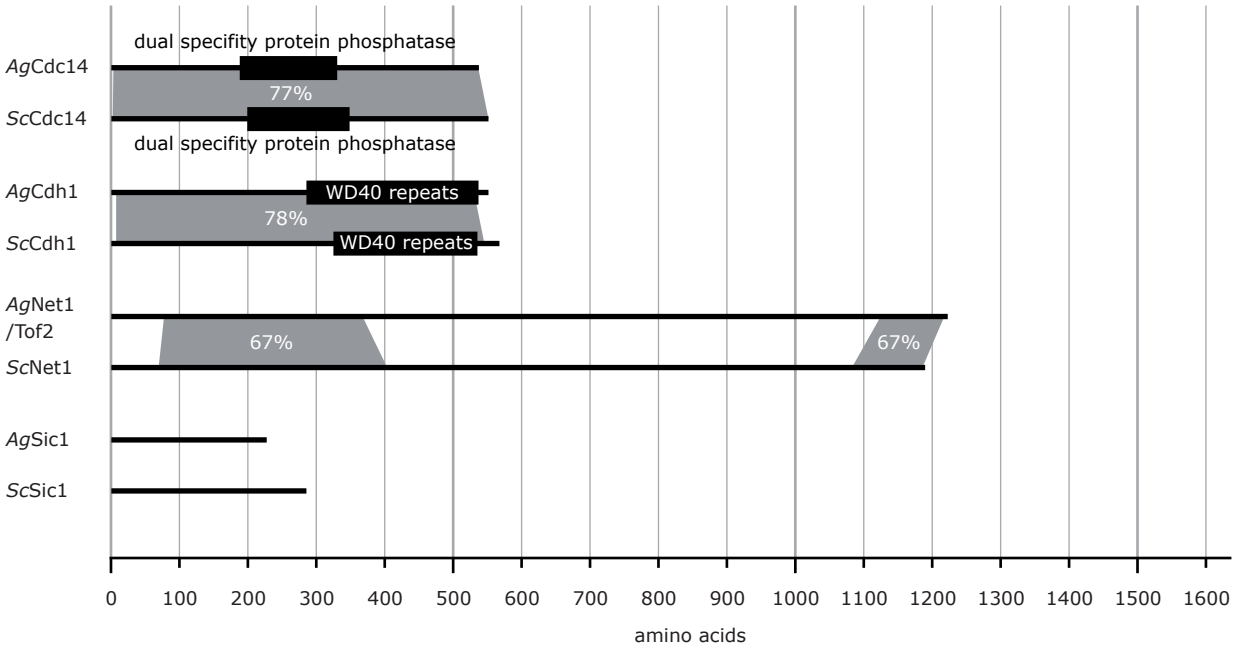

Figure 9: Sequence comparison of genes involved in termination of mitosis in *S. cerevisiae*. Grey areas indicate regions of high homology. Black bars depict all predicted domains and features. Higher identity homologs shown in case of twin genes. Second homologs depicted in supplemental figure 8.

2002), we hypothesised that this was also the case in *A. gossypii*. On this account, an *Ag*Cdc14-mCherry fusion was constructed (Katrin Hungerbühler, unpublished) and co-localized with *Ag*Tub4-YFP, an established component of the *A. gossypii* SPB (Lang *et al.,* 2010a). Single plane imaging confirmed that *Ag*Cdc14-mCherry indeed localizes to SPBs in anaphase nuclei (figure 11).

Additionally, a weak *Ag*Cdc14 signal is visible between the diving sister nuclei (figure 10, 7' 45" and figure 11). It is unclear whether this is unspecific nucleoplasmic localization reflecting the closed mitosis that *A. gossypii* undergoes (Lang *et al.,* 2010a), or protein enrichment at the elongating spindle mid-zone.

*Ag*Cdc14-GFP was also found to localize to developing septa. In time-lapse series, protein levels did not appear to vary during ongoing septum constriction (figure 12). This septal localization suggests a substantial pool of *Ag*Cdc14 present in the cytoplasm.

*Ag*Cdc14 is essential for progress through nuclear division cycle

To assess the role of *Ag*Cdc14 in the nuclear division cycle, the entire ORF was disrupted in a GFP-*Ag*Tub1 strain. *Agcdc14*Δ mutants were not viable and ceased growth approximately 12-20 hours after spore inoculation (figure 13, A). Typically, growth arrest occured in the bipolar or monopolar germling stage.

Investigation of GFP-*Ag*Tub1 in these deletion mutants indicated a malfunction of nuclear division (figure 13, B, top panel). Cells were shown to harbour only 2-3 nuclei at 8 hours after inoculation, compared to 10 or more in wt cells of comparable size. No nuclear division was recorded at this age in deletion mutants, implying that all mitotic activity was restricted to the first few hours of germination. It is plausible that these early germlings still contained residual *Ag*Cdc14 from the heterokaryotic mycelium used to harvest the spores for this experiment, and that the observed mitoses were only possible due to this "maternal effect".

Nuclei in terminal *Agcdc14*Δ GFP-*Ag*Tub1 mutants were exclusively found in interphase (figure 13, B, top panel, yellow arrowheads). This became apparent when comparing with GFP-*Ag*Tub1 cells, where metaphase (bottom panel, red arrowhead) and anaphase nuclei (blue arrowhead) were easily distinguishable.

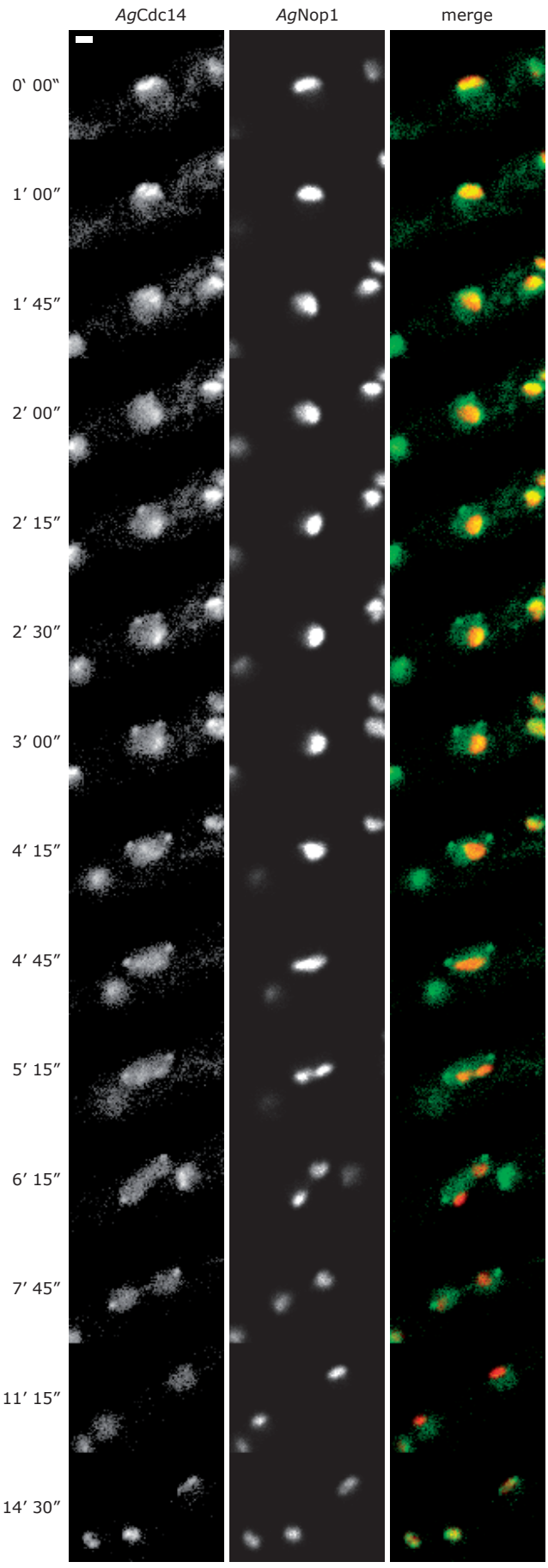

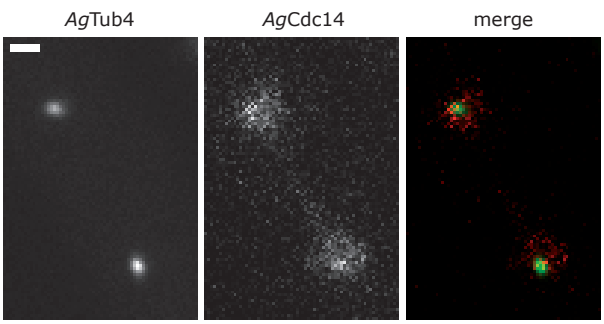

Figure 11: Colocalization of *Ag*Cdc14 and the SPB during anaphase. Still image from a time-lapse series tracking *Ag*Tub4-YFP and *Ag*Cdc14-yEGFP in a dividing nucleus. Only a single plane was captured in order to reduce the interval between channels to roughly 3 seconds. Scale bar depicts 1 μm.

Figure 10: Relocalization of *Ag*Cdc14 during anaphase in *A. gossypii*. Selection of timepoints illustrating the release and subsequent resequestration of *Ag*Cdc14-yEGFP from and into the nucleolus (visualized by *Ag*Nop1-mCherry), as a nucleus undergoes mitosis. Scale bar depicts 1 μm.

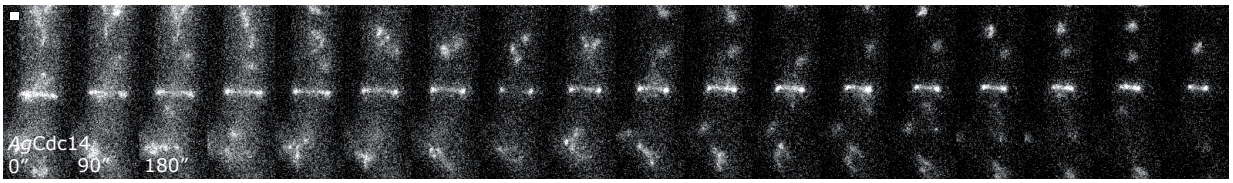

Figure 12: *Ag*Cdc14 at the septa. Time-lapse series showing *Ag*Cdc14-yEGFP localization to septum of 20 hour old mycelium. 3 minutes time interval. Scale bar depicts 1 μm.

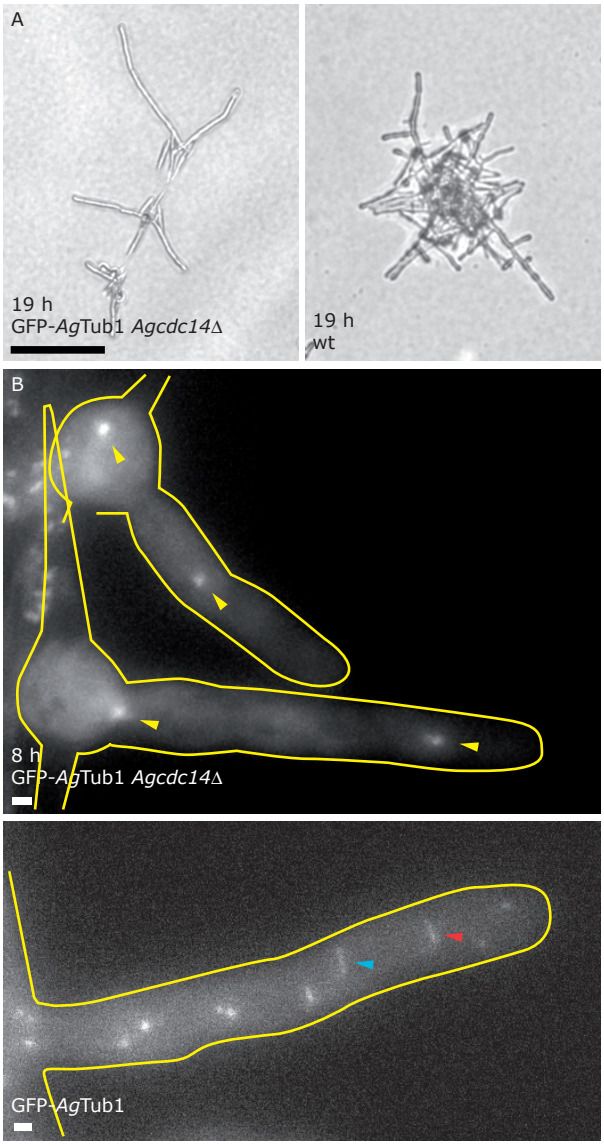

Figure 13: Phenotype of *Agcdc14*Δ mutant. (A) Exerpt from time-lapse series. Growth progression in *Agcdc14*Δ GFP-*Ag*Tub1 and wild-type reference strain at 19 hours after spreading of spores. (B) GFP-*Ag*Tub1 in 8 hour old *Ag*cdc14Δ germlings. Scale bar depicts 1 μm. MTOCs of interphase nuclei indicated by yellow arrows. (C) GFP-*Ag*Tub1 in 20 hour old wild-type reference strain. Red arrow: Spindle of metaphase nucleus. Blue arrow: Spindle of anaphase nucleus. Scale bar depicts 1 μm.

Discussion

Nuclear substructures were shown to be conserved in *A. gossypii* and *S. cerevisiae*. We observed similarities not only in size and shape of the nuclear envelope and the nucleolus, but also in their behaviour during mitosis. The trailing of the *Ag*Nop1-Cherry signal behind that of *Ag*H4-GFP is in agreement with observations in budding yeast (Granot and Snyder, 1991), and reflects distinctions made within the nucleus between different regions of the genome. Overall morphology of the *A. gossypii* nucleus is very much reminiscent of the *S. cerevisiae* counterpart.

The resemblance of the nucleolus in *A. gossypii* to that of *S. cerevisiae* hints at the possibility of retained functions. This is also suggested by the conservation observed on the amino acid level: homologs of all known RENT complex genes are present in *A. gossypii*.

The nucleolus apparently functions as the site for *Ag*Cdc14 regulation by sequestration. We were clearly able to observe *Ag*Cdc14-yEGFP co-localized with *Ag*Nop1-Cherry leave the nucleolus during anaphase and spread throughout the nucleoplasm and to the SPBs. Likely, *Ag*Cdc14 also exists at substantial concentrations in the cytoplasm, as we were able to observe clear signals at constricting septa. There, signal strength seemed independent of how close passing nuclei were. Quite possibly a significant cytoplasmic pool of *Ag*Cdc14 would be needed to sustain such a clear signal. This septal localization likely corresponds to the proposed role of *Sc*Cdc14 in actomyosin ring constriction at the bud neck (Bembenek *et al.,* 2005), where it is thought to dephosphorylate some yet unknown substrate involved in bud neck constriction. In a preliminary follow-up experiment, we looked at septum constriction (by means of *Ag*Hof1-GFP localization) in *Agcdc14*Δ germlings (supplemental figure 4, courtesy of summer intern Anaïs Sengler). Dynamics of *Ag*Hof1-GFP were unaffected, but a "maternal effect" of the heterokaryotic sporangia could not be ruled out.

*Ag*Cdc14 was shown to play an essential role in nuclear division cycle progression in *A. gossypii*. Deletion mutants could undergo mitosis during a very narrow time-frame at the beginning of germination (likely thanks to "maternal effect"), then all mitotic activity ground to a halt. Surprisingly, the observed nuclei all had single (or duplicated, but not separated) SPBs. This was unexpected, given that *Sc*Cdc14 ts-mutants in budding yeast arrest in telophase with elongated mitotic spindles. In *A. gossypii*, *Ag*Cdc14 may be needed in other parts of the cell cycle, such as prophase to metaphase transition or passage through S phase. This appears strange, considering that *Ag*Cdc14 is clearly released (and thus activated) during anaphase. Perhaps some visible aspects of M to G1 transition such as spindle breakdown are possible with no (or little maternal) *Ag*Cdc14, however proper priming of the nucleus for the next cycle cannot take place. A look at homologs in other eukaryotes may give additional clues for interpreting this outcome.

In *S. pombe*, *Sp*Clp1 (the *Sc*Cdc14 homolog) plays an important part in G2 to M transition. The mode of action is however inhibitory on mitotic entry, and deletion mutants (which are viable) display premature entry into mitosis at shorter cell lengths than in wt (Trautmann *et al.,* 2001). *Sp*Clp1 is already released from the nucleolus upon entry into mitosis and is also believed to inhibit Cdk activity. Upon release, *Sp*Clp1 localizes to SPBs, the mitotic spindle, the actomyosin ring and can also be detected in the cytoplasm.

In mammalian cells, details on the system are still scarce. Mammals have two *Sc*Cdc14 homolog isoforms, termed *m*Cdc14A and *m*Cdc14B. They localize to the centrosome and nucleolus respectively in interphase, but are then dispersed at onset of mitosis. *m*Cdc14A appears to play a role in the regulation of the centrosome cycle, mitosis, and cytokinesis (Kaiser *et al*., 2002), as well as meiosis I to meiosis II transition (Schindler and Schultz, 2009). *m*Cdc14B does not impede anaphase onset, mitotic exit, or cytokinesis. Also, segregation of rDNA repeats remained intact in *m*Cdc14B null mutants (Berdougo *et al*., 2008). In conclusion, it seems that despite *Sc*Cdc14-related phosphatases being conserved, they are not individually needed in mammalian cells to segregate sister genomes or complete cell division.

As for other filamentous fungi, it has been shown

that *An*Cdc14 is not essential in *Aspergillus nidulans*, which can grow and develop normally without this phosphatase (Son and Osmani, 2009). Orthologs of *Sc*Cdc14 were found across virtually all eukaryotic species, indicating a central role of this phosphatase since ancient times. Homologs have been found not be essential components of mitotic regulation in all organisms, however, like in *S. cerevisiae*, this is the case in *A. gossypii*. *S. cerevisiae* is the closest relative of *A. gossypii* on the phylogenetic tree (James *et al.,* 2006) for which published experimental data on this phosphatase is available. This close phylogenetic relationship is also reflected in the alignment of *Ag*Cdc14 with homologs in selected species (figure 14).

The terminal phenotypes of the null mutants are different in the *A. gossypii* and *S. cerevisiae*, for reasons not quite understood, however the timing of sequestration and release of the phosphatase from the nucleolus are the same, as are other localization characteristics. It will be interesting to investigate the regulatory basis of these events.

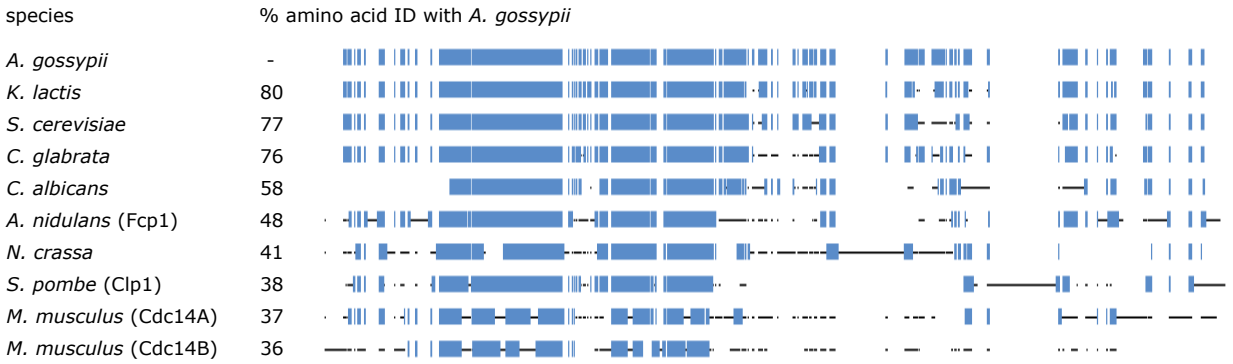

Figure 14: Multiple sequence alignment of homologs of *Ag*Cdc14 in selected species. Identified by PsiBLAST. Blue regions in alignment indicate areas of significant similarity (window of 10 aas). Black lines are unique sequences.

CHAPTER II

CHAPTER II: MEN HOMOLOGS IN *ASHBYA GOSSYPII*

Introduction

The fundamental question addressed in this chapter can be posed as such: Is there a functional MEN in *A. gossypii*? By strict definition the answer to this question would have to be "no". By most circulating definitions, "mitotic exit" also includes successful cytokinesis, which automatically implies a direct coupling of cell division to the nuclear division cycle. This, as has been described before, is clearly not the case in *A. gossypii*. We therefore rather asked: Are the genes there and if so, what do they do?

It is difficult to imagine a conserved MEN exercising the same function in a syncytium as in the unicellular setting of budding yeast, for reasons laid out in the general introduction, the function in mind being the conditional facilitation of M-phase to G1 transition. We therefore decided to focus predominantly on finding out whether disruption of the system would lead to any detectable perturbations in the nuclear division cycle of *A. gossypii*. The experiments described below were designed to gain as much information as possible on progression of nuclei through the division cycle, without ruling out any effect in unexpected cycle stages.

The most obvious readout of the MEN signalling pathway in budding yeast however is *Sc*Cdc14 release. Disrupting core components of the MEN in *S. cerevisiae*, such as *Sc*Tem1, leads to an arrest of the cell cycle at the M/G1 transition, with elongated mitotic spindles, and *Sc*Cdc14 still visibly retained within the nucleoli (figure 15, Shou *et al.,* 1999).

*Ag*Cdc14 was shown to be crucial for progression through the nuclear division cycle, and the observed release patterns suggest that the mode of regulation described in *S. cerevisiae* may be conserved in *A. gossypii*. Here we present results of investigations into the effect of disrupting the putative MEN homologs on *Ag*Cdc14 release and the effect on nuclear division stages in *A. gossypii*.

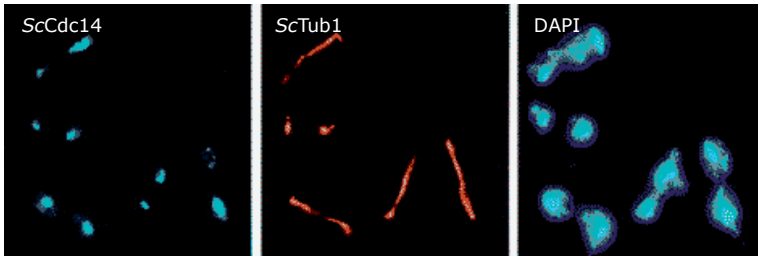

Figure 15: *Sctem1*Δ terminal phenotype. *Sc*CDC14-HA3 *Sctem1Δ::GAL1-ScTEM1* cells switched to glucose medium (*Sc*TEM1 off) after α-factor release (adapted from Shou *et al.,* 1999).

Materials and Methods

General

A. gossypii media, growth conditions, transformation, bioinformatic analysis, microscopy and strain verifications are as described in chapter I. Chitin staining (using Calcofluor White) was performed as described in Ayad-Durieux *et al.*, 2000.

Strain and plasmid construction

All plasmids and strains used in this study are listed in supplemental tables 5 and 6. All methods are as described in chapter I.

Construction of the plasmid pMF1 was analog to that of pMF8, described previously, using the primers AgTEM1_CL_Up and AgTEM1_CL_Down. A HindIII/SpeI digest of the product was sticky-end ligated into a pRS416 backbone, and verified by enzyme digestion and sequencing. pMF2 was then constructed using pMF1 as a backbone, analogous to pMF12 construction outlined in chapter I, using AgTEM1_F5 and AgTEM1_F2 and the template pAGT241. The resulting fusion plasmid was isolated from the co-transformed yeast cells and verified by enzyme digestion and sequencing of the yEGFP moiety as well as the C-terminus of *Ag*TEM1.

pMF3 was constructed in an analogous manner to pMF3, using the pre-existing plasmid clone (originally used for genome sequencing by Christine Mohr, documented in doctoral thesis) of the C-terminus of *Ag*LTE1, pAG7638, as a backbone and the oligonucleotide primers AgLTE1_F5 and AgLTE1_F2 for fusion cassette amplification. Verification was via digestion and sequencing.

pMF10 was constructed in an analogous manner, using the *Ag*PDS1 clone pAG11556 as a backbone, and pAGT211, combined with the primers PDS_F5 and PDS1_F2, to amplify the mCherry fusion cassette.

A. gossypii strains *Ag*Tem1-GFP and *Ag*Lte1-GFP were generated by transformation and genomic integration of fragments produced by digestion of pMF2 (with BssSI/BclI) and pMF3 (with BlpI) respectively. The *Ag*Pds1-Cherry *Ag*Cdc14-GFP strain was obtained by transforming fragments produced by digesting pMF10 with ClaI and SpeI (as well as XmnI for ARS disruption). *Ag*Tem1-yEGFP, *Ag*Lte1-yEGFP and *Ag*Pds1-mCherry were all functional.

All deletion mutants were generated as described in chapter I.

Anaphase measurements

The measurements of dividing nuclei as presented in figure 25 were performed by picking mycelium onto TL-slides, letting the cells recover for 2 hours, then imaging at 30 s intervals with 5 planes spaced 1 µm apart. Only tip-splitting hyphae were taken into consideration as this reflects healthy cells growing at accelerated speeds. Nuclei undergoing mitosis were determined and were measured for maximal *Ag*H4-GFP signal diameter at all time points. Nuclear cycle stages corresponding to the different diameters are illustrated in figure 16. Successful nuclear segregation is characterized by a fluctuating diameter, indicating independent movement of the sister nuclei.

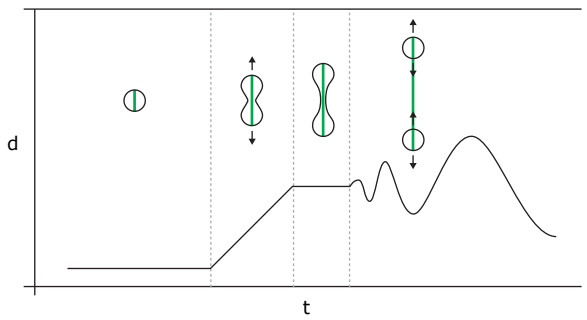

Figure 16: Anaphase measurements. Depiction of how measured length corresponds to nuclear division cycle stages. From left to right: pre-anaphase (G2/prophase/metaphase), anaphase, post-anaphase, G1.

Quantification of fractions of nuclei in different nuclear division cycle stages

Experiments presented in figure 27 were performed as follows: Tip-splitting hyphae were identified on TL-slides, indicating healthy growth, and short (8 minute) time-lapse movies were acquired, capturing

5 planes (1 µm apart) for the *Ag*H4-GFP signal, and 13 planes (0.5 µm apart) for the *Ag*TUB4-YFP signal at each time point (1 min time interval). The entire length of the movie was used to determine the category of nuclei in the third time frame, judging by the combined signals from the two channels acquired. Examples of nuclei assigned to different the categories are shown in figure 17.

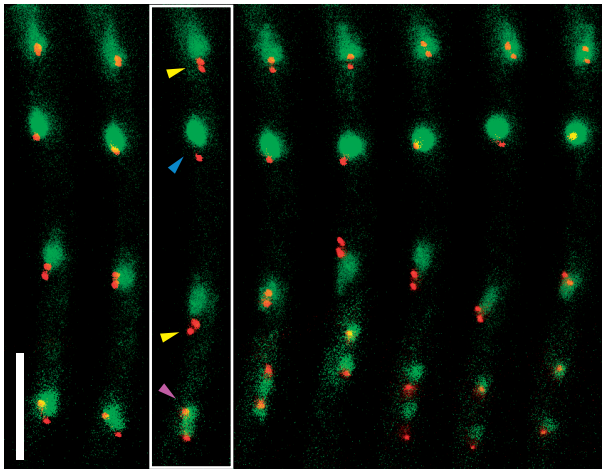

Figure 17: Nuclear division stage counts. Example of time-lapse series used for classification of nuclei. Maximal projection and overlay of *Ag*H4-GFP (green) and *Ag*Tub4-YFP (red) stacks. White border indicates time-frame used for count. Nuclei determined to be interphase (blue arrowhead), metaphase (yellow arrowheads, 2 SPBs paired on one nucleus, constant distance of 1 ± 0.2 µm), and anaphase (violet arrowhead, linearly segregating SPBs). Scale bar depicts 10 µm.

*Ag*Cdc14-yEGFP vs. *Ag*Pds1-mCherry dynamics

To generate the data presented in figure 30, cells harbouring *Ag*Pds1-mCherry and *Ag*Cdc14-yEGFP were imaged over 20-30 minutes on low fluorescent (ALF) TL-slides (due to weak *Ag*Pds1-mCherry signal), allowing for rare instances where mitotic events could be entirely followed through. For *Ag*Cdc14-yEGFP measurements, a minimal polygon shape was determined (example in figure 29, left panel) which would capture the entire area of the yEGFP signal without being altered in size during the course of the series (to be able to compare the different time points. The intensity of all pixels within this area was measured and the individual values sorted to form a histogramm of the data (figure 18). Going back to the raw images, intensity means were then calculated for sample areas within nucleolar foci (for core intensity of sequestered *Ag*Cdc14-yEGFP), within the nucleoplasm of anaphase nuclei (for intensity of released *Ag*Cdc14-yEGFP), and within the hyphae (for brightness of background fluorescence). In the example shown in figure 18, these values are 144, 128 and 104, respectively (blue dotted lines), and are used for the other timepoints later on. Based on these mean values, borders delimiting these catagories where defined. For example, all pixels with intensities over 138, were deemed to represent sequestered *Ag*Cdc14 (green markings), and could as such be counted. In this manner, numbers of pixels belonging to each category were determined for each time point, for each individual nucleus, and plotted against time. These resulting graphs could

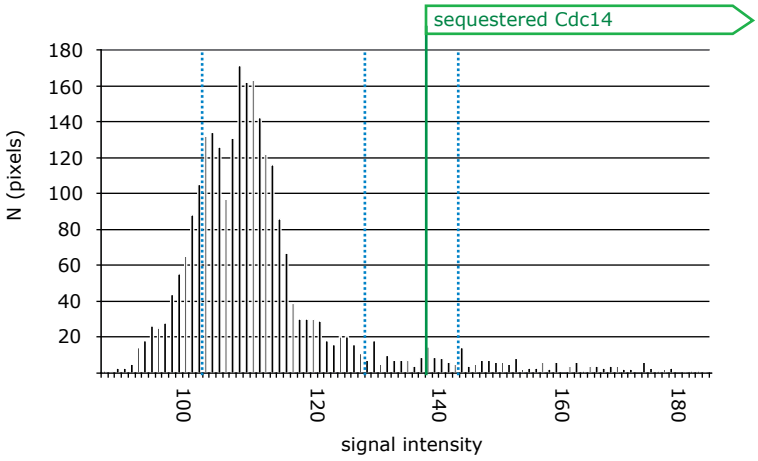

Figure 18: *Ag*Cdc14 vs *Ag*Pds1 measurements. Pixel intensity histogramm for one time point of one nucleus

then be combined on a common time axis and were scaled to correct for artefactual differences in signal intensities and boundary polygon shapes between experiments, leading to figure 30, “sequestered *Ag*Cdc14”. *Ag*Pds1-mCherry was treated in a analogous manner, but starting with a predefined 80 pixel large pseudo-circular area placed within the brightest part of the image, and without any classifications.

The entire set of *S. cerevisiae* genes involved in MEN is conserved in *A. gossypii*

Orthologs for all genes proposed to be involved in MEN signalling in *S. cerevisiae* were found to be annotated in the *A. gossypii* genome (Dietrich *et al.,* 2004). All orthologs are syntenic and computed amino acid identity values range between 19% for the SPB anchor (Lang *et al.,* 2010b) *Ag*Nud1 and 79% for *Ag*Cdc5 and *Ag*Dbf2/Dbf20 (table 2). Generally (and cautiously) speaking, many orthologs of core components of the MEN such as *Ag*Bub2, *Ag*Tem1, *Ag*Dbf2/Dbf20 or *Ag*Mob1 exhibited high identity scores of over 70%, whereas orthologs of peripheral network components such as *Ag*Kel1/Kel2, *Ag*Kin4/Frk1 had low identity values around 40%. Concerning notable differences in predicted Cdk phosphorylation motifs (which suggest a nuclear division cycle dependent role downstream of Cdk), *Ag*Cdc15 was shown to have 5 motifs less than *Sc*Cdc15, whereas *Ag*Dbf2/Dbf20, *Ag*Kel1/Kel2 and *Ag*Kin4/Frk1 all had significantly higher numbers of predicted Cdk consensus sequences than their *S. cerevisiae* orthologs.

All domains predicted for MEN component in *S. cerevisiae* were also predicted for the *A. gossypii* orthologs (figure 19), suggesting that principle molecular functions are conserved for these genes. Notably, no regions of particular high homology were calculated that do not overlap with domains of known function.

Localization patterns of MEN orthologs are analogous to *S. cerevisiae*

Given the sequence level conservation of the *S. cerevisiae* MEN pathway in *A. gossypii*, we were interested to see if functionality was also conserved. To study the aspect of localization, we constructed C-terminal yEGFP fusions for the putative GEF *Ag*Lte1 and GTPase *Ag*Tem1.

*Ag*Tem1-yEGFP was shown to localize to distinct foci reminiscent of *Ag*Tub4-YFP (figure 20), which is in agreement with the localization of *Sc*Tem1 to SPBs in *S. cerevisiae*. In time-lapse recordings of growing hyphae, by studying their movement for up to half an hour, we were able to identify *Ag*Tem1-yEGFP foci of dividing nuclei (yellow arrowhead) and follow them through the course of mitosis. We were interested to see if asymmetric, polar localization of *Ag*Tem1-yEGFP occurred at any stage of the nuclear division cycle, as is the case in *S. cerevisiae*. This was shown not to be the case (figure 20, B). *Ag*Tem1-yEGFP was distributed to both foci evenly, with no loss or gain of signal over time.

*Ag*Lte1-yEGFP also exhibited a localization pattern analogous to that of its *S. cerevisiae* ortholog. Observing young mycelia up to 20 h in age, we

***A. gossypii* ortholog**					***S. cerevisiae* 1st homolog**					***S. cerevisiae* 2nd homolog**		
common	systematic	aa	Cdk	synt.	systematic	aa	ID	null mutant	Cdk	common	systematic	aa
*Sc*BFA1	ACL090C	474	2	Y	YJR053W	574	34%	viable	1			
*Sc*BUB2	ADR131C	305	0	Y	YMR055C	306	76%	viable	0			
*Sc*CDC15	AER223C	903	2	Y	YAR019C	974	43%	lethal	7			
*Sc*CDC5	ACL006W	709	3	Y	YMR001C	705	79%	lethal	2			
*Sc*DBF2	ADR033W	578	5	Y	YGR092W	572	79%	double: lethal	2	*Sc*DBF20	YPR111W	564
*Sc*KEL1	ADL149W	1211	11	Y	YHR158C	1165	43%	double: viable	4	*Sc*KEL2	YGR238C	883
*Sc*KIN4	ACR119W	932	5	Y	YOR233W	865	38%	viable*	1	*Sc*FRK1	YPL141C	866
*Sc*LTE1	ACR292W	1439	7	Y	YAL024C	1435	46%	lethal at low t	9			
*Sc*MOB1	ADL236W	296	1	Y	YIL106W	314	72%	lethal	2			
*Sc*NUD1	ADR416W	757	1	Y	YOR373W	852	19%	lethal	1			
*Sc*TEM1	AER132W	233	0	Y	YML064C	245	72%	lethal	0			

Table 2: Homologs of MEN. aa: length in amino acids. Cdk: predicted number of Cdk phosphorylation motifs. *double deletion N/A

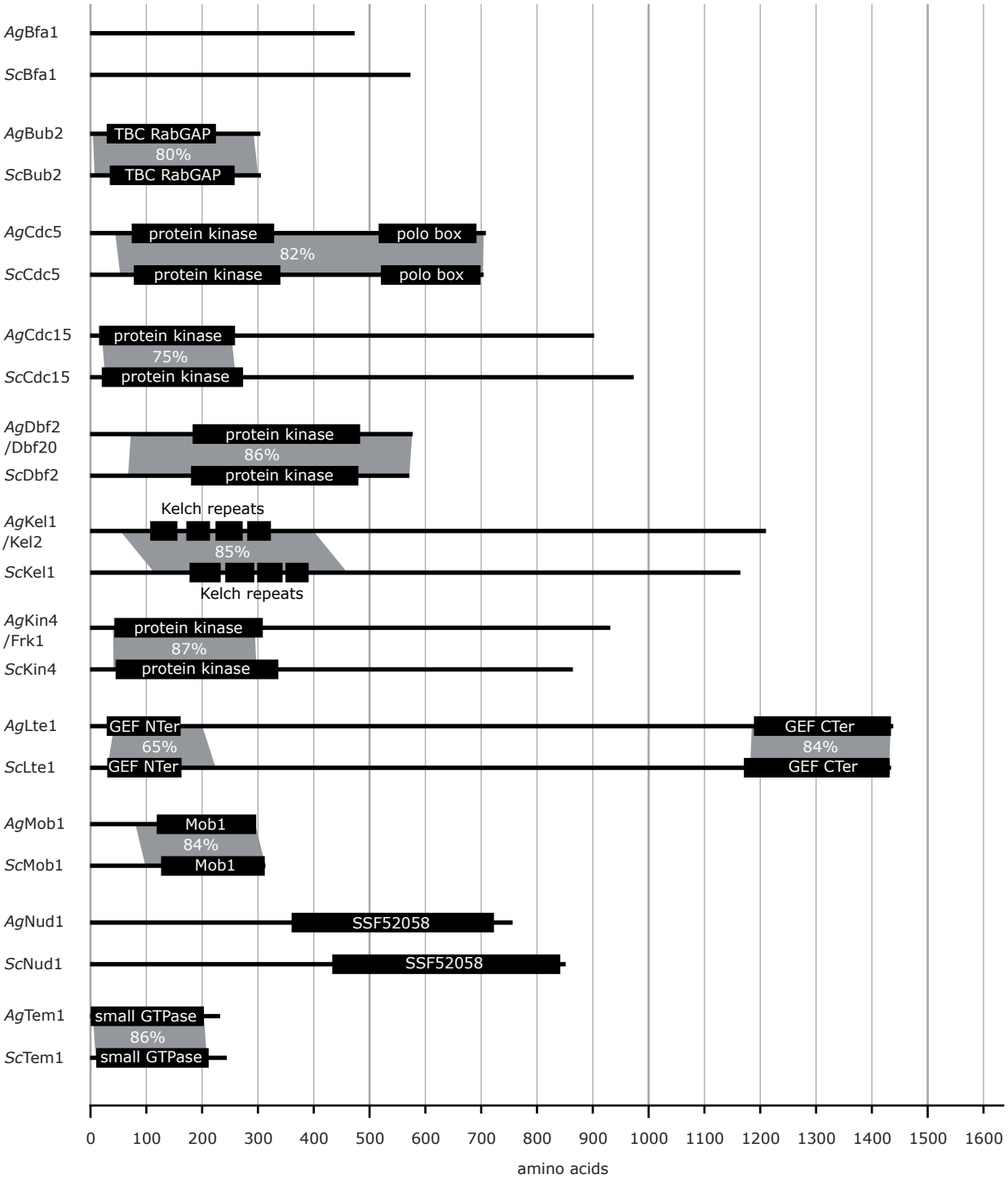

Figure 19: Sequence comparison of genes involved in MEN pathway. Grey areas indicate regions of high homology. Black bars depict all predicted domains and features. Higher identity homologs shown in case of twin genes. Second homologs depicted in supplemental figure 8.

could see a strong localization of *Ag*Lte1-yEGFP to the hyphal tip, with the signal strength declining towards the back, but sometimes still visible up to 10 mm from the tip (figure 21, A). The signal intensity was not the same at different branches of the same mycelium, sometimes missing entirely. In single-plane images, localization to the outer, cortical zone of the hyphal tip could be observed (figure 21, B).

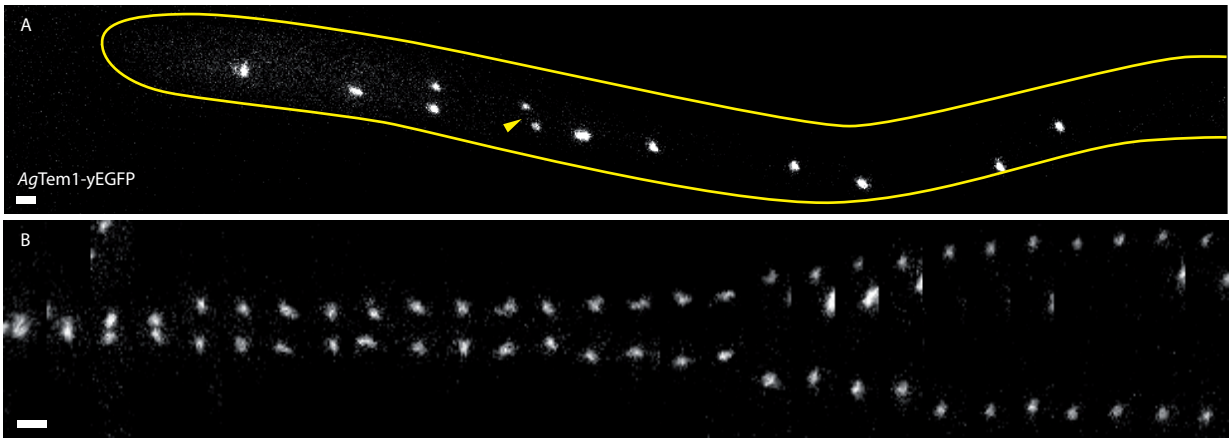

Figure 20: *Ag*Tem1 localization. (A) Still image from time-lapse series tracking *Ag*Tem1-yEGFP in growing hyphae. Arrowhead indicates nucleus chosen for montage. Projection of 11 Z-planes, 0.5 μm apart. Scale bar depicts 1 μm. (B) Montage of nucleus undergoing mitosis. 1 minute time interval. Scale bar depicts 1 μm.

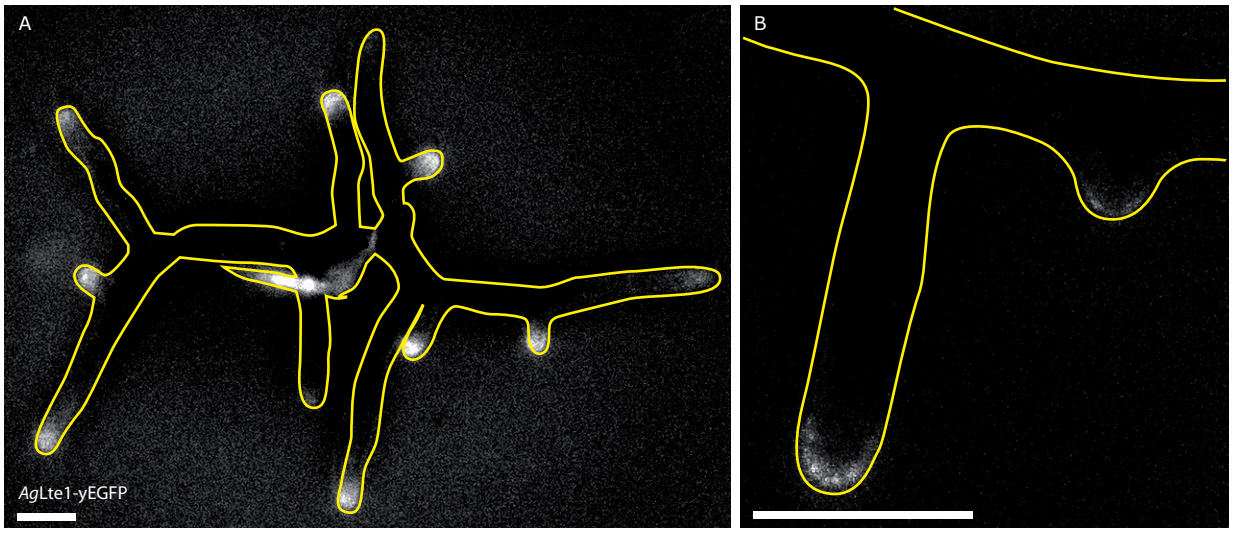

Figure 21: *Ag*Lte1 localization. (A) *Ag*Lte1-yEGFP in 20 hour old mycelium. Maximum intensity projection of 5 planes with Z-distance of 1 μm. Scale bar depicts 1 μm. (B) *Ag*Lte1-yEGFP in 22 hour old mycelium. Single plane. Scale bar depicts 1 μm.

MEN orthologs are not essential for growth but play a role in sporulation

Given the analogous localization patterns of *Ag*Lte1 and *Ag*Tem1 and the high sequence identity of MEN orthologs in general, an analogous cellular function of MEN components in *A. gossypii* is plausible. In order to clarify whether the *A. gossypii* orthologs of this pathway fulfill similar roles, we created single-gene deletions for putative core components and peripheral contributers *Ag*TEM1, *Ag*CDC15, *Ag*DBF2/DBF20, *Ag*MOB1, *Ag*LTE1, *Ag*KIN4/FRK1 and *Ag*KEL1/KEL2. Unexpectedly, viable, homokaryotic null mutants could be generated for all selected MEN related orthologs in *A. gossypii*. We then proceeded to conduct routine macroscopic growth assays. At the optimal growth temperature of 30°C, all strains exhibited radial growth speeds similar to wt, except *Agkin4/frk1*Δ and *Agkel1/kel2*Δ mutants, which (expressed as radial colony growth) grew approximately 10% slower (figure 22, A). Some mild growth impairments could be observed in all mutants at non-optimal temperatures, notably including an increased sensitivity to low temperatures in *Aglte1*Δ mycelia. Mycelial morphology at the edge of colonies was normal for all strains at 30°C, except for slight irregularities observed in *Agkin4/frk1*Δ mutants (figure 22, D). Circular areas of defined size (6 cm^2) were excised from the center of 6 day old colonies, and checked for spore content and weight of mycelium. The mutants *Agtem1*Δ, *Agcdc15*Δ,

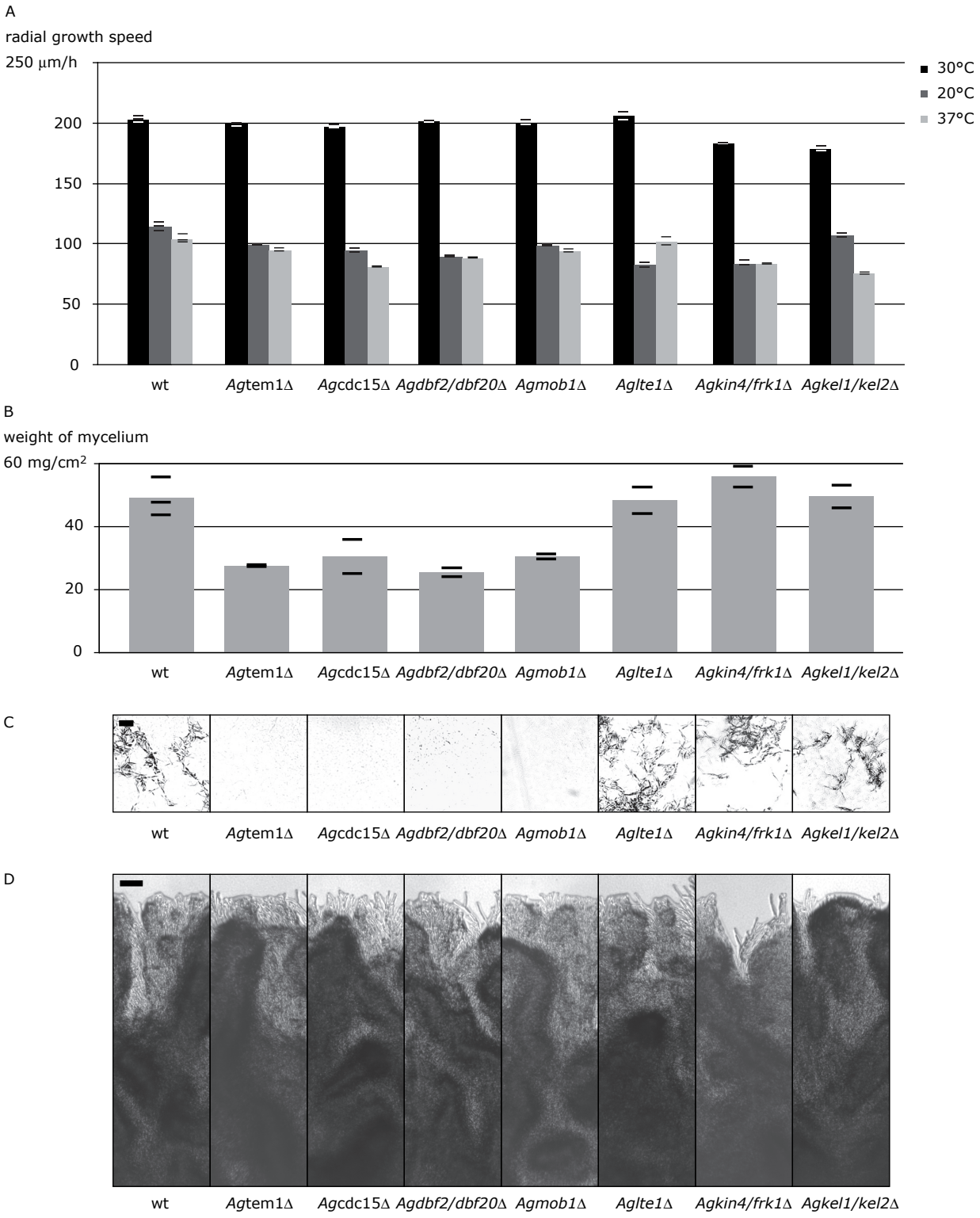

Figure 22: Macroscopic development of MEN mutants. (A) Radial growth speeds of mutants at 30°C, 20°C and 37°C after 5 days. Values represent the mean of 2 or 3 separate measurements done with individual strains, which are indicated by thin horizontal bars. (B) Weights of the inner 3 cm of mycelium taken for spore isolation from the growth assay plates. Mean values of 2 or 3 separate measurements, indicated by thin horizontal bars. (C) Samples taken from spore preparations of inner 3 cm of 6 day old colonies. Scale bar depicts 0.1 mm. (D) Edges of 6 day old colonies at 30°C. Scale bar depicts 0.1 mm.

*Agdbf2/dbf20*Δ and *Agmob1*Δ were shown to have severe sporulation deficiencies (figure 22, C). The same strains also accounted for less mass (figure 22, B) than wt, suggesting defects in later developmental stages. To gain understanding of these sporulation deficiencies, we transferred 1 day old mycelia to nutrient deprived liquid medium cultures in an attempt to trigger the sporulation programm at a young stage. Differences between wt and *Agtem1*Δ samples were observed within 48 hours of switching to low nutrients. Sporangia in mutant strains could not develop properly. This was likely caused by some defect in septation, as regular segmentation of bloating hyphae was not observed frequently in mutants (figure 23). The few spores observed to start forming after 72 hours in *Agtem1*Δ developed in non-compartmentalized sections of the hyphae (figure 23, B). These observations are in agreement to chitin stainings of *Agmob1*Δ mutant mycelia (using Calcofluor White), where well formed mature septa can only seldomly be seen (figure 24).

Effect of deletion of MEN orthologs in *A. gossypii* on anaphase nuclear dynamics

Because MEN null mutants such as *Sctem1*Δ in *S. cerevisiae* fail to exit mitosis and arrest with elongated spindles (Shirayama *et al.,* 1994), we measured anaphase dynamics of dividing nuclei in *Agtem1*Δ *Ag*H4-GFP hyphae by determining the diameter of the H4-GFP-signal in 1 minute intervals over the course of half an hour. No delay of events could be detected in *Agtem1*Δ mutants (figure 25, B), compared to wt (figure 25, A): Maximum spindle length (typically between 7 and 8 µm), duration of anaphase (typically 9 minutes) and time of spindle breakdown (indicated by independent oscillation movements of post-anaphase nuclei, typically around 15 minutes after onset of anaphase, but subject to variation) were all shown to be like wild-type.

The distribution of nuclei in growing hyphae upon deletion of putative MEN orthologs in *A. gossypii*

To aid in making assertions on mitotic activity in growing hyphae, we calculated the density of nuclei (*Ag*H4-yEGFP signals) in different regions which were defined by the distance from the growing tip. This spatial distinction arose from the assumption that mitotic activity may be affected in mutants dependent on the position within the hyphae, given the restricted localization of *Ag*Lte1-yEGFP to the foremost 10-15 µm of hyphal tips. Measurements showed a slight increase in distance between nuclei towards the backward regions of growing wild-type hyphae (figure 26). No significant differences to wild-type could be detected in *Agtem1*Δ or *Agdbf2/dbf20*Δ mutant strains. The overall average distance throughout all defined areas was calculated to be 4.47 ± 2.06 µm (1 SD, N = 193) for wild-type, 4.44 ± 2.82 µm (1 SD, N = 173) for *Agtem1*Δ and 4.58 ± 2.65 µm (1 SD, N = 199) for *Agdbf2/dbf20*Δ.

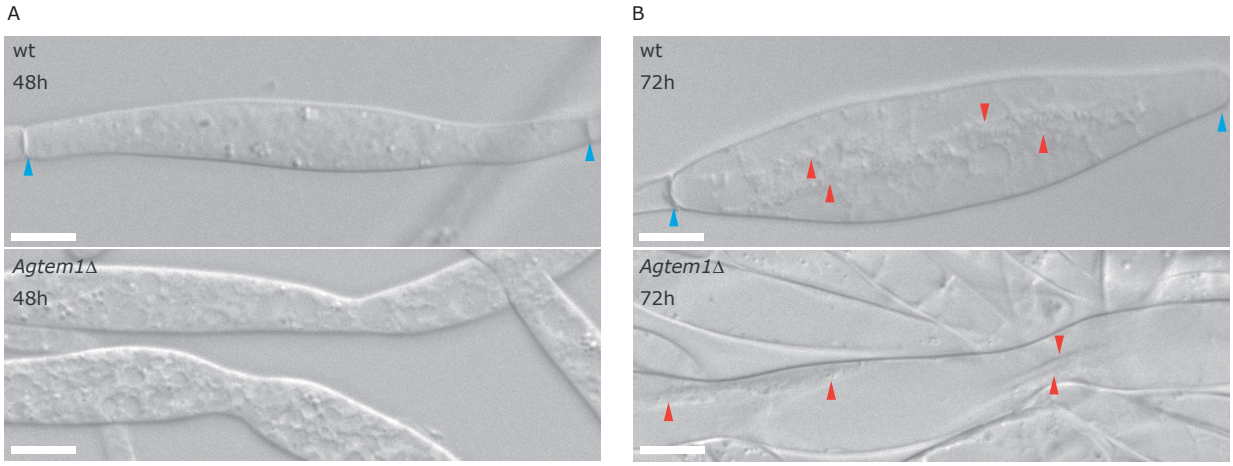

Figure 23: Sporangia and developing spores in *Agtem1*Δ. DIC images of hyphae after (A) 48 hours and (B) 72 hours in 1:4 diluted AFM liquid cultures. Blue arrowheads indicate mature septa. Red arrowhaeads indicate developing spores. Scale bars depict 10 µm.

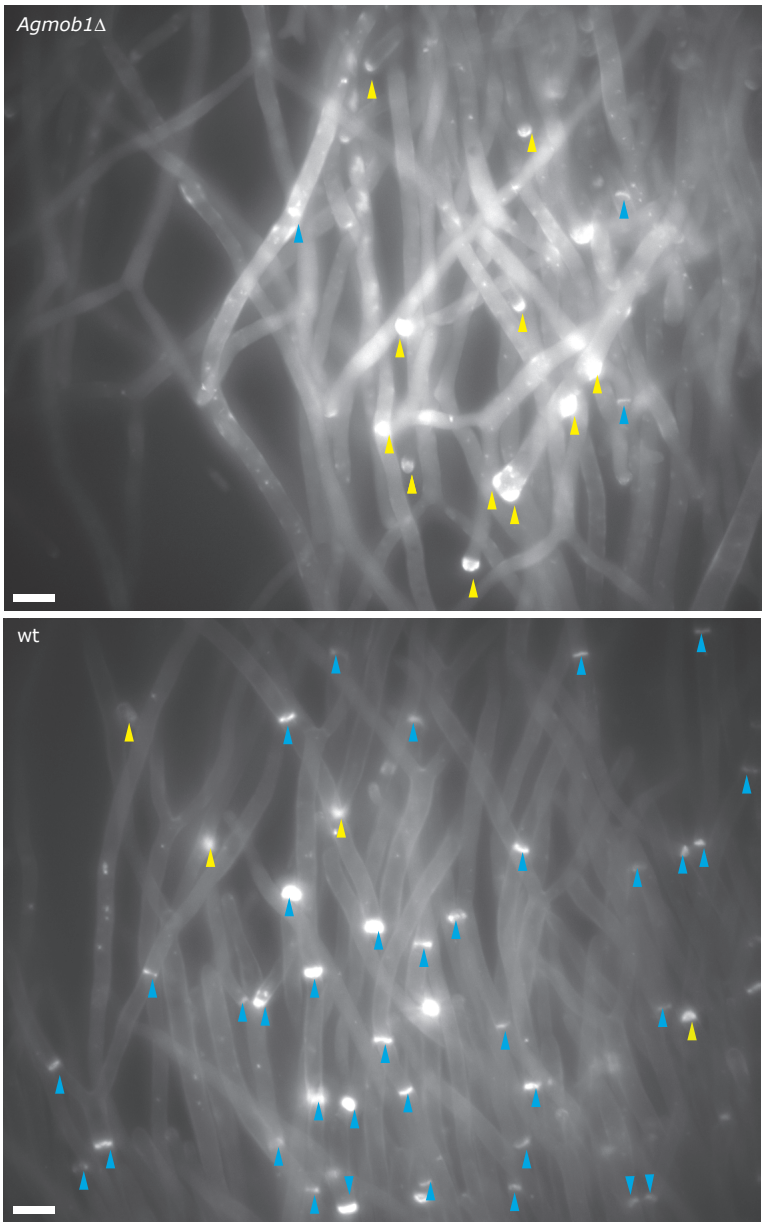

Figure 24: Septum staining in *Agmob1*Δ. Calcofluor White stainings visualizing chitin-harbouring septa in cells taken from o/n liquid AFM cultures inoculated with pieces of mycelium from edge of plate colonies. Chitin stains show at growing and emerging hyphal tips as well as at septa. Yellow arrowheads indicate chitin staining at polarized growth tip. Blue arrowheads indicate chitin staining at septa. Scale bar depicts 10 μm.

Quantifying nuclear division cycle stages in MEN ortholog mutants *Agtem1*Δ, *Agcdc15*Δ, *Agdbf2/dbf20*Δ and *Aglte1*Δ

Because nuclear density in the areas observed could potentially be maintained in cells with decreased mitotic frequency simply by distributing nuclei towards the front, a more detailed look at the mitotic cycle was necessary. We deleted *Ag*TEM1, *Ag*CDC15, *Ag*DBF2/DBF20 and *Ag*LTE1 in an *Ag*H4-GFP *Ag*Tub4-YFP background, so as to be able to differentiate whether individual nuclei were in interphase, metaphase or anaphase. We then inspected more than 300 nuclei for each strain, only taking into consideration fast growing hyphae which had recently undergone tipsplitting (detailed description of experiment in materials and methods section). In the wt reference strain, we found 86.6% interphase, 11.7% metaphase and 1.7% anaphase nuclei. Although these numbers are similar to results obtained for wild-type in similar experimental setups (Helfer and Gladfelter, 2006: 80%, 16% and 3%; Claudia Lang, doctoral thesis: 92%, 6% and 2%), the method may not detect all anaphase nuclei, mistaking them for interphase nuclei due to nuclear bypassing and crowded hyphae. MEN ortholog mutants *Agtem1*Δ, *Agcdc15*Δ, *Agdbf2/dbf20*Δ were shown to have increased fractions of metaphase

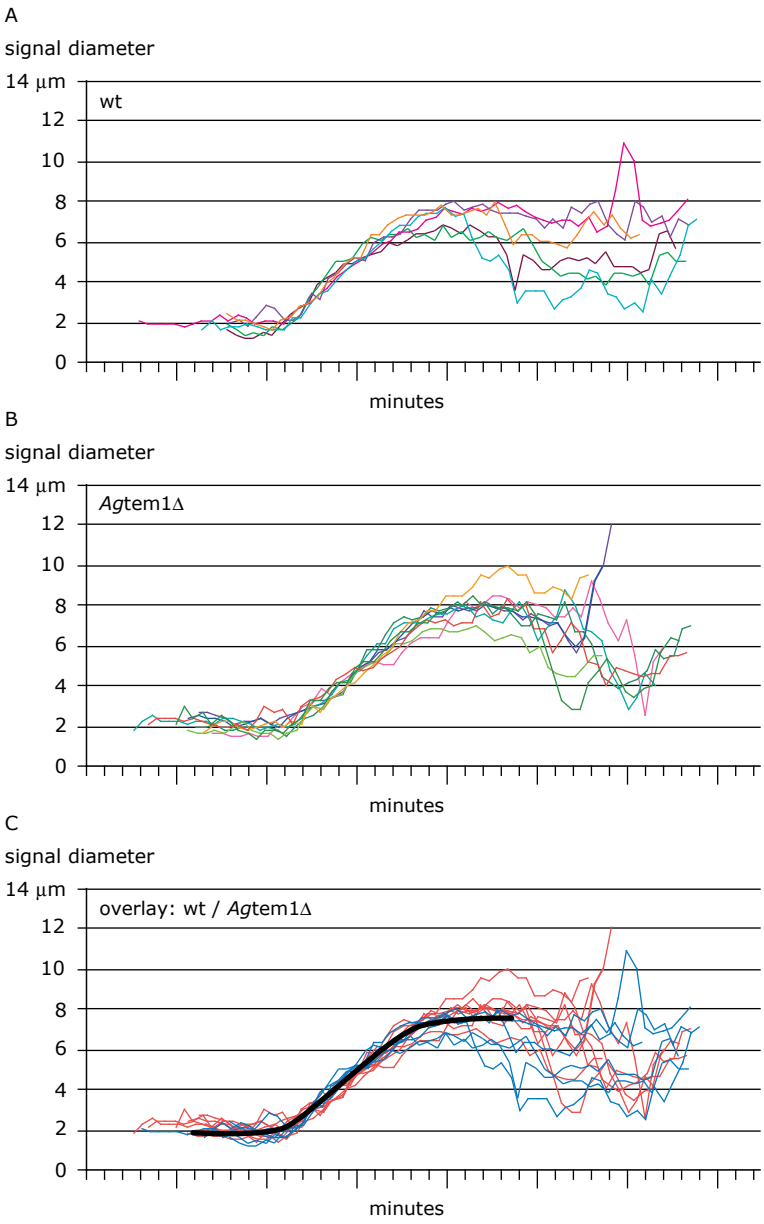

Figure 25: Anaphase dynamics in *Agtem1*Δ mutant. Overlay of multiple measurements of *Ag*H4-GFP signal diameter of mitotic nuclei in wild-type reference strain (*Ag*H4-GFP) (A) and *Agtem1*Δ (B) hyphae. Overlay achieved by translation along x-axis (synchronization of data, no scaling adjustments). (C) Overlay of wt (blue) and *Agtem1*Δ (red) measurements. Visual approximation of typical anaphase event provided by black curve.

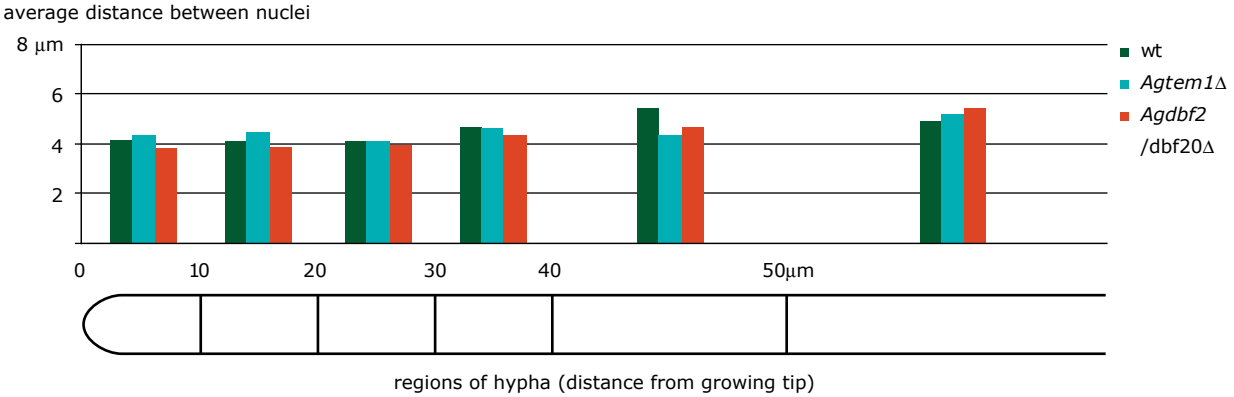

Figure 26: Distribution of nuclei in MEN mutants. Mean distances between nuclei in defined regions of hyphae (illustrated below) in wild-type reference strain (*Ag*H4-GFP) and MEN mutants.

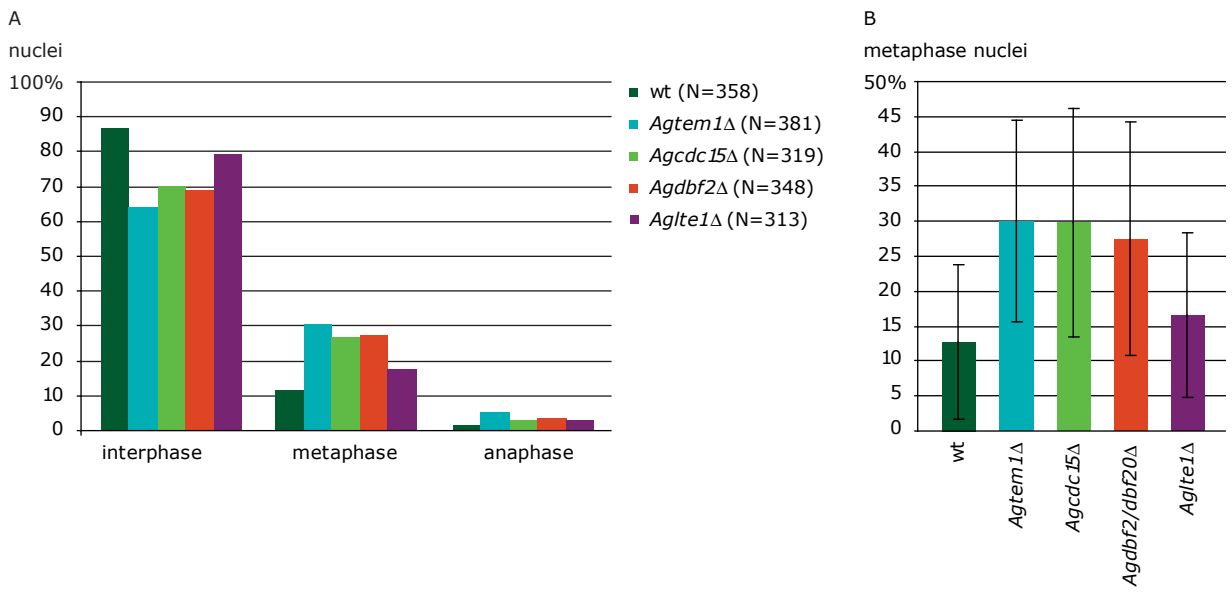

Figure 27: Occurence of metaphase nuclei in MEN mutants. (A) Percentages of total counted nuclei found to be in different nuclear division cycle stages in wild-type reference strain (*Ag*H4-GFP *Ag*Tub4-YFP) and MEN mutants. (B) Percentages of nuclei within individual hyphae found to be in metaphase. Error bars represent one standard deviation.

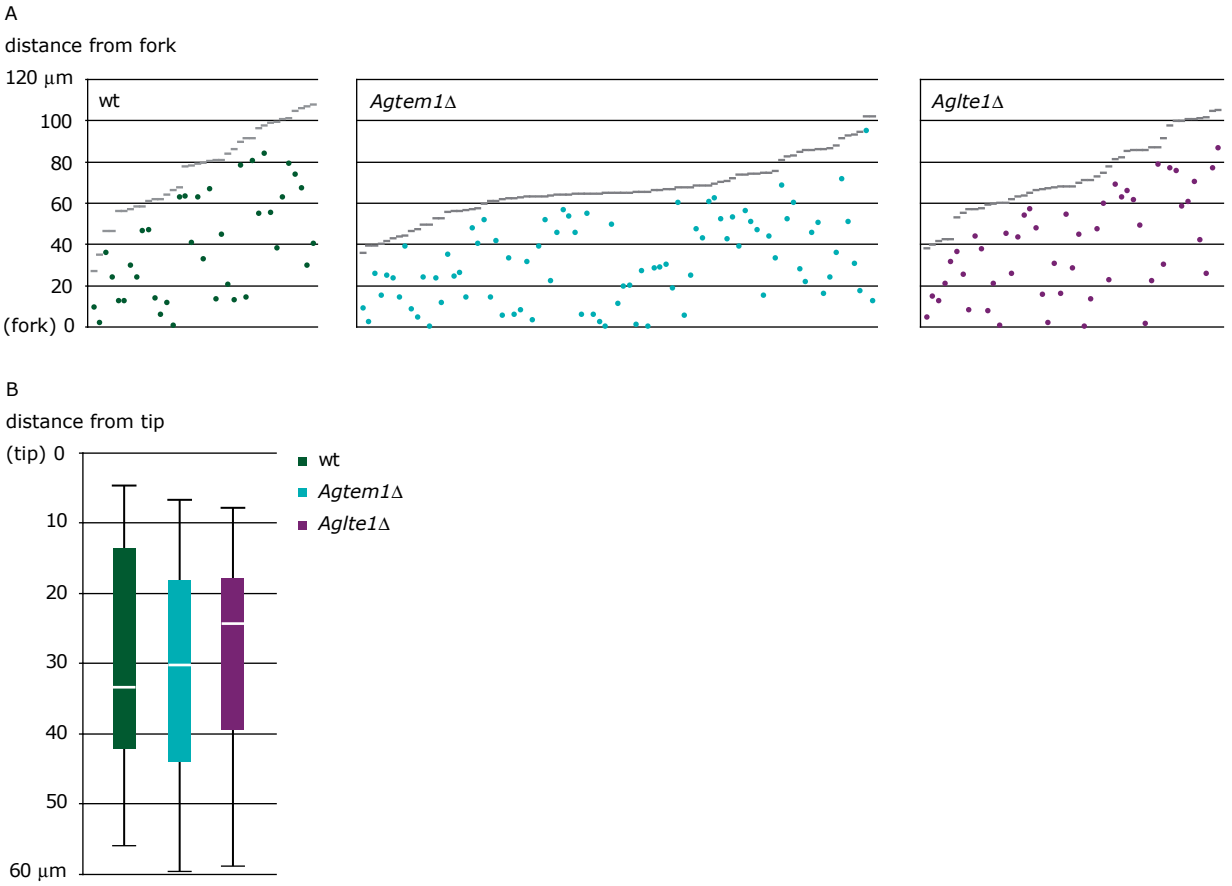

Figure 28: Positional distribution of metaphase nuclei within hyphae. (A) Distance of individual identified metaphase nuclei from the tip-splitting fork site in wild-type reference strain (*Ag*H4-GFP *Ag*Tub4-YFP) and MEN mutants. Dots represent metaphase nuclei, grey horizontal lines represent the tip of the hypha. Measurements are sorted along the x-axis by length of hyphae after the fork site. (B) Mean distance of metaphase nuclei from the hyphal tip in wild-type reference strain (*Ag*H4-GFP *Ag*Tub4-YFP) and MEN mutants. Whisker plot depicts 25th percentiles.

nuclei of approximately 27-30% (Figure 27, A). In *Aglte1*Δ cells, 17% of nuclei were found to be in metaphase. In order to demonstrate the large variation observed within strains, we also made separate percentage calculations for each individual hypha (as opposed to pooling all nuclei and calculating the overall mean), and then calculated the mean and SD from these values. In the resulting representation (figure 27, B), the mild enrichment of metaphase nuclei observed in the *Aglte1*Δ strain (17% versus 11.7% in wild-type) is almost reduced to wild-type values by this alternative form of data processing.

Spatial occurence of metaphase nuclei in *Agtem1*Δ

To investigate the possibility of a spatial dependence of these observations, we measured the position of nuclei identified as being in metaphase in selected mutants, relative to the hyphal tip and the fork site. We plotted these coordinates, but could not recognize any pattern. Occurence of metaphase nuclei was seemingly well dispersed and not found to be enriched in any defined area in wildtype, *Agtem1*Δ, *or Aglte1*Δ (Figure 28, A). No significant increase or decrease of metaphase nuclei was detected towards the hyphal tip in any of the strains, including *Aglte1*Δ, nor was there a detectable enrichment around the fork site, where septa are laid down in fast growing hyphae (Kaufmann and Philippsen, 2009), and entry into mitosis is therefore expected to be stimulated (Helfer and Gladfelter, 2006). These findings were also made apparent in whisker plots of the same data, representing distances of metaphase nuclei from the growing tip (Figure 28, B): Distribution of metaphase nuclei from tip of the cell is very similar between wild-type, *Agtem1*Δ, and *Aglte1*Δ.

*Ag*Cdc14 release dynamics in *Agcdc15*Δ mutants

Given that an immediate consequence of MEN signalling in *S. cerevisiae* is sustained release of *Sc*Cdc14 during later stages of anaphase, experiments were conducted to clarify the role of the *A. gossypii* orthologs in localization patterns of *Ag*Cdc14. To be able to detect minor changes in release dynamics, we introduced *Ag*Pds1-mCherry into our *Ag*Cdc14-GFP background strain. *Sc*Pds1, or securin, is an inhibitor of separase and is degraded in an APC-dependent manner, triggering the onset of anaphase (Cohen-Fix *et al*., 1996). The intention of including this marker was to provide an additional visual cue (the disappearence of *Ag*Pds1-Cherry) for the metaphase/anaphase transition as a temporal reference to base the timings of our observations of *Ag*Cdc14-yEGFP on. Isolated *Ag*Pds1-Cherry *Ag*Cdc14-GFP homokaryotic strains were viable and thus deemed functional. The ORF of *Ag*CDC15 was deleted in this strain, and time-lapse image series of both mCherry and GFP signals were acquired (Figure 29). *Ag*Cdc14 dynamics were shown to be very similar to what was observed in wild-type. Seemingly coincidental with the first signs of *Ag*Pds1 degradation, *Ag*Cdc14 would start to become visible at the SPBs, indicating initial release from the nucleolus. Around the time *Ag*Pds1 reached baseline levels, *Ag*Cdc14 release was to full extent. No return of *Ag*Pds1 could be made out in post-mitotic nuclei, where *Ag*Cdc14 was resequestered in the nucleoli. In order to provide quantitative data to these anecdotal observations, we measured various features of these dividing nuclei (full description in materials and methods): To quantify sequestered Cdc14, we calculated the number of high intensity yEGFP-channel pixels within fixed mitotic areas (figure 29, yellow polygonal shape in left column). For *Ag*Pds1 levels, we measued mCherry signals at the center of nuclei (figure 29, circular area in middle column). We also measured elongation of the mitotic spindle using the SPB signal of *Ag*Cdc14 which was always visible for the entire duration of anaphase. The measurements, although quite noisy (which was countered by overlaying the data), confirmed our prior observations (Figure 30). No significant differences were found between *Agcdc15*Δ and wild-type nuclei concerning the timing and sequence of such events as *Ag*Pds1 degradation, *Ag*Cdc14 release, spindle elongation or *Ag*Cdc14 resequestration.

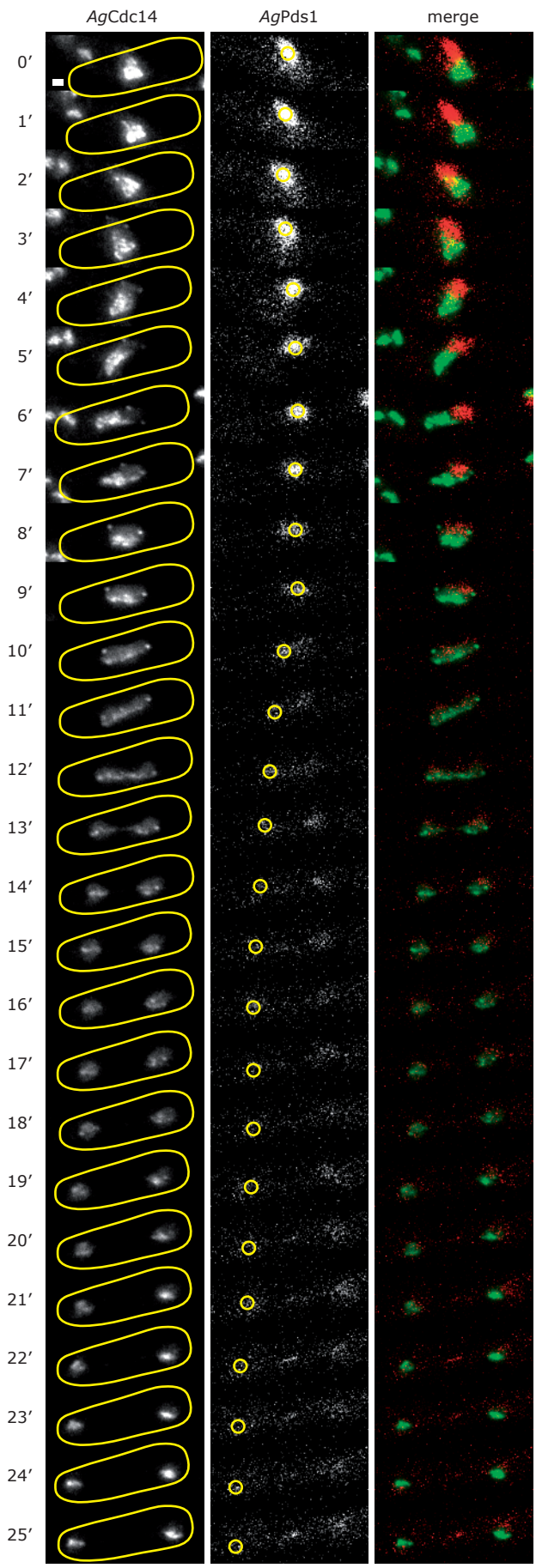

Figure 29: *Ag*Pds1 as a visual marker for initiation of anaphase. Time-lapse series of *Agcdc15*Δ *Ag*Cdc14-GFP *Ag*Pds1-mCherry nucleus undergoing mitosis. Yellow polygons demonstrate areas measured to generate data shown in next figure. 1 minute time interval. Scale bar depicts 1 μm.

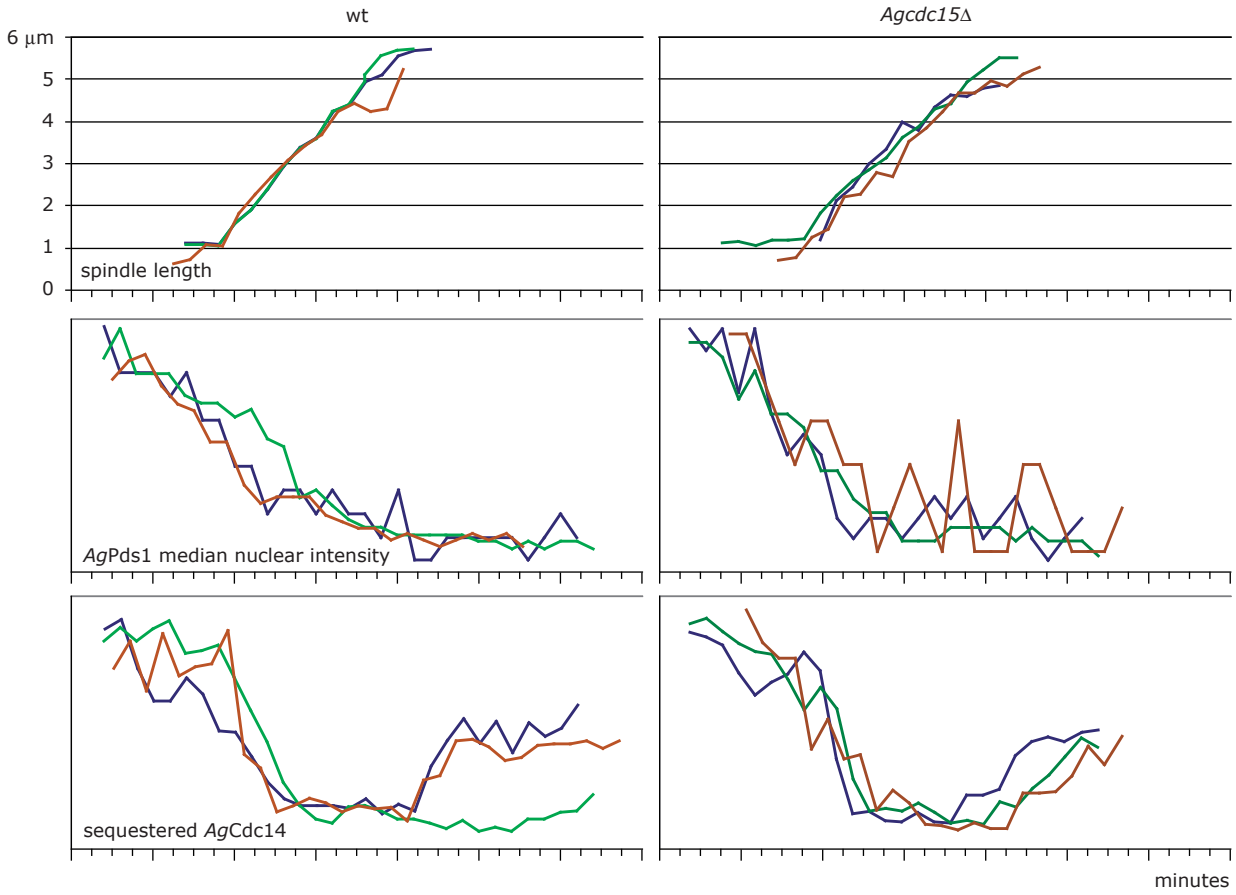

Figure 30: Dynamics of *Ag*Cdc14 release in *Agcdc15*Δ mutant. Measurement details in materials and methods section. Different colors indicate individual experiments. Overlay of measurements by translation along x-axis (synchronisation of data between experiments) and scaling along y-axis (mapping to comparable ranges). Spindle lengths (top panel) were not scaled vertically so units (μm) were retained. Other (signal intensity) measurements in arbitrary units due to scaling.

Discussion

On the amino acid level, *A. gossypii* carries the entire set of genes constituting the MEN in *S. cerevisiae*. High sequence identity values calculated for most core components of the signalling cascade and the identification of all predicted functional domains both speak in favor of a conserved role within the hyphae of *A. gossypii*.

This perception is enforced by the similarities in localization patterns observed for *Ag*Tem1 (at the SPBs) and *Ag*Lte1 (at the hyphal cortex). However, important differences exist. Notably, *Ag*Tem1 localizes to *both* SPBs of dividing nuclei, with no signs of signal fluctuation during the course of the nuclear division cycle. The assymmetrical pattern seen in *S. cerevisiae*, with *Sc*Tem1 localizing to the dSPB has been the subject of recent studies. Consequences of targeting *Sc*Tem1 to both SPBs could not be detected (Fraschini *et al*., 2006). The localization of *Sc*Tem1 is determined by the *Sc*Bfa1-*Sc*Bub2 complex (Pereira *et al*., 2000; Monje-Casas and Amon, 2009). *Sc*Bfa1-*Sc*Bub2 on the other hand seems to depend upon factors such as formins (Monje-Casas and Amon, 2009) and even *Sc*Lte1, which was shown to be crucial for correct polarity cap position (Geymonat *et al*., 2009). This suggests that the contribution of *Sc*Lte1 to mitotic exit may stem from its role in cell polarization. In this light, the localizations observed in *A. gossypii* could be interpreted as follows: *Ag*Lte1 likely plays a role in cell polarity, however it appears that this polarity cannot and is not inherited to the nuclei. The gradient observed, determining the anterior part of the hypha, is probably of to large a scale to be able to reliably differentiate between opposite SPBs of a highly motile, dividing nucleus. The symmetry of *Ag*Tem1 localization does not necessarily exclude a role of the protein in nuclear cycle regulation, however it does suggest that such a control system involving *Ag*Tem1 would likely function completely oblivious to the polarity of the cell, the sensing of which is seen as a defining feature of the MEN in *S. cerevisiae*.

The discovery that deletion mutants of MEN homologs in *A. gossypii* are viable and grow at wt-like speeds on plates is in strong contrast to the situation in budding yeast, where MEN signalling is essential for viability. The deficiencies of these mutants in spore production hint at a conserved role in sporulation and it is tempting to make a connection to the role of the MEN in spore formation in budding yeast. There, MEN components have been shown to play a role in and disassembly of meiosis II spindles, most likely by maintenance and shuttling of *Sc*Cdc14 release similar to mitosis. Furthermore, *Sc*Cdc15 is crucial for normal prospore membrane formation and nuclear capture (Pablo-Hernando *et al*., 2007). These events are initiated at the SPBs. It therefore plausible that the reduction in numbers of spores observed in the *A. gossypii* MEN homolog mutants could be traced back to developmental malfunctions such as flawed spore wall nucleation. However the few spores produced all had normal morphology, suggesting that spore development per se was unaffected, and that more likely the initiation of sporulation itself was disturbed. Looking at maturating hyphae, it became evident that the morphology of sporangia themselves were abnormal, with septation impaired. MEN components have been shown to localize to the bud neck and, more specifically, *Sc*Tem1, *Sc*Cdc15, *Sc*Dbf20 and *Sc*Dbf2 have been shown to be important for cytokinesis and controlling the re-polarization of the actin cytoskeleton (Corbett *et al.,* 2006). Sporulation deficiencies have also been observed in mutants of septation factors (Kaufmann, PhD thesis). What also stood out was the same common sporulation phenotype across all *Agtem1*Δ, *Agcdc15*Δ, *Agdbf2/dbf20*Δ and *Agmob1*Δ strains. This can be understood as an indication that the core signalling cascade as described in yeast may be intact in *A. gossypii*.

The investigation of the nuclei in *A. gossypii* MEN homolog mutants revealed great differences compared to MEN mutants in *S. cerevisiae*. Wild-type-like anaphase dynamics and timing of spindle breakdown in our mutant strains suggest a major deviation from the role established in budding yeast. Apparently, MEN homologs play no part in orchestrating the final steps in mitosis. Also, judging by nuclear density along the hyphae, no effect on

the nuclear division cycle as a whole could be made out either: wild-type values for nuclear density, combined with perfectly healthy growth speeds suggest that overall frequency of mitosis in these mutants is unperturbed. However, upon a more detailed look at different nuclear division cycle stages, a partial arrest in metaphase was discovered in the *Agtem1*Δ, *Agcdc15*Δ, *Agdbf2/dbf20*Δ and *Agmob1*Δ strains (once again suggesting that the core kinase cascade of the pathway is conserved). This is insofar surprising as it suggests a crucial role of these MEN signalling cascade homologs prior to anaphase. What could this function be? A healthy guess, at least timing-wise, would be triggering the degradation of *Ag*Pds1, an anaphase inhibitor (Gladfelter *et al.,* 2007). On the inside of the *S. cerevisiae* nucleus, the so-called spindle checkpoint inhibits the degradation of *Sc*Pds1 by complexing *Sc*Cdc20 until kinetochores are properly attached to MTs. Perhaps a similar system exists in *A. gossypii* involving MEN homologs ensuring the proper attachment of cMTs to the outer plaque of mitotic SPBs?

Or perhaps the MEN homologs directly mediate cytoplasmic pulling forces and the metaphase delay in mutants simply reflects the inability to efficiently elongate the mitotic spindle by internal forces only. In any case, the effect observed was not dependent on position of the nucleus within the hypha, meaning that the MEN homologs in *A. gossypii* do not help promoting (or allowing) mitosis close to growing tips for example. Anyhow, due to the observed timing of events (with *Ag*Cdc14 only fully released during anaphase) it seems unlikely that the MEN homologs would execute such a function via the *Ag*Cdc14 phosphatase.

What was further made evident in this experiment was the ability of nuclei to correct for prolonged metaphase by reducing the time spent in interphase. Apparently there is a regulatory system in place adjusting the frequency of mitosis in order to maintain an ideal density of nuclei in a variety of circumstances. This likely comes in handy throughout different stages of the life cycle of *A. gossypii*, when cells have to adapt to altering growth speeds and morphology as well as fractioning of the nuclear population by branching and tip-splitting. The simplest thinkable mechanism would be an instable factor diffusing from nuclei which can inhibit cell cycle progression of neighbouring nuclei.

Importantly, no role in *Ag*Cdc14 release could be detected for the MEN homolog *Ag*Cdc15. This further minimizes the possibility that the partial metaphase arrest observed in MEN homolog mutants is mediated via downstream *Ag*Cdc14, and likely marks a decoupling of the conserved signalling cascade from this important regulatory function first described in budding yeast. This does not rule out a regulatory function towards cytoplasmic *Ag*Cdc14.

This experiment also provided further important information on the nature of the partial metaphase seen in MEN homolog mutants in terms of time of action. The function involved in this arrest clearly precedes *Ag*Pds1 degradation, because no delay in spindle elongation was observed in nuclei where *Ag*Pds1 degradation was successfully triggered, when comparing our mutant to wild-type.

Having gathered evidence against a role of MEN homologs in *Ag*Cdc14 release, it will be interesting to see how the remaining system has adapted, or more precisely, what part FEAR homologs play in this important step of the nuclear division cycle.

CHAPTER III

CHAPTER III: FEAR HOMOLOGS IN *ASHBYA GOSSYPII*

Introduction

The discovery that MEN homologs in *A. gossypii* do not contribute to *Ag*Cdc14 release or M-phase to G1 transition raises the question whether the entire underlying regulatory machinery known from *S. cerevisiae* is uncoupled from these tasks, or if control over *Ag*Cdc14 activation has been bestowed upon a network made up of homologs of the FEAR pathway. Latter is certainly an exciting possibility in the light of the predictions discussed previously (Bosl and Li, 2005), however the need for the entire pathway as described for budding yeast is not completely self-evident in a multinucleate environment.

This chapter discusses investigations into the necessity of FEAR orthologs for successful progression through the nuclear division cycle in *A. gossypii*. As in the previous chapter, special attention is given to effects of mutations of the system on mitotic behaviour and *Ag*Cdc14 release. One possible consequence of the lack of contribution of MEN homologs to *Ag*Cdc14 release may be a detectable lack of robustness towards disruption of the putative FEAR regulatory pathway. If FEAR homologs were indeed discovered to play a role in *Ag*Cdc14 release, then such a decrease in functional redundancy may manifest itself in reduced viability of FEAR homolog deletion mutants, compared to *S. cerevisiae* counterparts. In budding yeast, deletion mutants of the FEAR pathway are all viable, with the exception of separase, and in synchronized experimental setups deletion or over-expression mutants will display temporal shifts in events such as *Sc*Cdc14 release (figure 31) or *Sc*Clb2-Cdk downregulation.

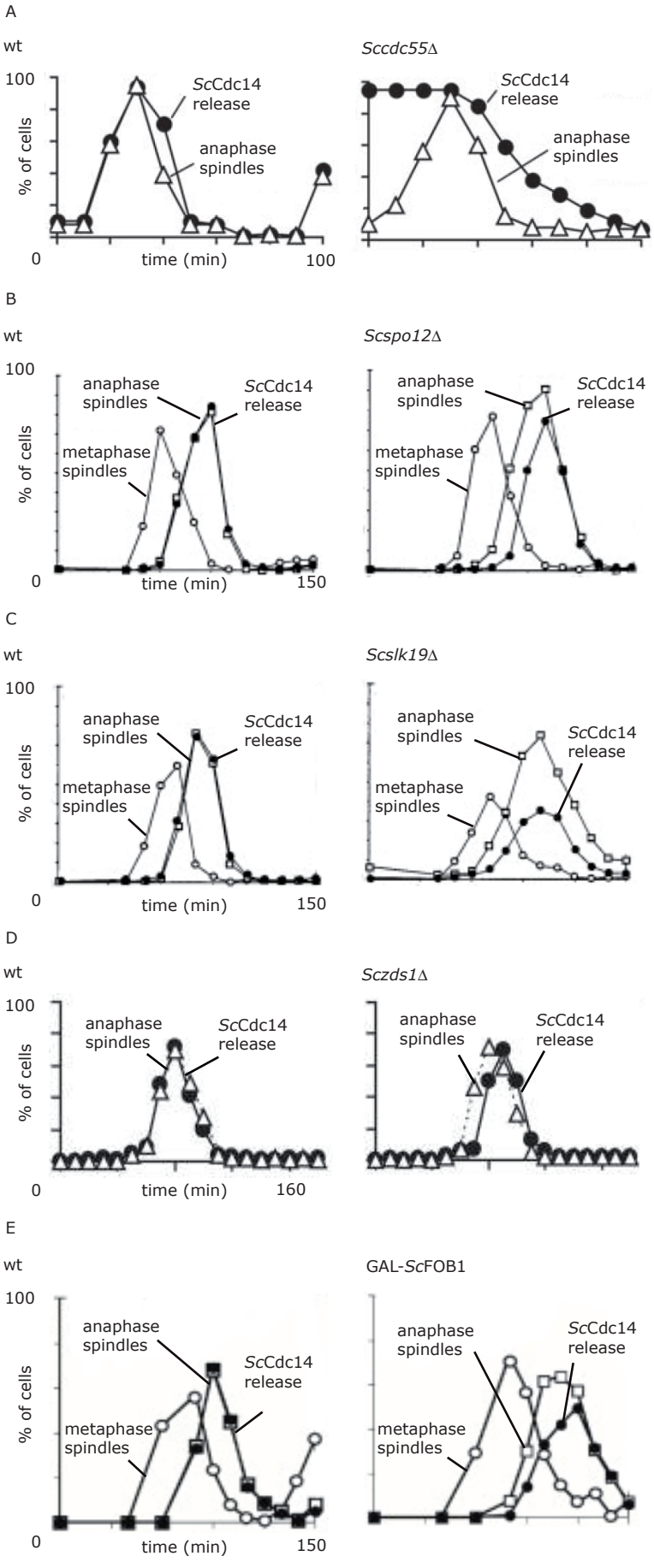

Figure 31: FEAR phenotypes. (A) Premature release of *Sc*Cdc14 in synchronized *Sccdc55*Δ cells (adapted from Queralt *et al.*, 2006). (B) Delayed release of *Sc*Cdc14 in pheromone synchronized *Scmad1*Δ *Scspo12*Δ cells (adapted from Stegmeier *et al.*, 2002). (C) Delayed and reduced release of *Sc*Cdc14 in pheromone synchronized *Scmad1*Δ *Scslk19*Δ cells (adapted from Stegmeier *et al.*, 2002). (D) Delayed release of *Sc*Cdc14 in pheromone synchronized *Sczds1*Δ cells (adapted from Queralt and Uhlmann, 2008). (E) Delayed release of *Sc*Cdc14 in pheromone synchronized, galactose induced *Scmad1*Δ GAL1-*Sc*FOB1 cells (adapted from Stegmeier *et al*., 2004).

Materials and Methods

General

A. gossypii media, growth conditions, transformation, bioinformatic analysis, microscopy, measurements and strain verifications are as described in the previous chapters. All plasmids and strains used are listed in supplemental tables 5 and 6.

Conservation of *S. cerevisiae* FEAR genes in *A. gossypii*

All budding yeast genes described in literature to be somehow involved in FEAR signalling were identified as annotated, syntenic ORFs in the *A. gossypii* genome (table 3). Relatively low amino acid sequence identity values (<=50%) were calculated for all *A. gossypii* FEAR orthologs, except for the putative subunits of the PP2A phosphatase complex (*Ag*CDC55, *Ag*PPH21/PPH22 and *Ag*TPD3), which had IDs ranging from 78% to 86%. The number of predicted Cdk phosphorylation motifs predicted was in only roughly within the same range for homologs, with the most notable difference being in *Ag*SLK19 (6 motifs in *A. gossypii* versus 3 in *S. cerevisiae*)

In a more detailed look at the amino acid sequence, we found all domains predicted for the *S. cerevisiae* genes to be predicted for the *A. gossypii* orthologs as well (figure 32). Such a high degree of homology however was not restricted to predicted domains. Within *Ag*Fob1 and *Ag*Slk19 for example, there were found to be highly conserved stretches located outside of identified domains, likely representing domains of yet to be clarified function themselves.

Effect of *Ag*CDC55 deletion on *Ag*Cdc14 sequestration and growth in *A. gossypii*

Given the apparent lack of function of MEN orthologs in *Ag*Cdc14 regulation in *A. gossypii*, we were curious to see to what extent FEAR orthologs play a role in this crucial task and set out to create a complete deletion collection of all orthologs of proposed FEAR network components. In a preliminary study, it could be shown that the putatitive FEAR ortholog *Ag*Cdc55 was essential for the viablity of young mycelia, as *Agcdc55*Δ mutants ceased growth, showed swelling and then lysed after approximately 24 hours (Valentin Tilloy, summer internship, supplemental figure 3). We then carried out the deletion of the *Ag*CDC55 ORF in a *Ag*Cdc14-yEGFP background strain and assessed GFP localization prior to lysis of the cells. In *Agcdc55*Δ, the *Ag*Cdc14-yEGFP localization pattern was at all times and in all nuclei reminiscent of the unsequestered signals we observed for anaphase nuclei in wild-type: The fusion protein exhibited a low intensity signal in what appears to be the nucleoplasm and bright foci at what we assume to be the SPBs (figure 33, A). Thus it seems that *Ag*Cdc14-yEGFP is constantly in a released state in these mutants.

Judging by the *Ag*Cdc14-yEGFP signals, the number of nuclei is strongly reduced in these mutants, compared to wild-type cells. Of all nuclei

***A. gossypii* ortholog**					***S. cerevisiae* 1st homolog**					***S. cerevisiae* 2nd homolog**		
common	systematic	aa	Cdk	synt.	systematic	aa	ID	null mutant	Cdk	common	systematic	aa
*Sc*CDC55	AFR195W	455	1	Y	YGL190C	526	78%	viable	1			
*Sc*ESP1	AAR089C	1618	0	Y	YGR098C	1631	50%	lethal	2			
*Sc*FOB1	AGR086C	534	1	Y	YDR110W	567	39%	viable	0			
*Sc*PDS1	AGR083W	295	1	Y	YDR113C	374	32%	lethal	3			
*Sc*PPH21	ADR099C	362	1	Y	YDL134C	370	89%	double: viable	1	*Sc*PPH22	YDL188C	378
*Sc*SLK19	AGR229W	705	6	Y	YOR195W	822	24%	viable	3			
*Sc*SPO12	ADL140C	63	0	Y	YHR152W	174	25%	double: viable	0	*Sc*BNS1	YGR230W	137
*Sc*TPD3	ACR279C	603	0	Y	YAL016W	636	78%	viable	0			
*Sc*ZDS1	AAL185W	1018	5	Y	YMR273C	916	34%	double: viable	3	*Sc*ZDS2	YML109W	943

Table 3: Homologs of FEAR pathway. aa: length in amino acids. Motifs: predicted number of Cdk phosphorylation motifs. Null: null mutant phenotype.

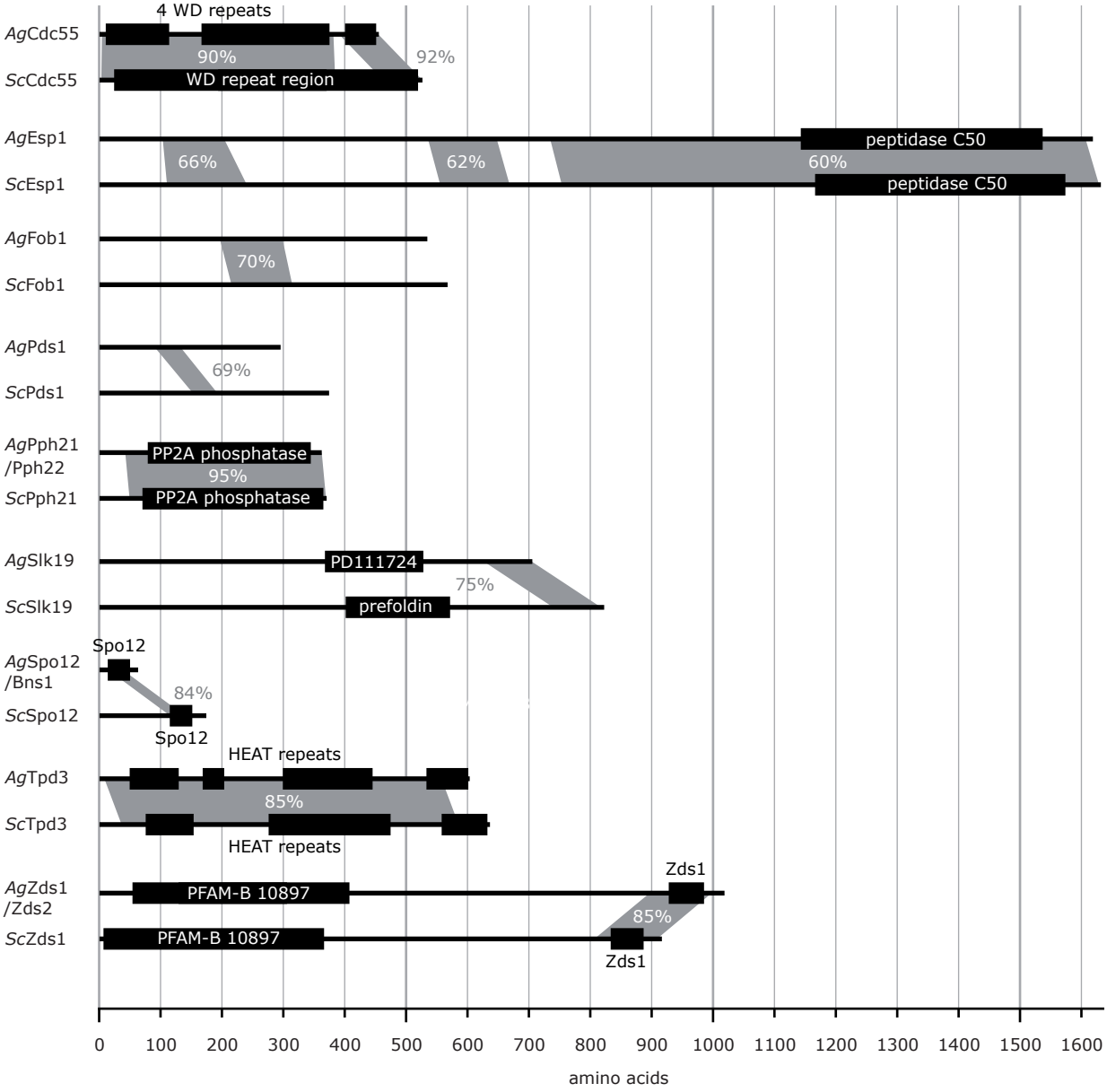

Figure 32: Sequence comparison of genes involved in FEAR pathway. Grey areas indicate regions of high homology. Black bars depict all predicted domains and features. Higher identity homologs shown in case of twin genes. Second homologs depicted in supplemental figure 8.

observed, almost all appeared to be in interphase, and only one instance of mitosis was captured by imaging (figure 33, B). In this incidence, it seemed that anaphase spindle elongation was not affected (in terms of duration and attained length), although it was not clear, due to lack of movement, if the nuclei could properly separate after maximum elongation was reached. Quite often, nuclei were observed that had remained connected by a continuous nucleoplasm, visible as a faint and mostly crooked *Ag*Cdc14-yEGFP signal (figure 33, A, yellow arrowhead). In the mutant strain, nuclei were also observed to be much larger than in wild-type, with diameters of more than 5 µm measured in most cases, making nuclei too large to properly pass through the hyphae in some places.

Effect of *Ag*SPO12/BNS1 deletion on mitosis and growth in *A. gossypii*

A notable phenotype discovered in our deletion collection is that of *Agspo12/bns1*Δ. We deleted the *Ag*SPO12/BNS1 ORF in an *Ag*H4-GFP to be able to monitor nuclear behaviour. Mutants would

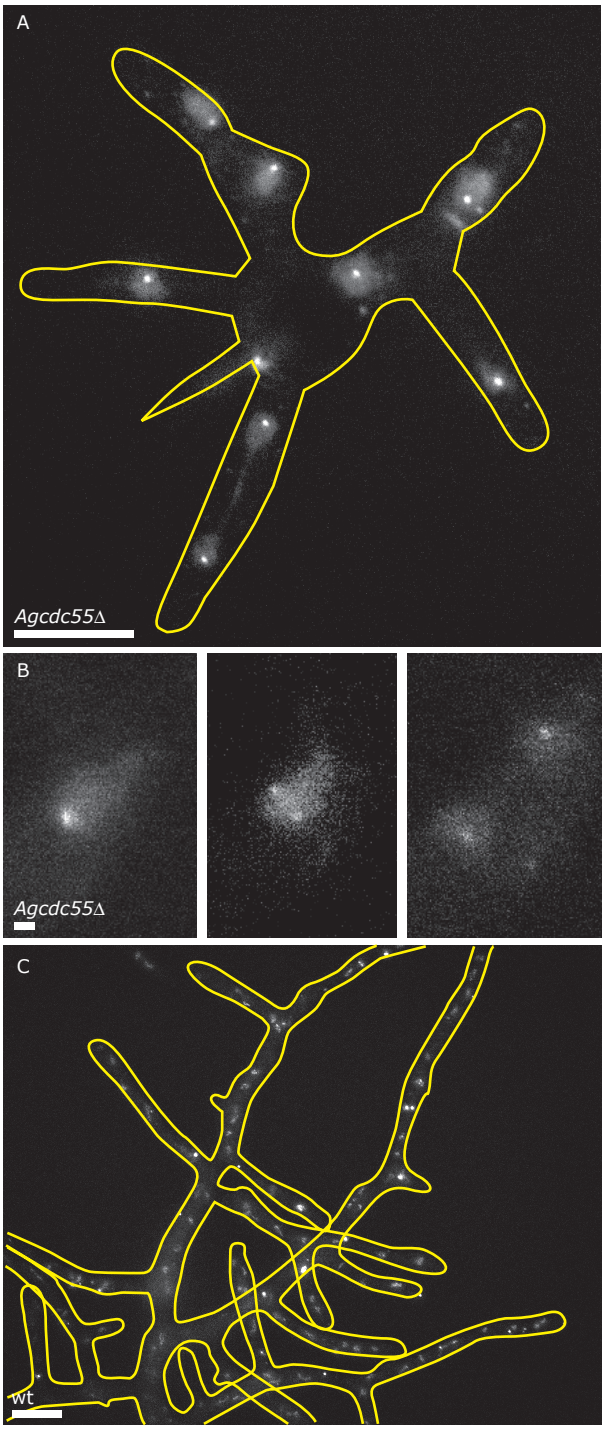

Figure 33: *Ag*Cdc14 release in *Agcdc55*Δ mutant. (A) *Ag*Cdc14-yEGFP signal in 18 hour old *Agcdc55*Δ mycelium. Maximum intensity projection of 11 planes with a Z-distance of 0.5 μm . Scale bar depicts 10μm. (B) *Ag*Cdc14-yEGFP signal in dividing nucleus of hour old *Agcdc55*Δ mycelium. Images taken 17 and 18 minutes apart, respectively. Scale bar depicts 1 μm. (C) *Ag*Cdc14-yEGFP signal in 18 hour old wild-type reference strain (*Ag*Cdc14-GFP). Maximum intensity projection of 11 planes with a Z-distance of 0.5 μm. Scale bar depicts 10 μm.

often cease growth at the germ bubble stage and occasionally could form primary germ tubes. In such cells we were able to monitor nuclei over a period of up to 14 hours (figure 34). Nuclei were in motion during the entire duration of the experiment, but mitosis was strongly impaired, as shown by time lapse imaging (figure 34, nucleus marked by yellow arrowhead is discussed in the following). Separation of DNA did not follow regular dynamics. Beginning and end of mitosis could not be identified and DNA was seemingly separated in multiple attempts over the course of approximately 4-5 hours. In first step, only part of the DNA is moved, creating 2 fractions with differing signal intensities (green arrowheads). In a second step, taking roughly 2 hours, more DNA is transferred, resulting in two equally bright nuclei. The nucleus located in the germ bubble exhibits more wild-type-like behaviour. This may be due to residual *Ag*Spo12/Bns1 protein retained in this area from the heterokaryotic mycelium the spores originate from.

Macroscopic phenotypes of non-lethal FEAR ortholog mutants

Not all FEAR ortholog disruptions had such severe effects. Deletions of *Ag*SLK19, *Ag*FOB1 and *Ag*ZDS1/ZDS2 were shown to be non-lethal. *Agslk19*Δ and *Agzds1/zds2*Δ however showed mild and strong growth phenotypes respectively at all tested temperatures (figure 35, A). *Agfob1*Δ did not show any sign of radial growth impairment. The reduction of radial growth speed in *Agslk19*Δ and *Agzds1/zds2*Δ correlated with decreased weight of the inner part of the colony (figure 35, B). Interestingly, these impairments were accompanied by a reduction of spore production in the *Agslk19*Δ (figure 35, C), but not in the *Agzds1/zds2*Δ strain. This sporulation defect was clear, but not as pronounced as observed in MEN mutants (Chapter 2, Figure 22, C). In addition, *Agslk19*Δ mycelia displayed frayed growth edges, with a visibly lower density of hyphae in the frontmost 0.5 mm of growing colonies (figure 35, D).

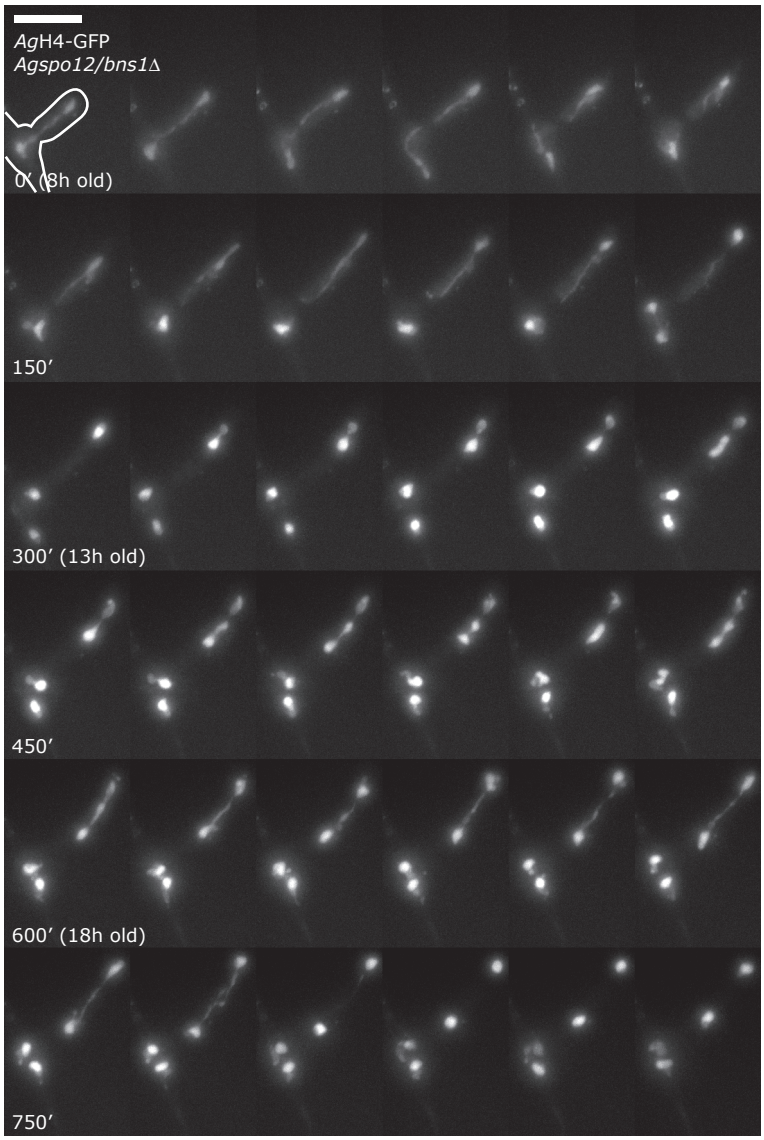

Figure 34: Behaviour of nuclei in *Agspo12/bns1*Δ mutant. Time lapse series of *Ag*H4-GFP in *Agspo12/bns1*Δ germling. 25 minute time interval beginning at 8 hours after spreading of spores. Scale bar depicts 10 μm.

Effect of *Ag*SLK19 deletion on mitosis in *A. gossypii*

We were interested to see if the observed growth defects were in connection with any mitotic deficiencies and investigated the density of nuclei (*Ag*H4-yEGFP signals) in pre-defined regions of post-tipsplitting hyphae as described in the previous chapter. The measurements show a clear increase in inter-nuclear distance in *Agslk19*Δ (figure 36). This effect was not limited to a specific region of the hyphae, but did seem slightly stronger towards the tip. This however is likely only due to large variation as a consequence of relatively small sample sizes (in turn being the cost of spatial resolution). Overall average distance in *Agslk19*Δ was calculated to be 11.34 ± 5.43 μm (1 SD, N = 111), more than double the values determined to be 4.47 ± 2.06 μm (1 SD, N = 193) for wild-type or 4.34 ± 2.25 μm (1 SD, N = 185) for *Agfob1*Δ.

Effect of *Ag*SLK19 on *Ag*Cdc14-yEGFP release

To investigate whether the decreased mitotic activity detected in *Agslk19*Δ was caused by compromised *Ag*Cdc14 regulation, we repeated the disruption in *Ag*Cdc14-yEGFP cells. *Ag*Cdc14-yEGFP sequestration and release seemed intact, with typical wild-type like localization patterns throughout anaphase (figure 37), although no precise quantification was undertaken.

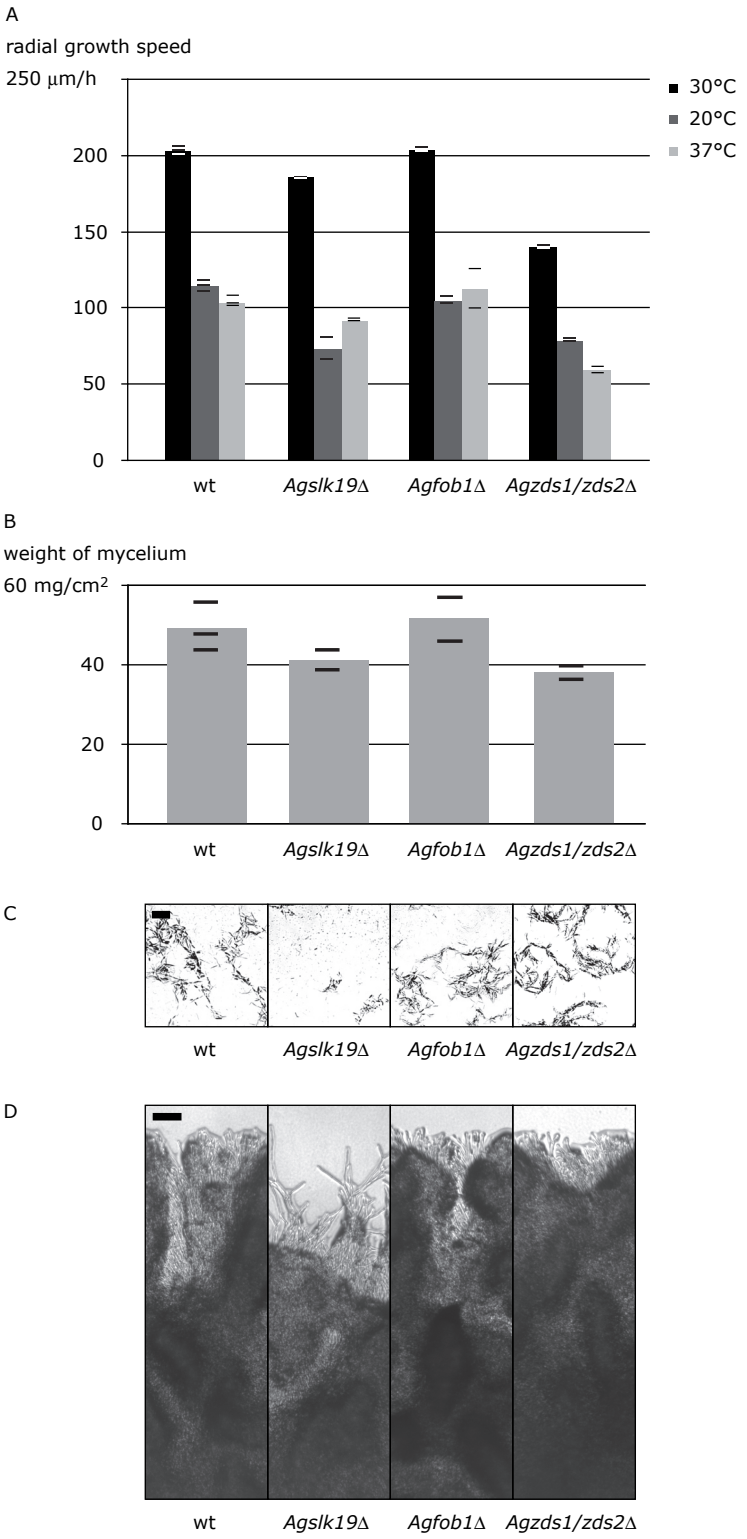

Figure 35: Macroscopic development of non-lethal FEAR mutants. (A) Radial growth speeds of mutants at 30°C, 20°C and 37°C after 5 days. Values represent the mean of 2 or 3 separate measurements done with individual strains, which are indicated by thin horizontal bars. (B) Weights of the inner 3 cm of mycelium taken for spore isolation from the growth assay plates. Mean values of 2 or 3 separate measurements, indicated by thin horizontal bars. (C) Samples taken from spore preparations of inner 3 cm of 6 day old colonies. Scale bar depicts 0.1 mm. (D) Edges of 6 day old colonies. Scale bar depicts 0.1 mm.

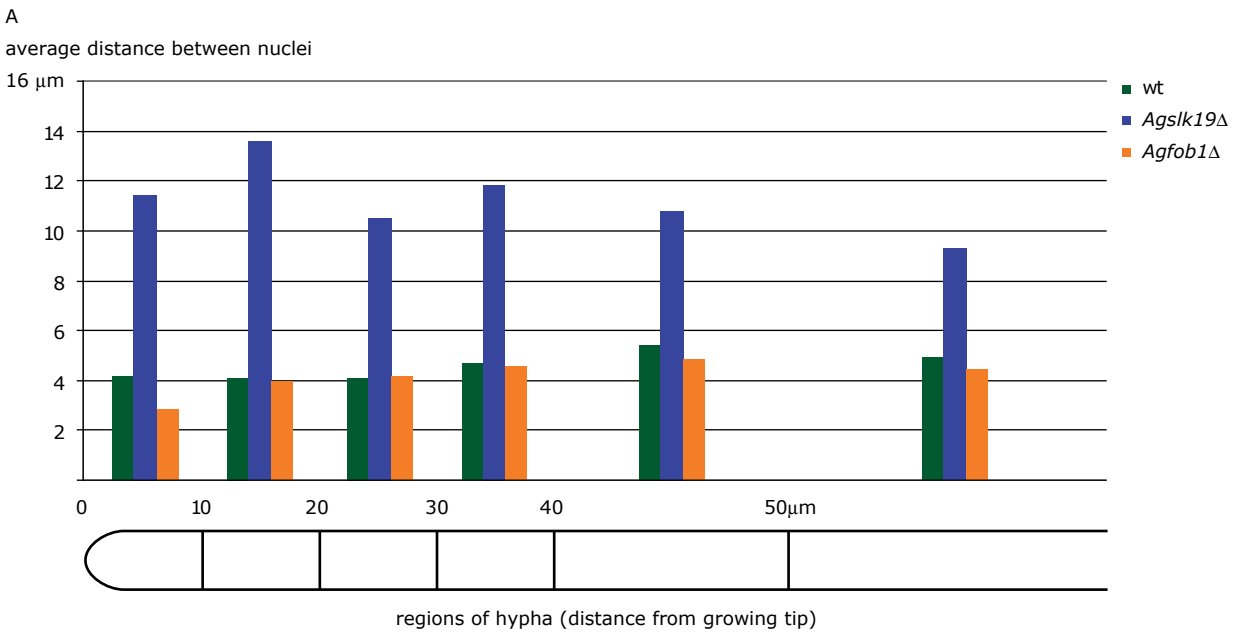

Figure 36: Distribution of nuclei in non-lethal FEAR mutants. Mean distances between nuclei in defined regions of hyphae (illustrated below) in wild-type reference strain (*Ag*H4-GFP) and MEN mutants.

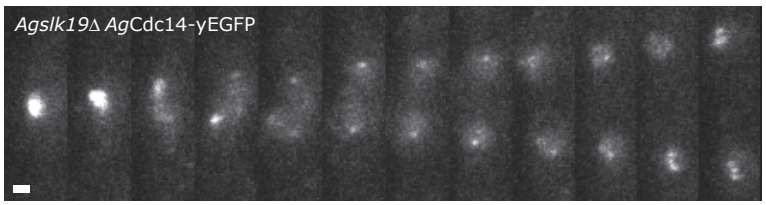

Figure 37: *Ag*Cdc14 release in *Agslk19*Δ mutant. Time lapse series of *Ag*Cdc14-yEGFP in mature *Agslk19*Δ mycelium. 1 minute time interval. Scale bar depicts 1 µm.

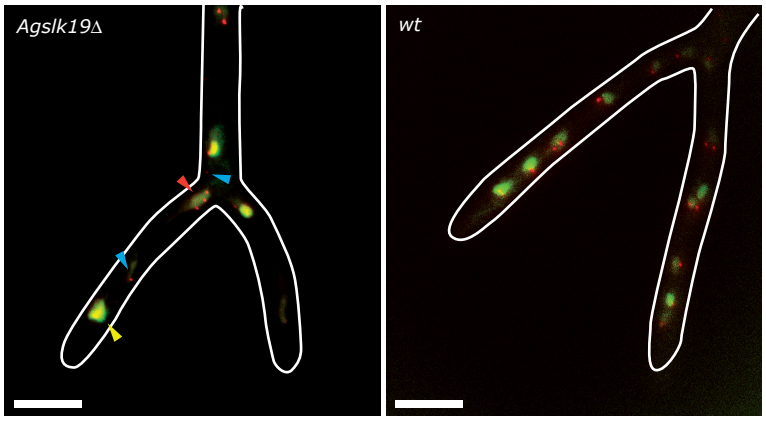

Figure 38: Nuclei and SPBs in *Agslk19*Δ mutant. Channel merge of *Ag*Tub4-YFP (red) and *Ag*H4-GFP (green) images of fast growing (as indicated by tip-splitting) hyphae on TL-slides. Yellow arrowhead indicates nucleus with no SPB. Red arrowhead indicates nucleus with 3 SPBs. Blue arrowheads indicate lone SPBs attached to no nucleus or nuclear fragment. Scale bars depict 10 µm.

Detailed look at nuclear division cycle stages in viable FEAR ortholog mutants

In *S. cerevisiae* FEAR and MEN share functional overlap in terms of their roles in *Sc*Cdc14 regulation. We repeated the experiment used in Chapter 2 to detect enrichment of metaphase nuclei with the FEAR ortholog mutants *Agslk19*Δ, *Agfob1*Δ and *Agzds1/zds2*Δ in order to find out if the functions indicated by partial metaphase arrest were also shared by these putative FEAR components.

Measurements as performed in the MEN ortholog mutants were not possible in *Agslk19*Δ. Upon inspection of *Ag*Tub4-YFP in the strains generated for the experiment, it became apparent that the nuclei in these mutants could not be catagorized

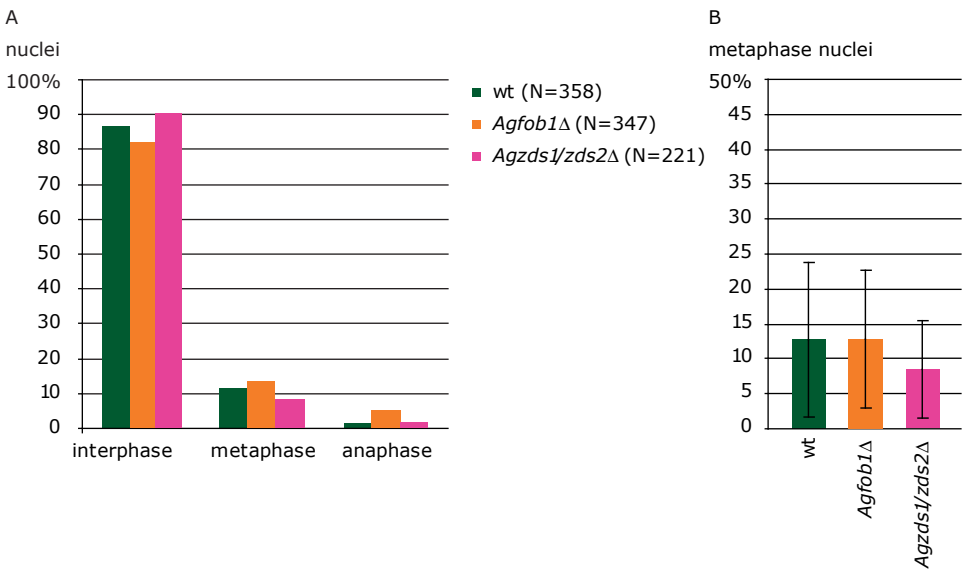

Figure 39: Occurence of metaphase nuclei in non-lethal FEAR mutants. (A) Percentages of total counted nuclei found to be in different nuclear division cycle stages in wild-type reference strain (*Ag*H4-GFP *Ag*Tub4-YFP) and FEAR mutants. (B) Percentages of nuclei within individual hyphae found to be in metaphase. Error bars represent one standard deviation.

in a fashion comparable to the data collected previously. Nuclei (or *Ag*H4-GFP patches) could often be observed which had three (figure 38, red arrowhead) or no SPBs (figure 38, yellow arrowhead). Also, there seemed to be detached SPBs within the cytoplasm, not stabily connected to any nuclei at all, or connected to what appears to be fragments of nuclei (figure 38, blue arrowheads). We also noticed morphological abnormalities of nuclei (aberrent shapes of *Ag*H4-GFP), something that had evaded our attention in our previous studies of nuclear density in *Agslk19*Δ mutants.

For *Agfob1*Δ and *Agzds1/zds2*Δ mutants, conventional catagorizations of nuclei could successfully be made using the combination of *Ag*H4-GFP and *Ag*Tub4-YFP signals. Quantifications showed that no significant enrichment of any stage of the nuclear division cycle could be detected in these strains (figure 39, A). Alternative data processing as described for the analogous experiment in Chapter 2 uncovered no apparent change in tendencies (figure 39, B): Percentage values of metaphase nuclei determined were 12.7 ± 11.1 % (1 SD, N = 358) for wild-type, 12.7 ± 9.9 % (1 SD, N = 347) for *Agfob1*Δ and 8.5 ± 7.0 % (1 SD, N = 221) for *Agzds1/zds2*Δ. Lower sample numbers were generated for *Agzds1/zds2*Δ mutants due to reduced capability to undergo tipsplitting in this particular experimental setup (a prerequisite for consideration, see materials and methods). This may be caused by the described reduction in growth speed.

Discussion

The results from the experiments with MEN homologs led to the question what role FEAR components may have in regulating anaphase events. Has the entire network in charge of bringing about exit from mitosis been reduced to a minimal set of genes comprised of FEAR homologs?

A. gossypii was found to have orthologs to all genes associated with FEAR in *S. cerevisiae*. Sequence identity values are slightly lower on average compared to the MEN homologs, and only components of the putative $PP2A^{AgCdc55}$ complex are highly conserved. Nevertheless, all predicted functional domains are present.

Deletion of *Ag*CDC55 was found to be lethal and provoked a striking phenotype concerning *Ag*Cdc14-yEGF release. In these cells, which halted all growth and lysed within 24 hours, *Ag*Cdc14 was found to be in permanent released form. This is in contrast to *Sccdc55*Δ cells which show premature release of *Sc*Cdc14, but successful, albeit delayed return to the nucleolus. This discrepancy seems to suggest that in *A. gossypii*, *Ag*Cdc55 downregulation might be sufficient for full, sustained release and thus may even belong to a sole pathway causing *Ag*Cdc14 activation.

What exactly leads to the death of *Agcdc55*Δ cells is not entirely clear. Despite permanent activation of *Ag*Cdc14, mitosis is not entirely abolished, however, nuclei expand to a remarkable size, possibly suggesting endo-reduplication, which could lead to all kinds of dosage dependent effects. Such drastic perturbations may also be detected and trigger apoptosis. Another cause for these aberrent nuclei could also be that *Ag*Cdc14 regulates nuclear membrane expansion during anaphase. *Ag*Cdc14 being constantly active throughout interphase would therefore lead to bloated nuclei. Or perhaps the observations rather reflect other effects of constantly low Cdk activity due to an antagonistic effect of *Ag*Cdc14.

Another drastic outcome was observed in *Agspo12/bns1*Δ mutants. Given the putative role as an inducer of *Ag*Cdc14 activation, the apparent failure to undergo nuclear abcission (and thus successfully exit mitosis) in these cells may well stem from failed release of the phosphatase. The inability to fully divide may be due to problems in rDNA segregation (which is strongly linked to *Sc*Cdc14 effector function). A high degree of conservation (five identical surrounding amino acids) of the phosphorylation site at S118 in *Sc*Spo12, which is essential for function within FEAR (Tomson *et al*., 2009), additionally speaks in favor of a conserved role of *Ag*Spo12/Bns1 in *Ag*Cdc14 regulation. The phenotype observed may stand in contrast to behaviour observed in *Agcdc14*Δ mutants, however full deletion of *Ag*CDC14 may also bring about other defects which mask late anaphase deficiencies. In this sense, perhaps the *Agspo12/bns1*Δ better reflects a lack of activated *Ag*Cdc14 during anaphase. To investigate sequestration specifically, we additionally constructed a *Agspo12/bns1*Δ strain carrying *Ag*Cdc14-yEGFP and could only see the phosphatase in its sequestered form (supplemental figure 6). Unfortunately however, these cells displayed even less viability than *Agspo12/bns1*Δ H4-GFP cells, with no germ tubes forming at all and no mitotic events successfully recorded. This may hint at compromised functionality of the *Ag*Cdc14-yEGFP construct.

*Agfob1*Δ mutants did not show any mitotic or developmental phenotype at all. This is similar to *S. cerevisiae* where *Sc*Fob1 deletion shows no phenotype in synchronized cells. Possibly, *Ag*Fob1 also only has a minor role as in *Ag*Cdc14 regulation, which, as in budding yeast, only becomes apparent in perturbed cell cycle progression.

*Agzds1/zds2*Δ cells display radial growth speed deficiencies, but have no apparent trouble proceeding through mitosis. Because *Sc*Zds1 is known to be potentially involved in many different areas (hence the alias “zillion different screens”) ranging from polarity (Zanelli and Valentini, 2005), sister chromatid cohesion (Heo *et al*., 1999), chromatin silencing (Roy and Runge, 2000) or cell wall integrity signalling (Griffioen *et al*., 2003), the causes for the observed reduced growth speeds cannot be conclusively deducted from our experiments. Concerning a possible function in FEAR, one may have anticipated at least a mild phenotype in nuclear division cycle progression, since the *Agcdc55*Δ mutant shows such clear

malfunctioning and *Ag*Zds1/Zds2 is a potential upstream inhibitor of the PP2A. In such a case we would have expected deficiences down the lines of *Agspo12/bns1*Δ. As it seems however, *Ag*Zds1/Zds2 may not be involved in $PP2A^{AgCdc55}$ downregulation. Perhaps in *A. gossypii*, $PP2A^{AgCdc55}$ is more directly inhibited by *Ag*Esp1-*Ag*Slk19 activity, and the inclusion of the seemingly polyvalent *Sc*Zds1 and *Sc*Zds2 in the FEAR pathway in budding yeast reflects a timing of polarity or cell-wall related events to occur during anaphase, a coordination that *A. gossypii* can do without.

*Agslk19*Δ mutants are viable, but have shown nuclear phenotypes reminiscent of the *Agspo12/bns1*Δ phenotype, however not quite as lethal. Mitosis seems to be heavily disturbed and hyphae carry only about half the nuclei that wild-type do. *Ag*Cdc14 appears to be released successfully, however we did not conduct an experiment to see if there is a delay in metaphase/anaphase transition, and cannot rule out a shift of events relative to *Ag*Pds1 degradation. Possibly, what we see is rather a result of malfunction of separase due to a loss of interaction with *Ag*Slk19. This would fit more nicely to the observations of more than two SPBs on some nuclei, which for example could be due to *Ag*Esp1 triggering *Ag*Cdc14 release and exit from mitosis without properly cleaving cohesin. Multiple SPBs were in fact also observed in many *Sc*esp1-1 cells at the restrictive temperature (McGrew *et al*., 1992). *Agesp1*Δ mutants were found to not be viable (supplemental figure 7). Concerning the reduced production of spores in *Agslk19*Δ mutants, the decrease seemed to be to a much smaller extent than in MEN homolog mutants and is likely caused by lower numbers of single SPB nuclei, rather than sporangium malformation.

FINAL DISCUSSION

The system promoting exit from mitosis has developed somewhat differently in the *A. gossypii* lineage, compared to *S. cerevisiae*. Whereas it seems that *Ag*Cdc14 has maintained a central role in the cell cycle as well as a conserved basis of regulation, the underlying pathways controlling this pivotal phosphatase are not conserved as such in *A. gossypii*. Homologs of the MEN still apparently function together as a G-protein coupled kinase cascade at the SPBs, this core signalling unit however seems to be uncoupled from any function in *Ag*Cdc14 release and exiting mitosis. The module appears to play a crucial role in septation, which calls to mind the septation initiation network (SIN) of *S. pombe*, which is required for (*Sc*Cdc14 ortholog) *Sp*Clp1-dependent septum formation and is largely made up of MEN homologs (supplemental figure 5).

The FEAR network on the other hand seems to be functionally conserved in *A. gossypii*, however in a reduced form. *Ag*Zds1/Zds2 and *Ag*Fob1 do not seem to play a role in *Ag*Cdc14 release, and *Ag*Slk19 may only be involved as a co-factor in cohesin cleavage, but not in FEAR activation. The reduced redundancy of the remaining system seems to have led to more drastic phenotypes of deletion mutants than in *S. cerevisiae*: *Ag*Spo12/Bns1 and the putative PP2A regulatory subunit *Ag*Cdc55 have obtained essential status. This is similar to the situation during meiosis I in *S. cerevisiae*, where FEAR is essential for proper *Sc*Cdc14 release, and MEN isn't. Meiosis I division notably takes place without ensuing cytokinesis and likely without other orientational cues.

How the regulatory network controlling exit from mitosis in *A. gossypii* might be wired can only be guessed at this moment, however we propose a rather stripped-down model (figure 40),

Interestingly, calculated sequence identity values for all genes in the system are either particularly high (over 70%) or rather low (below 50%) with no values in between (supplemental figure 2). This pattern may indicate points of particularly high evolutionary pressure on the system. To a certain degree high identity values also reflect areas of the network map that are thought to be still intact: The only highly conserved FEAR homologs are all part of the putative PP2A^{AgCdc55} phosphatase. On the MEN side of things, the cascade components *Ag*Tem1, *Ag*Dbf2/Dbf20 and *Ag*Mob1 are strongly conserved, and it seems that evolution has modified the cellular function of this signalling group by altering upstream and downstream elements, and not the pathway itself. Interestingly *Ag*Bub2 and *Ag*Cdc5 are also highly identical to their *S. cerevisiae* homologs. *Agbub2*Δ mutants, which were not investigated thoroughly in this work, were found to be viable (Sandrine Grava, personal communication). *Ag*Cdc5 will be particularly interesting to study, due to its involvement in both FEAR and MEN in *S. cerevisiae*. Interesting preliminary data has already been gathered (supplemental figure 9).

Can *A. gossypii* be viewed as a "primitive" system? In some ways, probably. Polarized growth is very likely to have predecessed cytokinesis in evolution due to its relative simplicity (clustering of a few factors is certainly more easily accomplished than constriction and controlled fusion of a membrane), and *A. gossypii* may very well resemble primordial organisms taking first steps in cell division. However in the case of *A. gossypii*, we can presume that ancestors were in fact "one nucleus per cell" organisms, and that the current morphology and life style has been attained by the loss of functions once possessed. This transpires from the fact that MEN homologs in several other organisms coordinate cytokinesis with the cell cycle, and from studies suggesting that the evolution of septation in *A. gossypii* is also strongly influenced by significant loss of function over the ages (Andreas Kaufmann, doctoral thesis). However the case, it is safe to say that coordination of nuclear division is bound to less conditions than in budding yeast, and that this is directly reflected in reduced complexity of the regulatory pathways.

What implications do these results bear for *S. cerevisiae*? To answer the question what imposing selective force is responsible for the complexity observed in budding yeast FEAR and MEN, it seems that the purpose of the "extra" components lies first

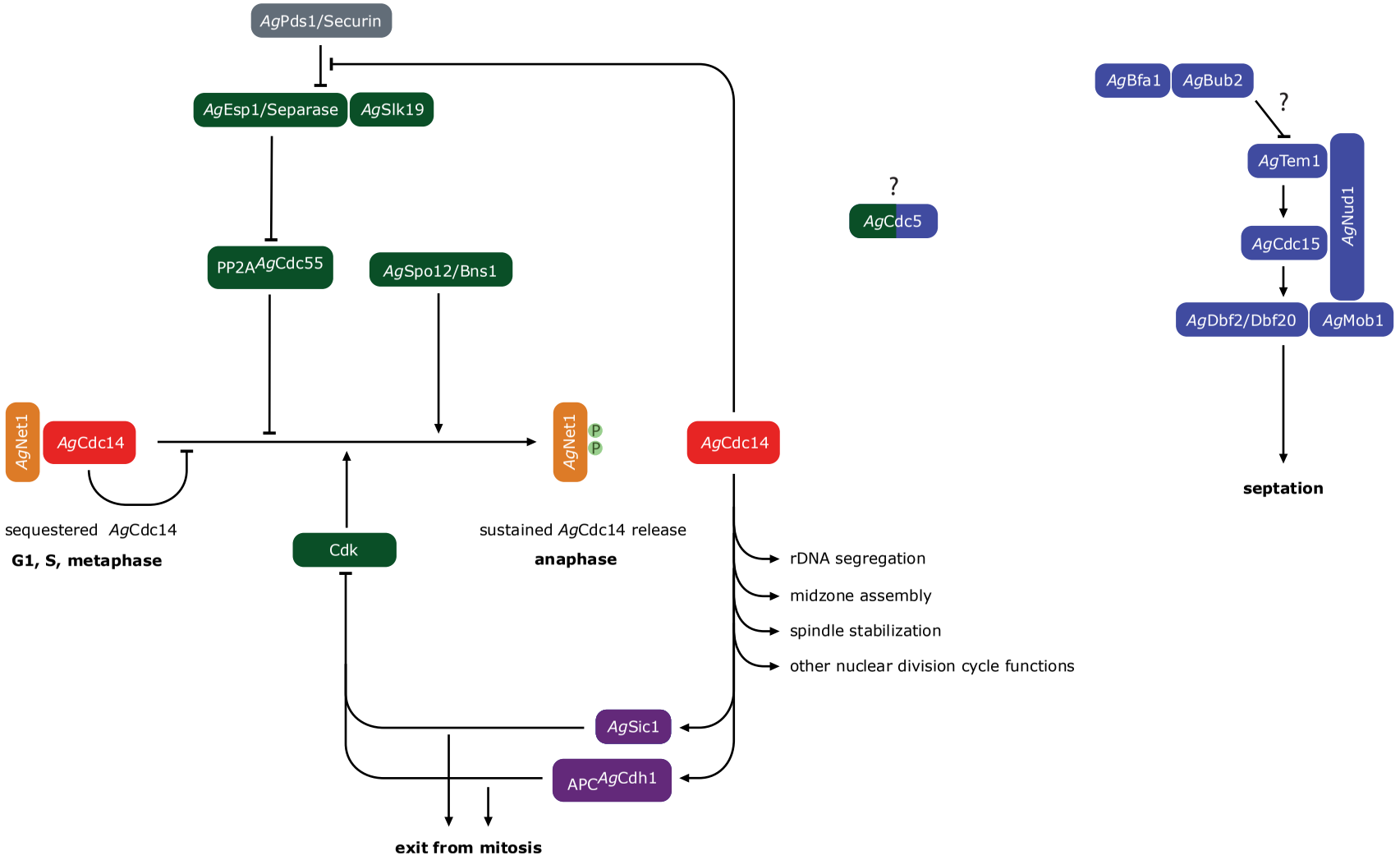

Figure 40: Possible wiring diagram of exit from mitosis homologs in *A. gossypii*. Based on pathways presented in introduction. Minimally reduced by nodes and connections that are suggested to be ruled out by experimental data. Question marks indicate important components where insufficient data has been generated to make presumptions.

and foremost in spatial regulation. The importance of feedback loops and other such circuitry motifs present in these parts of the network is not to be underestimated, however their significance is likely to have gradually grown over time, as they have not been conserved in the *A. gossypii* lineage.

The system described in *A. gossypii* may also provide grounds for clarifying unsolved questions that have been experimentally difficult to tackle in *S. cerevisiae*. It may for example prove useful to determine the precise role of *Sc*Cdc5 within mitotic exit (Its function in MEN is well described, it however remains as yet elusive how exactly *Sc*Cdc5 fits into FEAR). With MEN signalling obsolete, any contribution of *Ag*Cdc5 to *Ag*Cdc14 release could be interpreted as a function within FEAR.

Also, some questions remain open as to how *Sc*Spo12 antagonizes *Sc*Cdc14 sequestration (apart from interaction with *Sc*Fob1). Perhaps it will be easier to dissect its mode of action within the "simplified" *Ag*Cdc14 release pathway. In addition, study of *A. gossypii* MEN homologs may be of use to elucidate secondary functions in *S. cerevisiae* (such as their role at the bud neck) which are masked by their essential role in nuclear division.

APPENDIX

Appendix

Supplemental materials

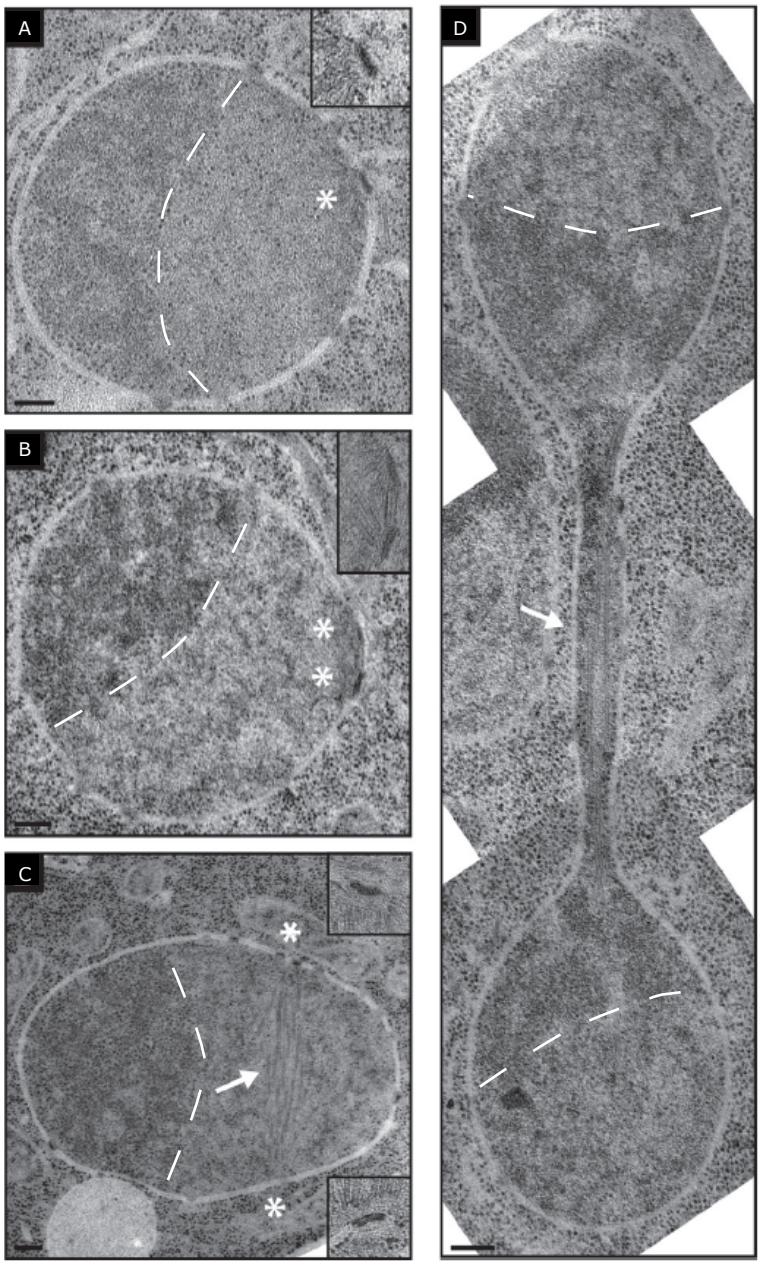

Supplemental figure 1: EM images of nuclear structures in *A. gossypii*. (A) single SPB, (B) duplicated SPB, (C) metaphase and (D) anaphase nuclei. White, dashed lines indicate the visible border between regions of different electron density thought to delimit the nucleolus. White arrows indicate mitotic spindles, asterisks indicate the position of SPBs. Scale bars depict 200 nm. Adapted from Lang *et al.,* 2010a.

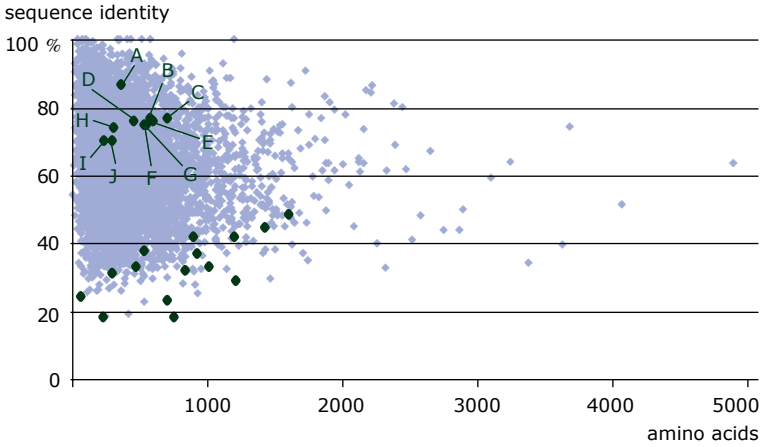

Supplemental figure 2: Amino acid sequence identities. Plotted against protein length. Blue: *A. gossypii* proteome. Green: Proteins discussed in this thesis (further details in tables provided in results section). (A) *Ag*Pph21/Pph22. (B) *Ag*Dbf2/Dbf20. (C) *Ag*Cdc5. (D) *Ag*Cdc55. (E) *Ag*Tpd3. (F) *Ag*Cdc14. (G) *Ag*Cdh1. (H) *Ag*Bub2. (I) *Ag*Tem1. (J) *Ag*Mob1.

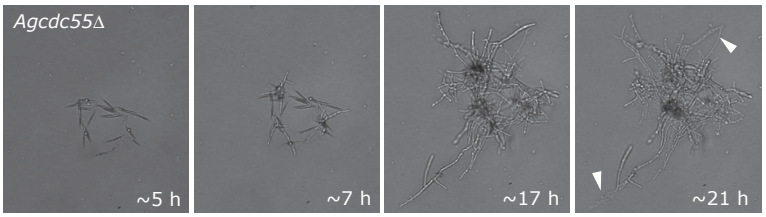

Supplemental figure 3: *Agcdc55*Δ growth. Exerpts from time-lapse movie of multiple *Agcdc55*Δ germlings growing on AFM full medium at 30°C. White arrows indicate sites of lysis. Images courtesy of Valentin Tilloy.

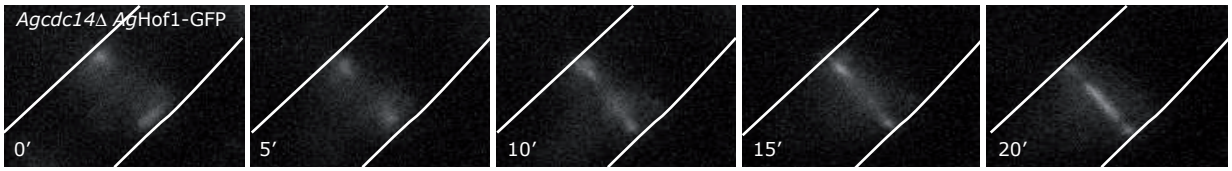

Supplemental figure 4: *Ag*Hof1-GFP dynamics in *Agcdc14*Δ. Maximum projections of 7 planes each picturing transition from bar to ring localization of *Ag*Hof1 in terminal bipolar germling. Constriction progression visible at 20 minutes. Image courtesy of Anaïs Sengler.

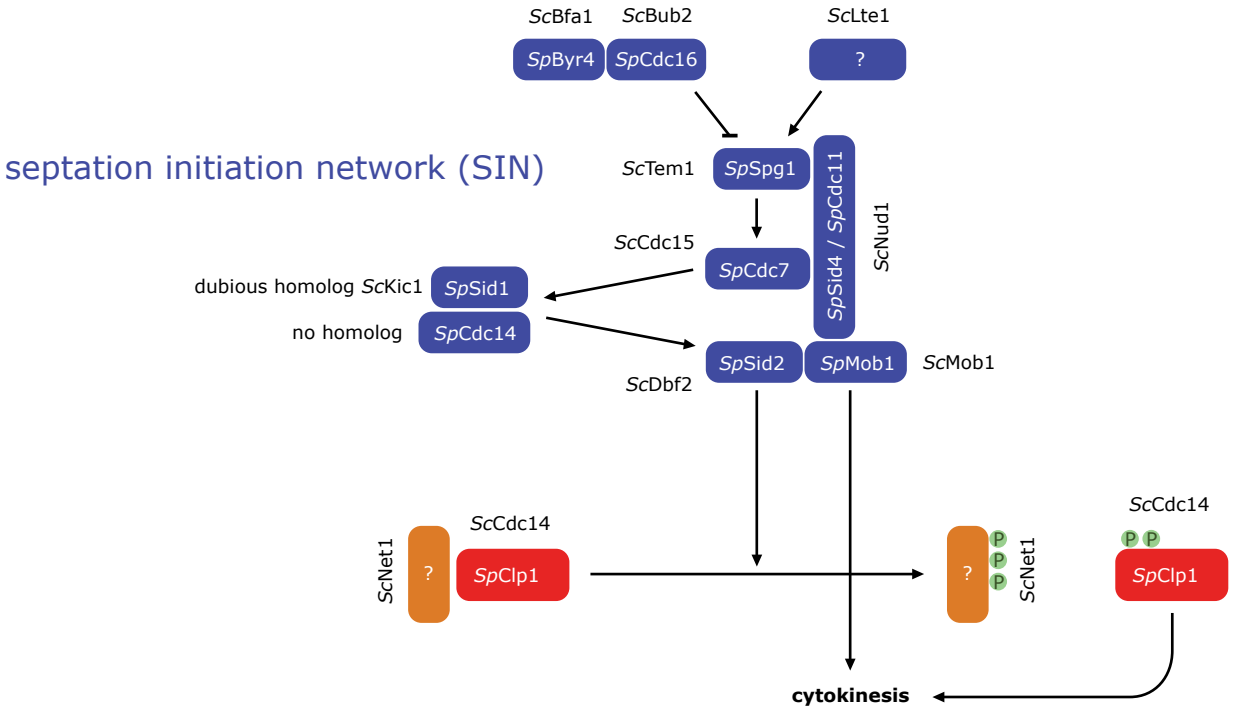

Supplemental figure 5: *S. pombe* SIN. Based on Bardin and Amon, 2001. *S. cerevisiae* homologs in black. *Sc*Kic1 identified by PsiBLAST as dubious homolog of *Sp*Sid1, not found to be mentioned in literature.

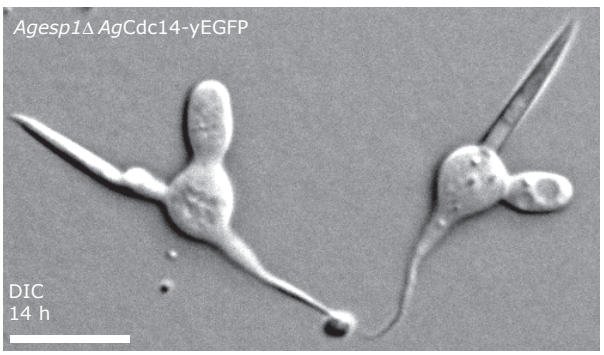

Supplemental figure 6: *Ag*Cdc14-yEGFP *in Agspo12*Δ mutants. *Agspo12*Δ germlings after 21 h on nutrients.

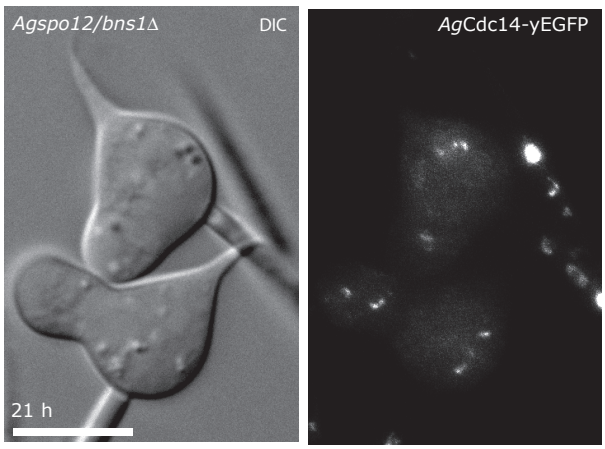

Supplemental figure 7: *Agesp1*Δ mutants. *Agesp1*Δ germ bubbles after 14 h on nutrients.

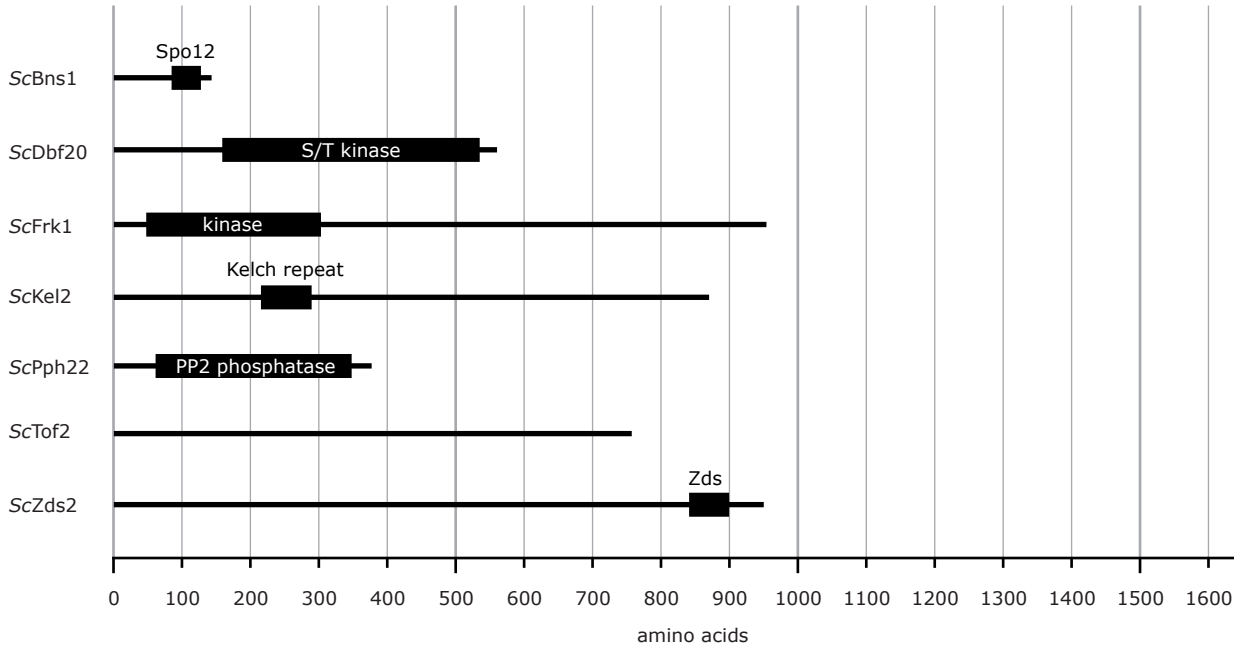

Supplemental figure 8: Predicted domains of 2nd homologs. Black bars represent predicted features.

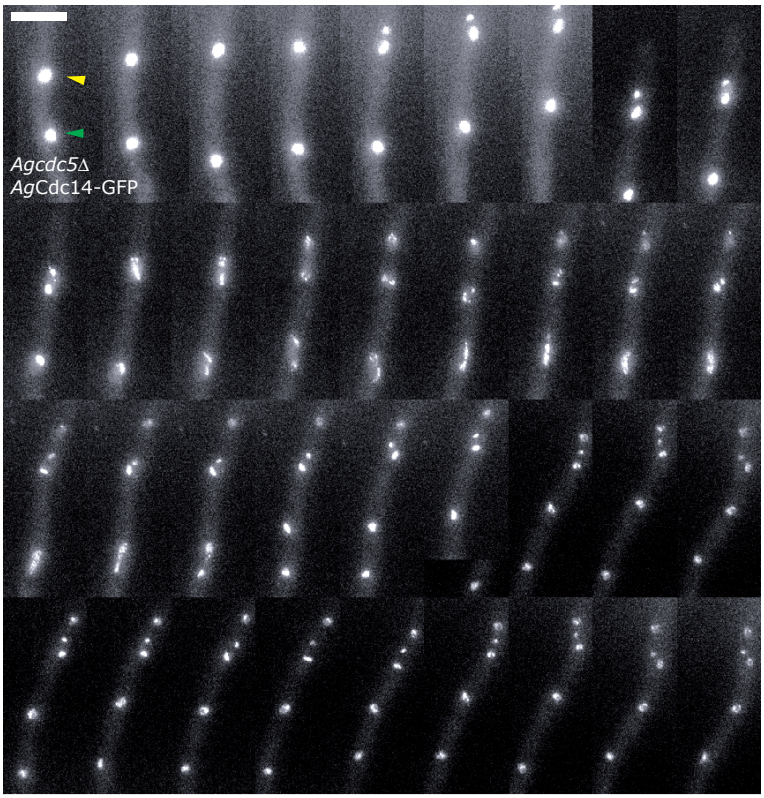

Supplemental figure 9: Preliminary *Agcdc5*Δ *Ag*Cdc14-GFP. Preliminary because: 1) only C-terminally verification possible 2) only one transformant obtained 3) mixed phenotype observed: most homokaryotic germlings died very early. This time-lapse series was taken of homokaryotic mycelium that survived the germling stage and grew very slowly on plates. Yellow arrow: Nucleus which attempts to undergo mitosis with partial *Ag*Cdc14 release, however doesn't fully separate. Green arrow: Nucleus which undergoes mitosis apparently without *Ag*Cdc14 release, and with irregular spindle elongation. Time interval: 45 seconds. Maximal projection of 5 Z-planes. Scale bar depicts 10 μm. Shift of imaging field between 7th and 8th frame.

Verification PCRs

All oligos used for verification PCRs are listed further below and were ordered at Microsynth, CH-9436 Balgach. Both N-terminal and C-terminal products were aimed for in deletion mutants, however, in some cases (marked with *) only one side could be verified due to failed annealing of the oligonucleotides. Calculated PCR fragment sizes are listed below the gel scans. A legend of the gel scan labels as well as generic figures illustrating the different kinds of reaction products are given in Figure 41. Numbers in brackets next to the strain name denote individual strains isolated.

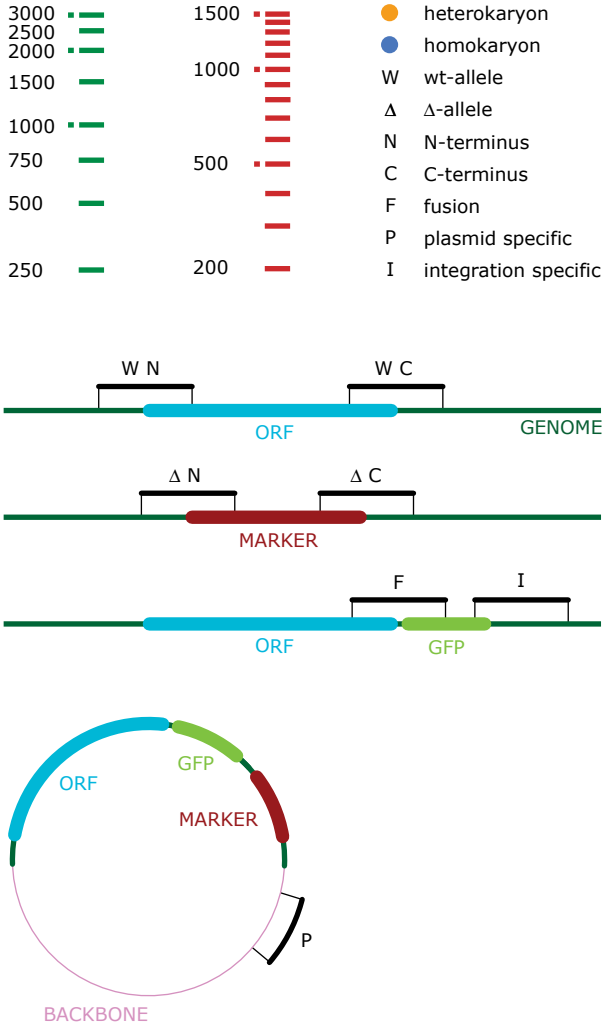

Figure 41: Verification gel scans. Top left: DNA ladder scales used on following pages representing Promega 1kb (blue) and Invitrogen 100bp (red) commercial benchtop ladders. Top right: legend of gel scan labels. Bottom: Illustrations of different kinds of PCR products (letters in legend) indicating different genotypes. From top to bottom: Wild-type allele / deletion allele / GFP (or other fluorescent protein) fusion integrated into genomic locus / GFP fusion on plasmid.

*Ag*Nup49-yEGFP GFP-*Ag*Tub1 (2/3)

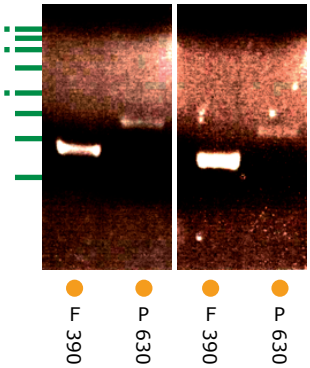

*Agcdc14*Δ GFP-*Ag*Tub1 (2)

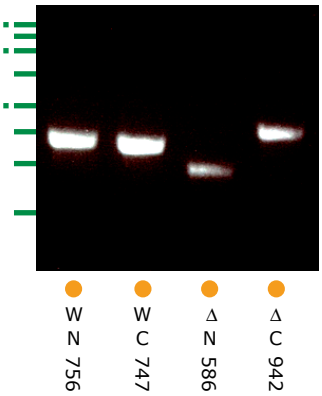

*Agcdc15*Δ *Ag*Tub4-YFP AgH4-GFP (3)

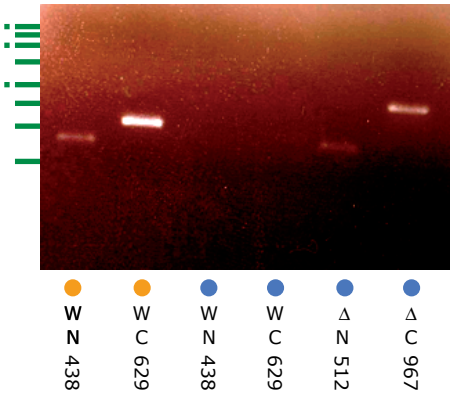

*Agcdc15*Δ *Ag*Pds1-mCherry AgCdc14-GFP (2)

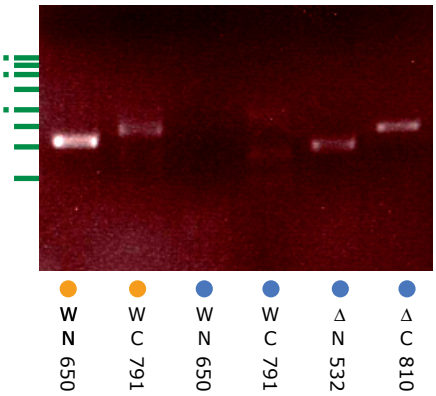

*Agcdc55*Δ AgCdc14-GFP (1/2)

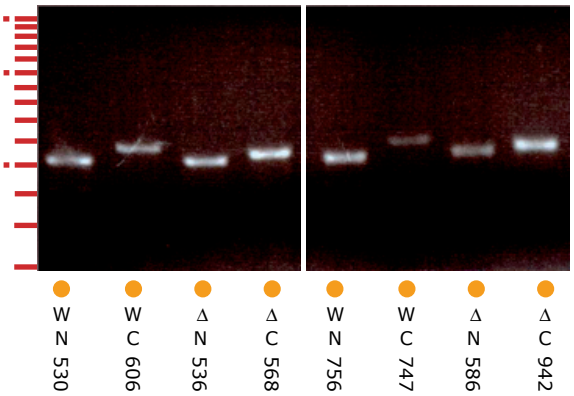

*Agdbf2/dbf20*Δ *Ag*Tub4-YFP AgH4-GFP (1/3)*

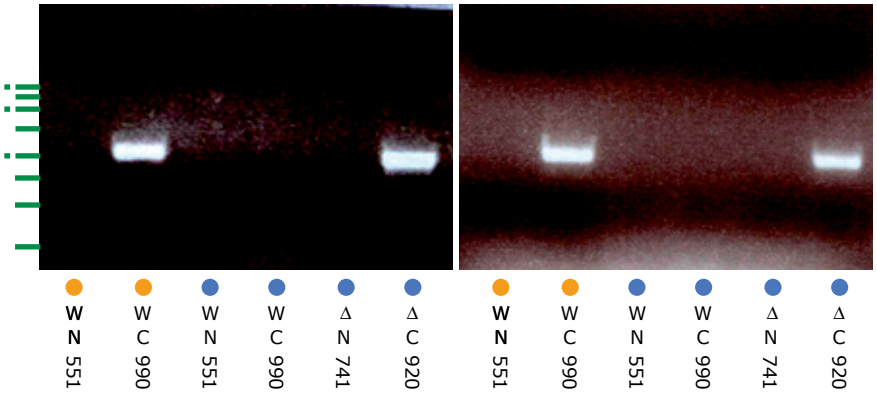

*Agfob1*Δ *Ag*H4-GFP (2/5)

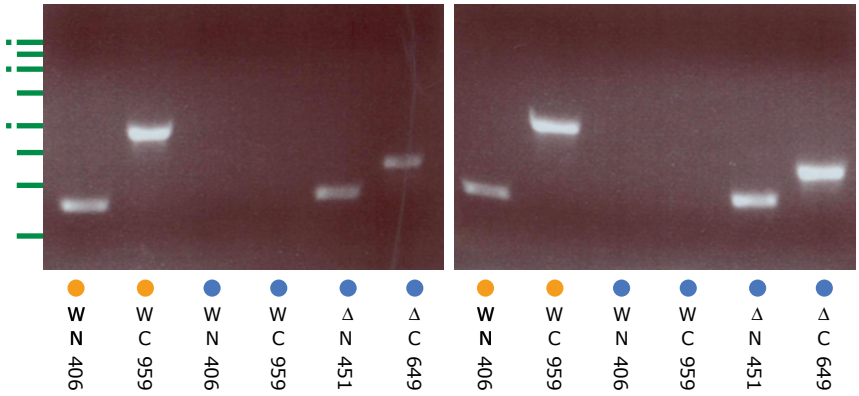

*Agfob1*Δ *Ag*Tub4-YFP *Ag*H4-GFP (2/3)

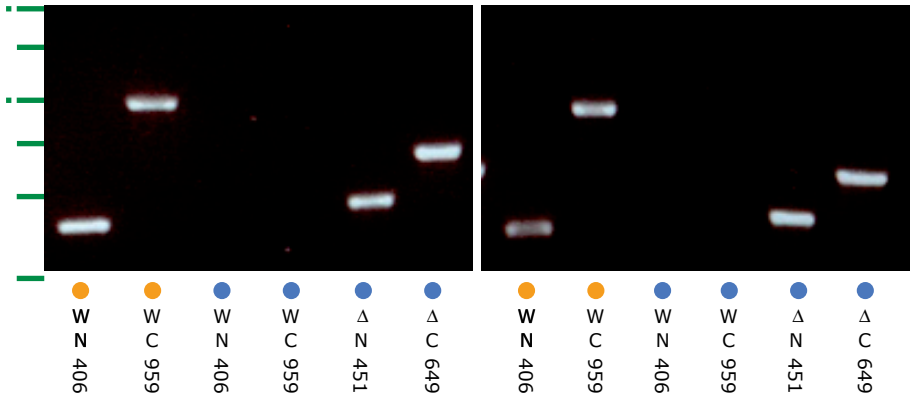

*Agkel1/kel2*Δ *Ag*H4-GFP (7/8)

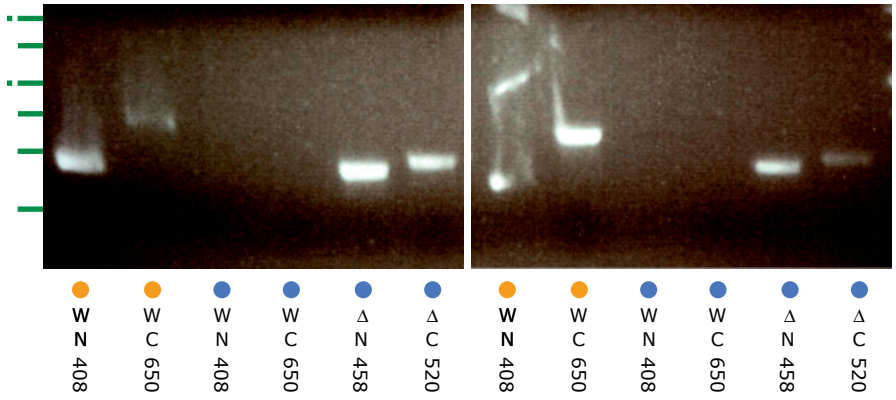

*Agkin4/frk1*Δ *Ag*H4-GFP (1/2)

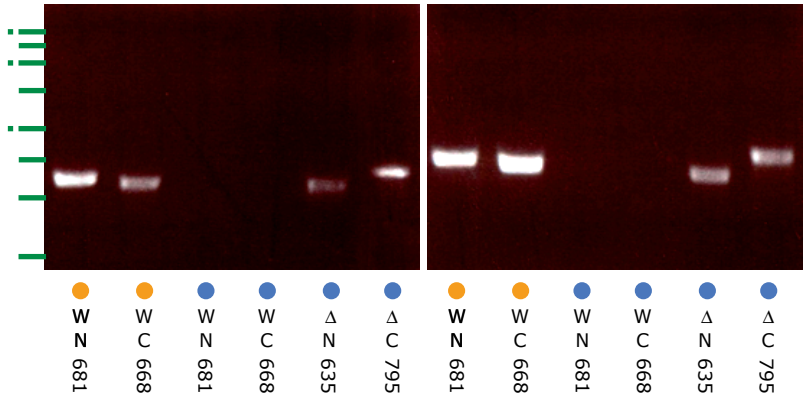

*Aglte1*Δ *Ag*H4-GFP (9/11)*

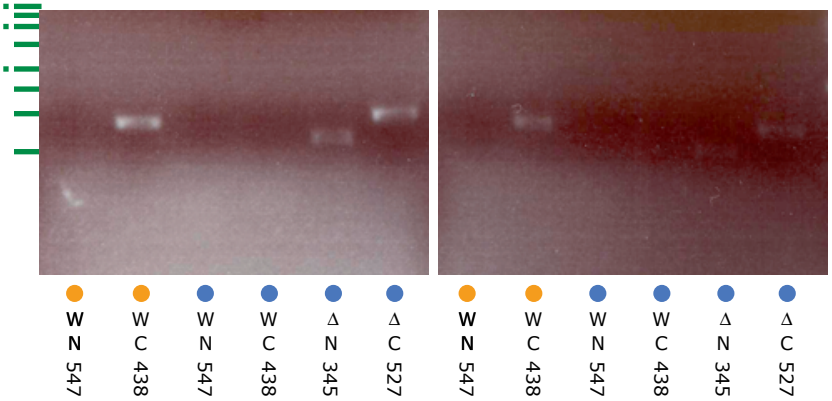

*Ag*Lte1-GFP (9/11)

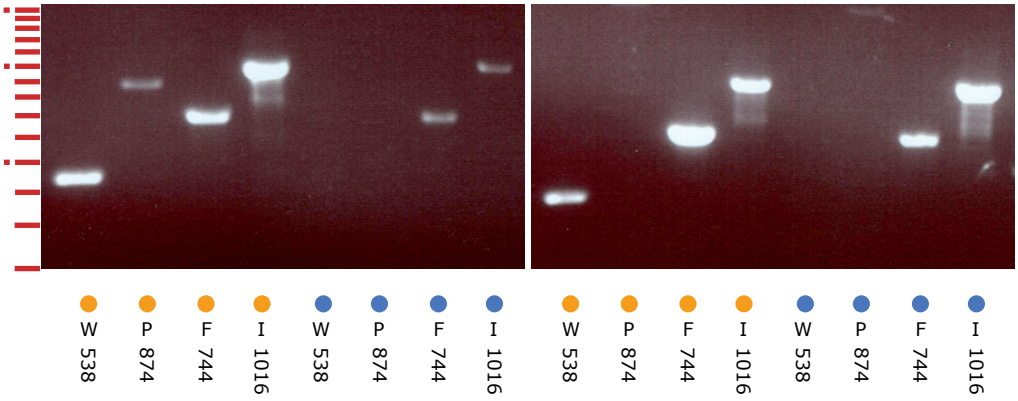

*Aglte1*Δ *Ag*Tub4-YFP *Ag*H4-GFP (10/12)*

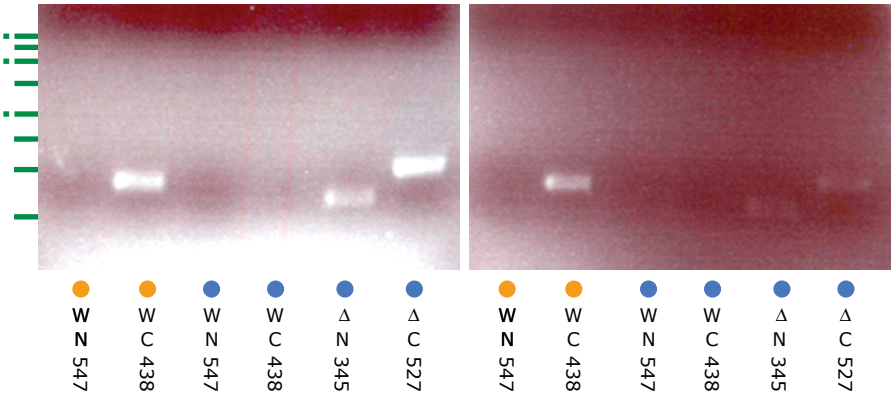

*Agmob1*Δ *Ag*H4-GFP (3)

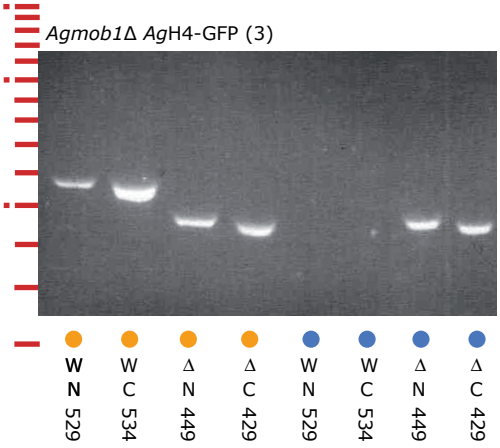

*Ag*Nop1-Cherry *Ag*Cdc14-GFP (11)

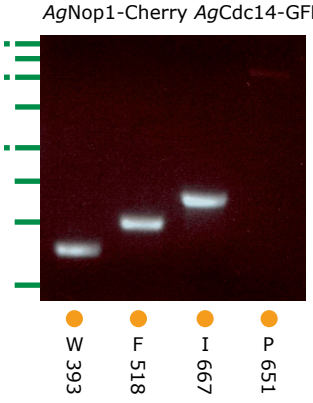

*Ag*Nop1-Cherry *Ag*Cdc14-GFP (11)

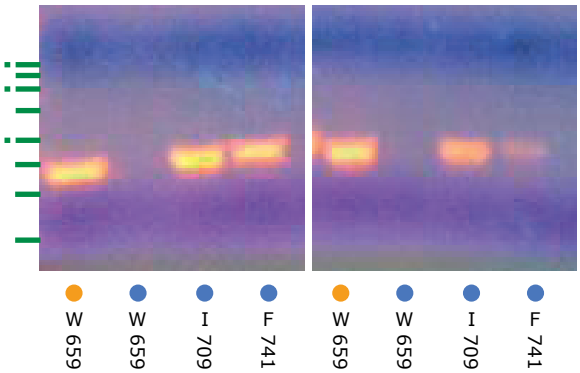

*Agslk19*Δ *Ag*H4-GFP (1/2)

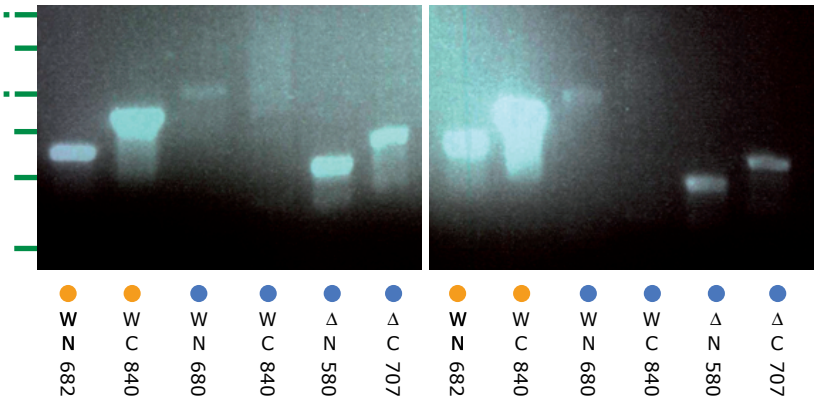

*Agslk19*Δ *Ag*Tub4-YFP *Ag*H4-GFP (7)

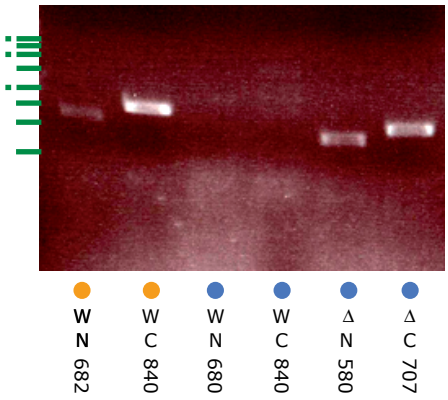

*Agslk19*Δ *Ag*Cdc14-GFP (4)

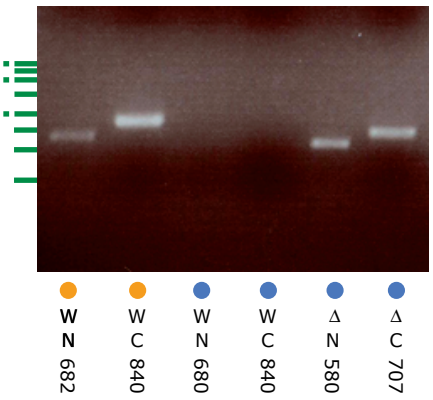

*Agspo12/bns1*Δ *Ag*H4-GFP (1/2)

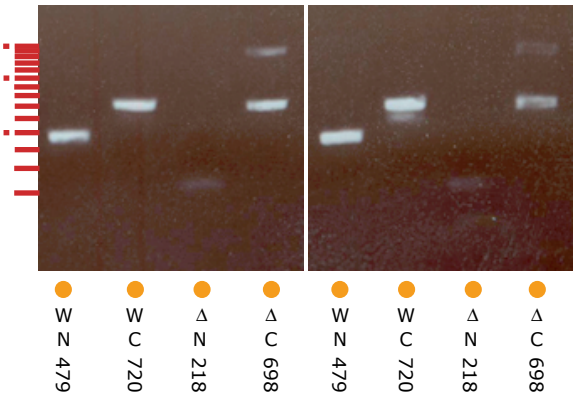

*Agspo12/bns1*Δ *Ag*Cdc14-GFP (15)

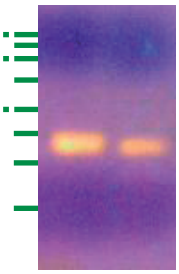

*Agtem1*Δ *Ag*H4-GFP (5/6)

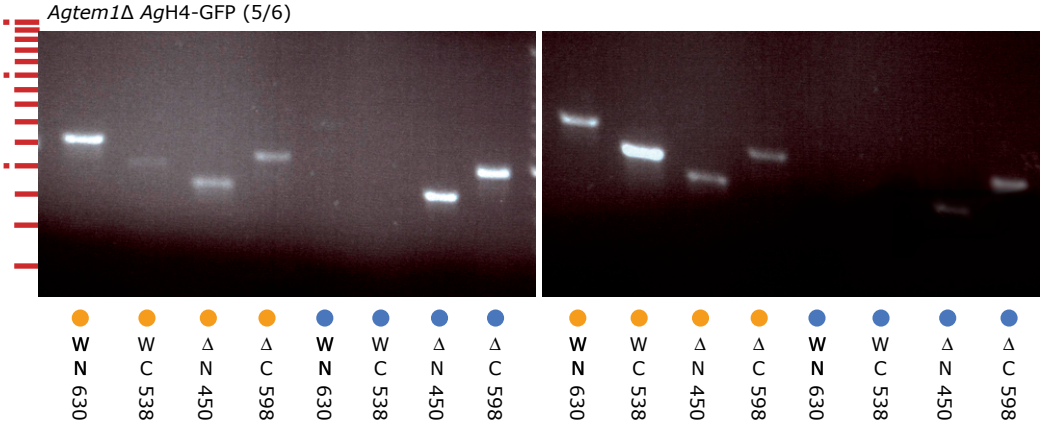

*Agtem1*Δ *Ag*Tub4-GFP *Ag*H4-GFP (1/2)*

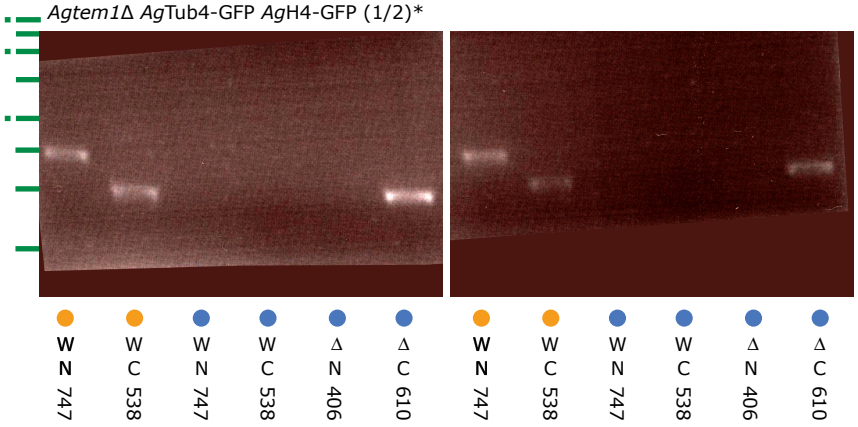

*Ag*Tem1-GFP (2/3)

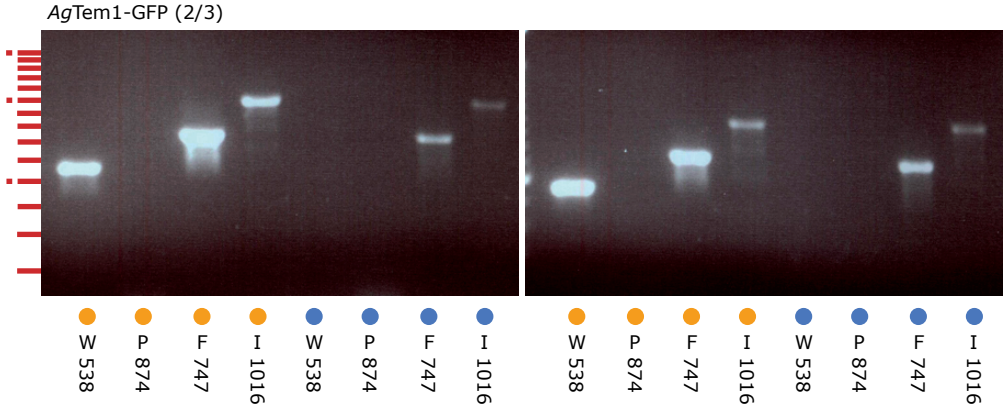

*Ag*Tub4-YFP H4-GFP (2)

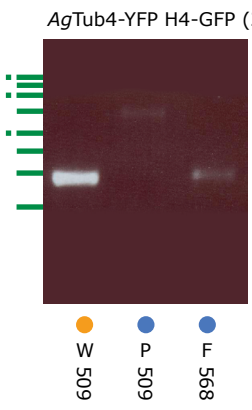

*Agzds1/zds2*Δ *Ag*Tub4-GFP *Ag*H4-GFP (5/8)*

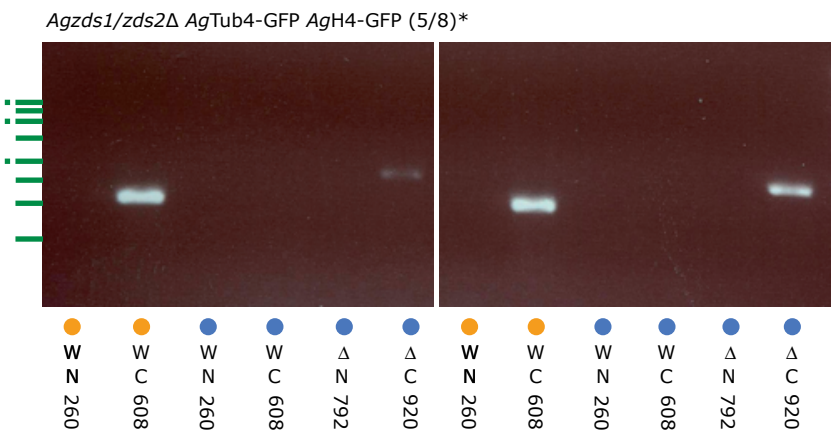

Oligonucleotide list

Primer	Sequence	Use
AgCdc15-G1	CTTCCTGCCACCACTGGAAGAG	V
AgCdc15-G4	GAACCATGAGCTTGGAAGTGGG	V
AgCdc15-I1	GTCAGCAGCAGGTTGGCCGC	V
AgCdc15-I2	CTTCTAGCAGACCGTCTTCAC	V
AgCdc15-S1	GGGTTTGAAGTTATTCTTCTTCAAGGAGGTTTACACGGTTGGTGGAGAAGGGCTAGGGATAACAGGGTAAT	V
AgCdc15-S2	CCTGATGGTAATCTCCTGGGTACTAGAAATCCGTCAGAATCATGCAACGGCCGAGGCATGCAAGCTTAGATCT	V
AgCdc55-G1	CCTCGAAAGATAGGCGAGCAGTACC	V
AgCdc55-G4	GCTCCTGCGGCGGCAGTTATTGAC	V
AgCdc55-I1	CGAATTCTGCATCATGGCTCTG	V
AgCdc55-I2	CGTCCTCCAGGCGGACAAATC	V
AgLTE1_F5	TGTATATCAGTGCGTTGTCTCATGAGGAAATTGGATATTTAACTTCCTTTGGTGACGGTGCTGGTTTA	F/D
AgLTE1_GEN_S1	CCGTTGCGGGCTCCGGCAGTATATAACGCAGAGCCGAACGCCAGCGCTAGGGATAACAGGGTAAT	D
AgLTE1_GEN_S2	ACATATGAATGAATTTACAAAAGGAGTGACAGCCATCCAGCATTAAGGCATGCAAGCTTAGATCT	D
AgLTE1T_F2	ACTCTAAATTTGATCCGACGGTCATAGACATCACATATGAATGAATTTACCATGATTACGCCAAGCTTGC	F/D
AgTEM1_CL_Down	AGGGACTCCGAAGCTTTAAAAAATCGGGAGCCCACG	C
AgTEM1_CL_Up	AGATGACTGCACTAGTCGCACCGCTGCTGGCGCGCT	C
AgTEM1_F2	ATGTTGCTCGCTGATTGACGCCATTATTATTCTCCACCTGCCGCTGTGCCCATGATTACGCCAAGCTTGC	F/D
AgTEM1_F5	ATCATGGACGTTATCGACAACCAGAACACATACGGAATATGGCGGAGCAAGGTGACGGTGCTGGTTTA	F/D
AgTEM1_GEN_S1	ATACGGGAAGACTATTGAGGTGGCATATGATAGGGGGAGTGTAAGGCTAGGGATAACAGGGTAAT	D
AgTEM1_GEN_S2	ATTATTCTCCACCTGCCGCTGTGCCGATCCCATTTGTTAGCAGGCAGGCATGCAAGCTTAGATCT	D
Cdc14-G1	CAGCGTGCCGCAGCCAAATC	V
Cdc14-G4	CTCTCGTATTTGGGTCTGTAGG	V
Cdc14-I1	GTACGAGCACCATGTAGCAGCAG	V
Cdc14-I2	CACTTCGAGAGTCCATCATAG	V
Cdc14-S1	GCAGGTGTTGAAGCCACTCAAACATTGGTAGGAGGTTCAAGTCAAGAGCTGCGCTAGGGATAACAGGGTAAT	D
Cdc14-S2	GGTACGGTACAATTCGGTTGAAGAAGAGACATAATGATTCTTACGAGTTCAGGCATGCAAGCTTAGATCT	D
CDC15_F2	GCAAGCTTGGCGTAATCATGTTATGATTTACTTAATTATGTTTCTCAATATGGCGATGCCCAAAC	D
CDC15_N*S1	CACGGTTGGTGGAGAAGGCTGAAAAAAATAGCGGACGTCCCAAGGATGGGTACCACTCTTGACGAC	D
CDC15_N*S2	TGGGCATCGCCATATTGAGAAACATAATTAAGTAAATCATAATTAGGGGCAGGGCATGCTCATGTAG	D
CDC5_F2	GGTTTGAGATTAAACCGTTAGGAGTATGTAAAAGTGTATATATTGCATGATTACGCCAAGCTTGC	D
CDC5_NS1	CCGCCAATTAATACCCCTCTTCCCATCCACACAACTGAAAGCACTCCAGTGAATTCGAGCTCGG	D
CDC55_F2	TTCAGTGGCTTTTTGCATACTGAGGTGTCAGTAGGTGTACTTCCACATGATTACGCCAAGCTTGC	D
CDC55_NS1	CTAAACCTTTGCGTAGCCACTCATCGGGCCGGAAACCACGTCGGCCCAGTGAATTCGAGCTCGG	D
DBF2_F2	TAAGAATGCGATAAATGCTCGTAAAGCGACCTCATGGATGGGCTGTGTCGCATGATTACGCCAAGCTTGC	D
DBF2_N*S1	GGCGAGGGGAACAGAGGCATTCAGGGAGACACGAAGGCGAAAAAAATGGGTACCACTCTTGACGAC	D
DBF2_N*S2	CGATAAATGCTCGTAAAGCGACCTCATGGATGGGCTGTGTCGTCAGGGGCAGGGCATGCTCATGTAG	D
DBF2_NS1	AATCTGGCGAGGGGAACAGAGGCATTCAGGGAGACACGAAGGCGAAAAAACCAGTGAATTCGAGCTCGG	D
G2.2	CATCTACTATATGTAAGTATACGGCCCC	V
G2.3	GGAGGTAGTTTGCTGATTGG	V
G2_MF	CGACGCCGTCACAAACAACC	V
G2_MF_B	CTTGGTTATGGCGCCCTCAC	V
G2_MF_C	AAGCGCCTACGCTTGACATC	V
G3.3	ATGTTGGACGAGTCGGAATC	V
G3_MF	TCGGAATCGCAGACCGATAC	V
KEL1_F2	GGCCGGGGGAATATTAGGTGTGGCCCTCTTACGAACGTTTTGGCTGGCCACATGATTACGCCAAGCTTGC	D
KEL1_NS1	CAACAGGCGAGAAGACATCTGTCAAACTGCCAGAGCCAACAAGTAGCGAGCCAGTGAATTCGAGCTCGG	D
KIN4_F2	GCCAATATGAAAACATGCTACACGATACATACTCAACTAGATAAACATGATTACGCCAAGCTTGC	D
KIN4_NS1	GCGCAAGGCCAGCGAGAGAGTGTTTACGGCGGCAGACAAGGCAGGCCAGTGAATTCGAGCTCGG	D
L2 MF	GTTCCGGCCTCTCACCTTTC	V
L2.3	TATATGCGTCAGGCGACCTC	V
L3 MF	ACCCTATCGCCACTATCTTG	V
L3.3	ACCCTATCGCCACTATCTTG	V
MOB1_N*S1	CCTAGAGCGCGGAGGTCCAGGCTATGTCATTTCTACAGAACTTGTATGGGTACCACTCTTGACGAC	D
MOB1_N*S2	TGGTTACATACCTAACGGTGTAGTGACTTCGAGCAGGAGCGTTTAGGGGCAGGGCATGCTCATGTAG	D

Primer	Sequence	Use
N2	CGGTAAGCCGTGTCGTCAAG	V
N3	TGGAGGTCACCAACGTCAAC	V
NOP1_F2	GCAGAACAGGAATGTAGCAGCAGGCTCGCCCTGCTGTGCCAACGGCGCGGCATGATTACGCCAAGCTTGC	F
NOP1_F5	ACGAAAGAGACCACTGTATCGTCATTGGCAGATACATGAGAAGCGGCTTGGGTGACGGTGCTGGTTTA	F
NOP1BamHIdown	AGGGACTCCGGGATCCAAGAAAAGGCTATTTTACAA	V
NOP1SpeIup	AGATGACTGCACTAGTCGCCACTACGCGCCAACGGT	V
PDS1_F2	TGTCGTGGCTAAATACATAACTTGTACATAGTATGCATGCGTCGTATTAGCATGATTACGCCAAGCTTGC	D
PDS1_F5	TTGCCGTTGGTGAGGGATTGGATTCTAAGGACCTACATTCTCTATTAGACGGTGACGGTGCTGGTTTA	D
SLK19_F2	GCGGTAGTCATGTGACTCAGTTATGCAATTGGGGCGACGGCCTCCGGGAGCATGATTACGCCAAGCTTGC	D
SLK19_NS1	AGCGAGTAGGGCTCTGAAGCGGTTGGTTTGGTGCGAGAGAGCGCATATAGCCAGTGAATTCGAGCTCGG	D
SPO12_F2	ATTCCAATATATGATGATCCTGTCGATAGTGTTATATAACAACCTCTTCCCATGATTACGCCAAGCTTGC	D
SPO12_NS1	ATGTGCACGCGAAGGGCGTCGGGAGCGTGCACAAGAGTCTCCACAAGGCGCCAGTGAATTCGAGCTCGG	D
V1_(CDC15)	TCCGGCTAGATGCGTGATCC	V
V1_(DBF2)	CCCTGCGTCTACATACTCTG	V
V1_(MOB1)	GCGATGGCACGTGATGAAAG	V
V1_CDC15	GGGATAGATCGCCACAGGAG	V
V1_CDC15_08	TCCTGCCACCACTGGAAGAG	V
V1_CDC5	CGGCTTATTGAGAGGTTCTG	V
V1_CDC55	AGCAGTACCGAAGACTTCAC	V
V1_CDC55	TCTCCAGCGACTTCAAGTAG	V
V1_DBF2	AGACATCCTTGCCCGGATCG	V
V1_DBF2_C	CGCAGCAAGTTCCGCCTCTC	V
V1_DBF2_E	GCCGCCGCTTCCGCGCCCAC	V
V1_ESP1_B	GGCATACAGGGTACAAAGTG	V
V1_KEL1	CTTGCTGGTGTATGCTAAGG	V
V1_KIN4	ACGAATAGATCCGCGTGTTG	V
V1_LTE1	CTGTACGAGAGCGCATGAGC	V
V1_LTE1_B	TGGGCCGAGAGTCACAAAGC	V
V1_LTE1_E	GTTACGAGCCCGCTCAGAAG	V
V1_LTE1_F	TTGCTGCTGTCTGCGGTGTG	V
V1_MOB1	GCTCGACCTCTGAGTCTGTG	V
V1_NEW_KEL1	CGCTCGCGTTATGCTCCATC	V
V1_SLK19	CTAGCTGTGGTGAACGTTTG	V
V1_SPO12	AGACAGTAGTGGAGGCTTTC	V
V1_TEM1	TGTTCCTCCGCCCATTGCTC	V
V1_TEM1_B	CATGGGTGCCGATGTATGGG	V
V1_ZDS1	TCTACCGAACCGTTCACAAG	V
V2*NAT1	GTGTCGTCAAGAGTGGTACC	V
V2_(CDC15)	TCCTTATCCGCCAGCTGTGC	V
V2_(DBF2)	AGACGGTGTCGGTGGTGAAG	V
V2_(MOB1)	GCCGTGTTCCATTTGAACCC	V
V2_CDC15	TCTGGGCAAGGTGGGTAATG	V
V2_CDC15_08	CATACGCGCCCTTGCCAATC	V
V2_CDC5	CTTCCGGTTCTGTAAGTTGC	V
V2_DBF2	CCATCTCGCCCTCAAAGCTC	V
V2_ESP1_B	CAAAGTCCGCCATCAATACG	V
V2_KEL1	ACTTGTGCGAGTTCACGTTC	V
V2_KIN4	TCGCGGTAGATCTTGATCTC	V
V2_LTE1	GCAGGAAGTCCTGCGCAAAG	V
V2_LTE1_B	ACGCCCACGTCTTCTTGAGG	V
V2_LTE1_C	ATCTCGCCCAGCGACCAATC	V
V2_LTE1_ext	CGCAACGGTGATCCGTCTAC	V
V2_MOB1	GCCGTGTTCCATTTGAACCC	V
V2_NAT1	GTGTCGTCAAGAGTGGTACC	V
V2_NEW_KEL1	TGCACCAGCTTCACCCTGTC	V
V2_SLK19	TTGAGGTCGTCCTGGATGTC	V

Primer	Sequence	Use
V2_SPO12	GAACATCGCCTTGTGGAGAC	V
V2_TEM1	CGTACCGCATGCTCGTCTTC	V
V2_ZDS1	ACTCATCCTCGCTCATTGAC	V
V3*NAT1	ACATGAGCATGCCCTGCCCC	V
V3_(CDC15)	TGCAGCTCCTCCTCATTCTC	V
V3_(DBF2)	GGCAGATATGGCCAAGTACG	V
V3_(MOB1)	TCAACCTGCAGACGGTACTC	V
V3_CDC15	CTTGTATACCACGCCATACG	V
V3_CDC15_08	TGGGCAAGGTGGGTAATGAC	V
V3_CDC5	GCCCAAAGAGTTGAACAGAC	V
V3_CDC5_V	GGTGGCGAATCACTACAGTC	V
V3_CDC55	TTGCCGCTCGTGATTACTTG	V
V3_DBF2	CCAAGTACGCCGACGTCTTC	V
V3_KEL1	CAGGACATCAGCAACCATTC	V
V3_KIN4	CAGTGGCGTTGAGTTATGTC	V
V3_LTE1	CAGCTCATGGCGCTTAATTG	V
V3_MOB1	GCCTGTTCTCCGAGGAGTTC	V
V3_NAT1	ACATGAGCATGCCCTGCCCC	V
V3_SLK19	AAGGAGGACGAGCTAAACAG	V
V3_SPO12	TTGGAGGACGTCTAGGGAAG	V
V3_TEM1	CTCACGTCAATCCGCGAATG	V
V3_ZDS1	ATCCAAAGCGGGAACTACGG	V
V4_(CDC15)	TCGCTCTTCACGGCACATTC	V
V4_(DBF2)	GTCGCAGAGCTCGAACGAAG	V
V4_(MOB1)	CGCCAGCCAAAGTCCACAAG	V
V4_CDC15	CCTGCTCCAACCCATTTATC	V
V4_CDC15_08	ATTCTCATGGCGCAACCCAG	V
V4_CDC5	TCTTCGCCGCATACAAAGTG	V
V4_CDC5_V	CCGGCTGTAACTGGTTTGAG	V
V4_CDC55	TGTCGCTGCTCTACTGTTAC	V
V4_DBF2	CAGTGCCAGACACCTCTTCC	V
V4_KEL1	ATTAGGTGTGGCCCTCTTAC	V
V4_KIN4	GTTGTCAGAGCCAAGTTCAG	V
V4_LTE1	CCGACGGTCATAGACATCAC	V
V4_LTE1_uncloned	GGACAATAGGCGTGTTAACC	V
V4_MOB1	CCTGGCCCAATAGCGTCATC	V
V4_SLK19	CGTAAATCAGCCGGTATTGC	V
V4_SPO12	AGGACTACGTCGAACTCAAG	V
V4_TEM1	CCAGTGTCCGAGCACTTTAC	V
V4_TEM1_uncloned	CCTTTATGCCCTTGTGAACC	V
V4_ZDS1	GCAGCAGCTCATCGACAAAG	V
Zds1/2_F2	TGCTGTATCATGATATGAAATGCAACCATTTCACCGAAGTACAAAAAAATCATGATTACGCCAAGCTTGC	D
Zds1/2_NS1	GGCAGGTAGAGCGGGGCCAGAGAGTGCGAGCGAGGCTGAAAAGCAGGAAACCAGTGAATTCGAGCTCGG	D

Table 4: Oligos used in this study. 5′ to 3′. V: Verification. D: Deletion casstette. F: Fusion cassette. C: Cloning of genomic locus.

Strain list

Strain	Genotype	Reference
*Ag*Nup49-GFP GFP-*Ag*Tub1	*pAgNUP49-yEGFP[AgNUP49-yEGFP-GEN3] Agade2::AgADE2-GFP-AgTUB1 Agleu2Δ Agthr4Δ*	This study
*Agcdc14*Δ GFP-*Ag*Tub1	*Agcdc14::GEN3 Agade2::AgADE2-GFP-AgTUB1 Agleu2Δ Agthr4Δ*	This study
*Agcdc15*Δ *Ag*Tub4-YFP *Ag*H4-GFP	*Agcdc15::GEN3 Agade2::AgADE2-AgHHF1-GFP AgTUB4-YFP-AgLEU2 Agleu2Δ Agthr4Δ*	This study
*Agcdc15*Δ *Ag*Pds1-Cherry *Ag*Cdc14-GFP	*Agcdc15::LEU2 AgPDS1-mCherry-NAT1 AgCDC14-yEGFP-GEN3 Agleu2Δ Agthr4Δ*	This study
*Agcdc55*Δ *Ag*Cdc14-GFP	*Agcdc55::GEN3 AgCDC14-yEGFP-NAT1 Agleu2Δ Agthr4*	This study
*Agdbf2/dbf20*Δ *Ag*Tub4-YFP *Ag*H4-GFP	*Agdbf2/dbf20::NAT1 Agade2::AgADE2-AgHHF1-GFP AgTUB4-YFP-AgLEU2 Agleu2Δ Agthr4Δ*	This study
*Agfob1*Δ *Ag*H4-GFP	*Agfob1::GEN3 Agade2::AgADE2-AgHHF1-GFP Agleu2Δ Agthr4Δ*	This study
*Agfob1*Δ *Ag*Tub4-YFP *Ag*H4-GFP	*Agfob1::GEN3 Agade2::AgADE2-AgHHF1-GFP AgTUB4-YFP-AgLEU2 Agleu2Δ Agthr4Δ*	This study
*Agkel1/kel2*Δ *Ag*H4-GFP	*Agkel1/kel2::GEN3 Agade2::AgADE2-AgHHF1-GFP Agleu2Δ Agthr4Δ*	This study
*Agkin4/frk1*Δ *Ag*H4-GFP	*Agkin4/frk1::GEN3 Agade2::AgADE2-AgHHF1-GFP Agleu2Δ Agthr4Δ*	This study
*Aglte1*Δ *Ag*H4-GFP	*Aglte1::GEN3 Agade2::AgADE2-AgHHF1-GFP Agleu2Δ Agthr4Δ*	This study
*Ag*Lte1-GFP	*AgLTE1-yEGFP-GEN3 Agleu2Δ Agthr4Δ*	This study
*Aglte1*Δ *Ag*Tub4-YFP *Ag*H4-GFP	*Aglte1::GEN3 Agade2::AgADE2-AgHHF1-GFP AgTUB4-YFP-AgLEU2 Agleu2Δ Agthr4Δ*	This study
*Agmob1*Δ *Ag*H4-GFP	*Agmob1::NAT1 Agade2::AgADE2-AgHHF1-GFP Agleu2Δ Agthr4Δ*	This study
*Ag*Nop1-Cherry *Ag*Cdc14-GFP	*AgNOP1-mCherry-NAT1 AgCDC14-yEGFP-GEN3 Agleu2Δ Agthr4Δ*	This study
*Ag*Nop1-Cherry *Ag*H4-GFP	*pMF12[AgNOP1-mCherry-NAT1] Agade2::AgADE2-AgHHF1-GFP Agleu2Δ Agthr4Δ*	This study
*Ag*Nop1-Cherry *Ag*H4-GFP *Ag*Tub4-YFP	*pMF12[AgNOP1-mCherry-NAT1] Agade2::AgADE2-AgHHF1-GFP AgTUB4-YFP-AgLEU2 Agleu2Δ Agthr4Δ*	This study
*Ag*Pds1-Cherry *Ag*Cdc14-GFP	*AgPDS1-mCherry-NAT1 AgCDC14-yEGFP-GEN3 Agleu2Δ Agthr4Δ*	This study
*Ag*Tub4-YFP *Ag*Cdc14-GFP *Ag*Nop1-Cherry	*pTUB4-YFP[TUB4-YFP LEU2] AgCDC14-yEGFP-GEN3 AgNOP1-mCherry-NAT1 Agleu2Δ Agthr4Δ*	This study
*Agslk19*Δ *Ag*H4-GFP	*Agslk19::GEN3 Agade2::AgADE2-AgHHF1-GFP Agleu2Δ Agthr4Δ*	This study
*Agslk19*Δ *Ag*Tub4-YFP *Ag*H4-GFP	*Agslk19::GEN3 Agade2::AgADE2-AgHHF1-GFP AgTUB4-YFP-AgLEU2 Agleu2Δ Agthr4Δ*	This study
*Agslk19*Δ *Ag*Cdc14-GFP	*Agslk19::GEN3 AgCDC14-yEGFP-NAT1 Agleu2Δ Agthr4Δ*	This study
*Agspo12/bns1*Δ *Ag*H4-GFP	*Agspo12/bns1::GEN3 Agade2::AgADE2-AgHHF1-GFP Agleu2Δ Agthr4Δ*	This study
*Agspo12/bns1*Δ *Ag*Cdc14-GFP	*Agspo12/bns1::GEN3 AgCDC14-yEGFP-NAT1 Agleu2Δ Agthr4Δ*	This study
*Agtem1*Δ *Ag*H4-GFP	*Agtem1::GEN3 Agade2::AgADE2-AgHHF1-GFP Agleu2Δ Agthr4Δ*	This study
*Agtem1*Δ *Ag*Tub4-YFP *Ag*H4-GFP	*Agtem1::GEN3 Agade2::AgADE2-AgHHF1-GFP AgTUB4-YFP-AgLEU2 Agleu2Δ Agthr4Δ*	This study
*Ag*Tem1-GFP	*AgTEM1-yEGFP-GEN3 Agleu2Δ Agthr4Δ*	This study
*Ag*Tub4-YFP *Ag*H4-GFP	*Agade2::AgADE2-AgHHF1-GFP AgTUB4-YFP-AgLEU2 Agleu2Δ Agthr4Δ*	This study
*Agzds1/zds2*Δ *Ag*Tub4-YFP *Ag*H4-GFP	*Agzds1/zds2::GEN3 Agade2::AgADE2-AgHHF1-GFP AgTUB4-YFP-AgLEU2 Agleu2Δ Agthr4Δ*	This study
*Ag*Cdc14-Cherry *Ag*Tub4-YFP	*AgCDC14-mCherry-NAT1 AgTUB4-YFP-AgLEU2 Agleu2Δ Agthr4Δ*	K. Hungerbühler
*Agcdc55*Δ *Ag*H4-GFP	*Agcdc55::GEN3 Agade2::AgADE2-AgHHF1-GFP Agleu2Δ Agthr4Δ*	V. Tilloy
Δ*l*Δ*t*	*Agleu2Δ Agthr4Δ*	C. Altmann-Jöhl
GFP-*Ag*Tub1	*Agade2::AgADE2-GFP-AgTUB1 Agleu2Δ Agthr4Δ*	C. Birrer
*Ag*H4-GFP	*Agade2::AgADE2-AgHHF1-GFP Agleu2Δ Agthr4Δ*	H. Helfer
*Agnet1/tof2*Δ *Ag*Cdc14-GFP	*Agnet1/tof2::GEN3 AgCDC14-yEGFP-NAT1 Agleu2Δ Agthr4Δ*	C. Correia
*Agcdc14*Δ *Ag*Hof1-GFP	*Agcdc14::GEN3 AgHOF1-yEGFP-NAT1 Agleu2Δ Agthr4Δ*	A. Sengler

Table 5: Strains used in this study. Listed alphabetically, except for foreign strains, which are listed last.

Plasmid list

Plasmid	Description	Derived from	Reference
pMF1	*AgTEM1* clone	pRS416	This study
pMF2	*AgTEM1-yEGFP-GEN3*	pMF1	This study
pMF3	(C-ter) *AgLTE1-yEGFP-GEN3*	pAG7638	This study
pMF8	*AgNOP1* clone	pRS416	This study
pMF10	*AgPDS1-mCherry-NAT1*	pAG11556	This study
pMF12	*AgNOP1-mCherry-NAT1*	pMF8	This study
pAG7638	*AgLTE1* C-terminus clone	-	Christine Mohr, doctoral thesis
pAG11556	*AgPDS1* clone	-	Christine Mohr, doctoral thesis
pAGT100	*NAT1* cassette	-	Kaufmann, 2009
pAGT120	*LEU2* cassette	-	Kaufmann, 2009
pAGT140	*GEN3* cassette	-	Kaufmann, 2009
pAGT211	linker-*mCherry-NAT1*	-	Kaufmann, 2009
pAGT241	linker-*yEGFP-GEN3*	-	Kaufmann, 2009
pRS416	*MCS* in *lacZ*	-	Sikorski and Hieter, 1989
pNUP49-yEGFP	*NUP49-yEGFP-GEN3*	-	Sandrine Grava, unpublished
pCB50	*AgTub4-YFP-AgLEU2*	-	Claudia Lang, doctoral thesis
pTUB4-YFP	*AgTub4-YFP-AgLEU2 ARS*	-	Claudia Lang, doctoral thesis

Table 6: Plasmids used in this study. Construction of plasmids descibed in materials and methods section.

References

Alberti-Segui, C., Dietrich, F., Altmann-Johl, R., Hoepfner, D., and Philippsen, P. (2001). Cytoplasmic dynein is required to oppose the force that moves nuclei towards the hyphal tip in the filamentous ascomycete Ashbya gossypii. J Cell Sci *114*, 975-986.

Altmann-Johl, R., and Philippsen, P. (1996). AgTHR4, a new selection marker for transformation of the filamentous fungus Ashbya gossypii, maps in a four-gene cluster that is conserved between A. gossypii and Saccharomyces cerevisiae. Mol Gen Genet *250*, 69-80.

Altschul, S. F., Madden, T. L., Schaffer, A. A., Zhang, J., Zhang, Z., Miller, W., and Lipman, D. J. (1997). Gapped BLAST and PSI-BLAST: a new generation of protein database search programs. Nucleic Acids Res *25*, 3389-3402.

Asakawa, K., Yoshida, S., Otake, F., and Toh-e, A. (2001). A novel functional domain of Cdc15 kinase is required for its interaction with Tem1 GTPase in Saccharomyces cerevisiae. Genetics *157*, 1437-1450.

Ayad-Durieux, Y., Knechtle, P., Goff, S., Dietrich, F., and Philippsen, P. (2000). A PAK-like protein kinase is required for maturation of young hyphae and septation in the filamentous ascomycete Ashbya gossypii. J Cell Sci *113 Pt 24*, 4563-4575.

Azzam, R., Chen, S. L., Shou, W., Mah, A. S., Alexandru, G., Nasmyth, K., Annan, R. S., Carr, S. A., and Deshaies, R. J. (2004). Phosphorylation by cyclin B-Cdk underlies release of mitotic exit activator Cdc14 from the nucleolus. Science *305*, 516-519.

Bardin, A. J., and Amon, A. (2001). Men and sin: what's the difference? Nat Rev Mol Cell Biol *2*, 815-826.

Bardin, A. J., Visintin, R., and Amon, A. (2000). A mechanism for coupling exit from mitosis to partitioning of the nucleus. Cell *102*, 21-31.

Becskei, A., and Serrano, L. (2000). Engineering stability in gene networks by autoregulation. Nature *405*, 590-593.

Bembenek, J., Kang, J., Kurischko, C., Li, B., Raab, J. R., Belanger, K. D., Luca, F. C., and Yu, H. (2005). Crm1-mediated nuclear export of Cdc14 is required for the completion of cytokinesis in budding yeast. Cell Cycle *4*, 961-971.

Berdougo, E., Nachury, M. V., Jackson, P. K., and Jallepalli, P. V. (2008). The nucleolar phosphatase Cdc14B is dispensable for chromosome segregation and mitotic exit in human cells. Cell Cycle *7*, 1184-1190.

Bosl, W. J., and Li, R. (2005). Mitotic-exit control as an evolved complex system. Cell *121*, 325-333.

Cohen-Fix, O., and Koshland, D. (1999). Pds1p of budding yeast has dual roles: inhibition of anaphase initiation and regulation of mitotic exit. Genes Dev *13*, 1950-1959.

Cohen-Fix, O., Peters, J. M., Kirschner, M. W., and Koshland, D. (1996). Anaphase initiation in Saccharomyces cerevisiae is controlled by the APC-dependent degradation of the anaphase inhibitor Pds1p. Genes Dev *10*, 3081-3093.

Corbett, M., Xiong, Y., Boyne, J. R., Wright, D. J., Munro, E., and Price, C. (2006). IQGAP and mitotic exit network (MEN) proteins are required for cytokinesis and re-polarization of the actin cytoskeleton in the budding yeast, Saccharomyces cerevisiae. Eur J Cell Biol *85*, 1201-1215.

D'Aquino, K. E., Monje-Casas, F., Paulson, J., Reiser, V., Charles, G. M., Lai, L., Shokat, K. M., and Amon, A. (2005). The protein kinase Kin4 inhibits exit from mitosis in response to spindle position defects. Mol Cell *19*, 223-234.

De Wulf, P., Montani, F., and Visintin, R. (2009). Protein phosphatases take the mitotic stage. Curr Opin Cell Biol *21*, 806-815.

Dietrich, F. S., Voegeli, S., Brachat, S., Lerch, A., Gates, K., Steiner, S., Mohr, C., Pohlmann, R., Luedi, P., Choi, S*., et al.* (2004). The Ashbya gossypii genome as a tool for mapping the ancient Saccharomyces cerevisiae genome. Science *304*, 304-307.

Dunkler, A., and Wendland, J. (2007). Use of MET3 promoters for regulated gene expression in Ashbya gossypii. Curr Genet *52*, 1-10.

Fraschini, R., D'Ambrosio, C., Venturetti, M., Lucchini, G., and Piatti, S. (2006). Disappearance of the budding yeast Bub2-Bfa1 complex from the mother-bound spindle pole contributes to mitotic exit. J Cell Biol *172*, 335-346.

Fraschini, R., Venturetti, M., Chiroli, E., and Piatti, S. (2008). The spindle position checkpoint: how to deal with spindle misalignment during asymmetric cell division in budding yeast. Biochem Soc Trans *36*, 416-420.

Gattiker, A., Rischatsch, R., Demougin, P., Voegeli, S., Dietrich, F. S., Philippsen, P., and Primig, M. (2007). Ashbya Genome Database 3.0: a cross-species genome and transcriptome browser for yeast biologists. BMC Genomics *8*, 9.

Geymonat, M., Spanos, A., de Bettignies, G., and Sedgwick, S. G. (2009). Lte1 contributes to Bfa1 localization rather than stimulating nucleotide exchange by Tem1. J Cell Biol *187*, 497-511.

Geymonat, M., Spanos, A., Smith, S. J., Wheatley, E., Rittinger, K., Johnston, L. H., and Sedgwick, S. G. (2002). Control of mitotic exit in budding yeast. In vitro regulation of Tem1 GTPase by Bub2 and Bfa1. J Biol Chem *277*, 28439-28445.

Gietz, R. D., Schiestl, R. H., Willems, A. R., and Woods, R. A. (1995). Studies on the transformation of intact yeast cells by the LiAc/SS-DNA/PEG procedure. Yeast *11*, 355-360.

Gladfelter, A. S. (2006). Nuclear anarchy: asynchronous mitosis in multinucleated fungal hyphae. Curr Opin Microbiol *9*, 547-552.

Gladfelter, A. S., Hungerbuehler, A. K., and Philippsen, P. (2006). Asynchronous nuclear division cycles in multinucleated cells. J Cell Biol *172*, 347-362.

Gladfelter, A. S., Sustreanu, N., Hungerbuehler, A. K., Voegeli, S., Galati, V., and Philippsen, P. (2007). The anaphase-promoting complex/cyclosome is required for anaphase progression in multinucleated Ashbya gossypii cells. Eukaryot Cell *6*, 182-197.

Grandi, P., Schlaich, N., Tekotte, H., and Hurt, E. C. (1995). Functional interaction of Nic96p with a core nucleoporin complex consisting of Nsp1p, Nup49p and a novel protein Nup57p. Embo J *14*, 76-87.

Granot, D., and Snyder, M. (1991). Segregation of the nucleolus during mitosis in budding and fission yeast. Cell Motil Cytoskeleton *20*, 47-54.

Griffioen, G., Swinnen, S., and Thevelein, J. M. (2003). Feedback inhibition on cell wall integrity signaling by Zds1 involves Gsk3 phosphorylation of a cAMP-dependent protein kinase regulatory subunit. J Biol Chem *278*, 23460-23471.

Gruneberg, U., Campbell, K., Simpson, C., Grindlay, J., and Schiebel, E. (2000). Nud1p links astral microtubule organization and the control of exit from mitosis. Embo J *19*, 6475-6488.

Hanahan, D. (1983). Studies on transformation of Escherichia coli with plasmids. J Mol Biol *166*, 557-580.

Helfer, H., and Gladfelter, A. S. (2006). AgSwe1p regulates mitosis in response to morphogenesis and nutrients in multinucleated Ashbya gossypii cells. Mol Biol Cell *17*, 4494-4512.

Heo, S. J., Tatebayashi, K., and Ikeda, H. (1999). The budding yeast cohesin gene SCC1/MCD1/RHC21 genetically interacts with PKA, CDK and APC. Curr Genet *36*, 329-338.

Higuchi, T., and Uhlmann, F. (2005). Stabilization of microtubule dynamics at anaphase onset promotes chromosome segregation. Nature *433*, 171-176.

Hofken, T., and Schiebel, E. (2002). A role for cell polarity proteins in mitotic exit. Embo J *21*, 4851-4862.

Holt, L. J., Krutchinsky, A. N., and Morgan, D. O. (2008). Positive feedback sharpens the anaphase switch. Nature *454*, 353-357.

Hu, F., Wang, Y., Liu, D., Li, Y., Qin, J., and Elledge, S. J. (2001). Regulation of the Bub2/Bfa1 GAP complex by Cdc5 and cell cycle checkpoints. Cell *107*, 655-665.

Huang, J., and Moazed, D. (2003). Association of the RENT complex with nontranscribed and coding regions of rDNA and a regional requirement for the replication fork block protein Fob1 in rDNA silencing. Genes Dev *17*, 2162-2176.

Hungerbuehler, A. K., Philippsen, P., and Gladfelter, A. S. (2007). Limited functional redundancy and oscillation of cyclins in multinucleated Ashbya gossypii fungal cells. Eukaryot Cell *6*, 473-486.

Hunter, S., Apweiler, R., Attwood, T. K., Bairoch, A., Bateman, A., Binns, D., Bork, P., Das, U., Daugherty, L., Duquenne, L.*, et al.* (2009). InterPro: the integrative protein signature database. Nucleic Acids Res *37*, D211-215.

Hwang, W. W., and Madhani, H. D. (2009). Nonredundant requirement for multiple histone modifications for the early anaphase release of the mitotic exit regulator Cdc14 from nucleolar chromatin. PLoS Genet *5*, e1000588.

James, T. Y., Kauff, F., Schoch, C. L., Matheny, P. B., Hofstetter, V., Cox, C. J., Celio, G., Gueidan, C., Fraker, E., Miadlikowska, J.*, et al.* (2006). Reconstructing the early evolution of Fungi using a six-gene phylogeny. Nature *443*, 818-822.

Jaspersen, S. L., Charles, J. F., Tinker-Kulberg, R. L., and Morgan, D. O. (1998). A late mitotic regulatory network controlling cyclin destruction in Saccharomyces cerevisiae. Mol Biol Cell *9*, 2803-2817.

Jaspersen, S. L., and Morgan, D. O. (2000). Cdc14 activates cdc15 to promote mitotic exit in budding yeast. Curr Biol *10*, 615-618.

Kahana, J. A., Schnapp, B. J., and Silver, P. A. (1995). Kinetics of spindle pole body separation in budding yeast. Proc Natl Acad Sci U S A *92*, 9707-9711.

Kaiser, B. K., Zimmerman, Z. A., Charbonneau, H., and Jackson, P. K. (2002). Disruption of centrosome structure, chromosome segregation, and cytokinesis by misexpression of human Cdc14A phosphatase. Mol Biol Cell *13*, 2289-2300.

Kaizu, K., Moriya, H., and Kitano, H. (2010). Fragilities caused by dosage imbalance in regulation of the budding yeast cell cycle. PLoS Genet *6*, e1000919.

Kamieniecki, R. J., Liu, L., and Dawson, D. S. (2005). FEAR but not MEN genes are required for exit from meiosis I. Cell Cycle *4*, 1093-1098.

Kaufmann, A. (2007). Polarized growth and septation in the filamentous ascomycete Ashbya gossypii, analyzed by live cell imaging, PhD thesis, University of Basel.

Kaufmann, A. (2009). A plasmid collection for PCR-based gene targeting in the filamentous ascomycete Ashbya gossypii. Fungal Genet Biol *46*, 595-603.

Kaufmann, A., and Philippsen, P. (2009). Of bars and rings: Hof1-dependent cytokinesis in multiseptated hyphae of Ashbya gossypii. Mol Cell Biol *29*, 771-783.

Knechtle, P., Dietrich, F., and Philippsen, P. (2003). Maximal polar growth potential depends on the polarisome component AgSpa2 in the filamentous fungus Ashbya gossypii. Mol Biol Cell *14*, 4140-4154.

Köhli, M. (2007). From polarity establishment to fast hyphal growth in the filamentous fungus Ashbya gossypii, PhD thesis, University of Basel.

Kohli, M., Galati, V., Boudier, K., Roberson, R. W., and Philippsen, P. (2008). Growth-speed-correlated localization of exocyst and polarisome components in growth zones of Ashbya gossypii hyphal tips. J Cell Sci *121*, 3878-3889.

Konig, C., Maekawa, H., and Schiebel, E. (2010). Mutual regulation of cyclin-dependent kinase and the mitotic exit network. J Cell Biol *188*, 351-368.

Lang, C. (2009). The organization of the microtubule cytoskeleton and its role on nuclear dynamics in the multinucleate hyphae of Ashbya gossypii revealed by live cell imaging and electron microscopy, PhD thesis University of Basel.

Lang, C., Grava, S., Finlayson, M., Trimble, R., Philippsen, P., and Jaspersen, S. L. (2010). Structural mutants of the spindle pole body cause distinct alteration of cytoplasmic microtubules and nuclear dynamics in multinucleated hyphae. Mol Biol Cell *21*, 753-766.

Lang, C., Grava, S., van den Hoorn, T., Trimble, R., Philippsen, P., and Jaspersen, S. L. (2010). Mobility, microtubule nucleation and structure of microtubule-organizing centers in multinucleated hyphae of Ashbya gossypii. Mol Biol Cell *21*, 18-28.

Lew, D. J., and Burke, D. J. (2003). The spindle assembly and spindle position checkpoints. Annu Rev Genet *37*, 251-282.

Lopez-Aviles, S., Kapuy, O., Novak, B., and Uhlmann, F. (2009). Irreversibility of mitotic exit is the consequence of systems-level feedback. Nature *459*, 592-595.

Lu, Y., and Cross, F. R. (2010). Periodic cyclin-Cdk activity entrains an autonomous Cdc14 release oscillator. Cell *141*, 268-279.

Maekawa, H., Priest, C., Lechner, J., Pereira, G., and Schiebel, E. (2007). The yeast centrosome translates the positional information of the anaphase spindle into a cell cycle signal. J Cell Biol *179*, 423-436.

Mah, A. S., Elia, A. E., Devgan, G., Ptacek, J., Schutkowski, M., Snyder, M., Yaffe, M. B., and Deshaies, R. J. (2005). Substrate specificity analysis of protein kinase complex Dbf2-Mob1 by peptide library and proteome array screening. BMC Biochem *6*, 22.

McGrew, J. T., Goetsch, L., Byers, B., and Baum, P. (1992). Requirement for ESP1 in the nuclear division of Saccharomyces cerevisiae. Mol Biol Cell *3*, 1443-1454.

Mohl, D. A., Huddleston, M. J., Collingwood, T. S., Annan, R. S., and Deshaies, R. J. (2009). Dbf2-Mob1 drives relocalization of protein phosphatase Cdc14 to the cytoplasm during exit from mitosis. J Cell Biol *184*, 527-539.

Monje-Casas, F., and Amon, A. (2009). Cell polarity determinants establish asymmetry in MEN signaling. Dev Cell *16*, 132-145.

Movshovich, N., Fridman, V., Gerson-Gurwitz, A., Shumacher, I., Gertsberg, I., Fich, A., Hoyt, M. A., Katz, B., and Gheber, L. (2008). Slk19-dependent mid-anaphase pause in kinesin-5-mutated cells. J Cell Sci *121*, 2529-2539.

Nash, R., Weng, S., Hitz, B., Balakrishnan, R., Christie, K. R., Costanzo, M. C., Dwight, S. S., Engel, S. R., Fisk, D. G., Hirschman, J. E., *et al.* (2007). Expanded protein information at SGD: new pages and proteome browser. Nucleic Acids Res *35*, D468-471.

Neiman, A. M. (2005). Ascospore formation in the yeast Saccharomyces cerevisiae. Microbiol Mol Biol Rev *69*, 565-584.

Nickas, M. E., Schwartz, C., and Neiman, A. M. (2003). Ady4p and Spo74p are components of the meiotic spindle pole body that promote growth of the prospore membrane in Saccharomyces cerevisiae. Eukaryot Cell *2*, 431-445.

Pablo-Hernando, M. E., Arnaiz-Pita, Y., Nakanishi, H., Dawson, D., del Rey, F., Neiman, A. M., and Vazquez de Aldana, C. R. (2007). Cdc15 is required for spore morphogenesis independently of Cdc14 in Saccharomyces cerevisiae. Genetics *177*, 281-293.

Pereira, G., Hofken, T., Grindlay, J., Manson, C., and Schiebel, E. (2000). The Bub2p spindle checkpoint links nuclear migration with mitotic exit. Mol Cell *6*, 1-10.

Pereira, G., and Schiebel, E. (2003). Separase regulates INCENP-Aurora B anaphase spindle function through Cdc14. Science *302*, 2120-2124.

Philips, J., and Herskowitz, I. (1998). Identification of Kel1p, a kelch domain-containing protein involved in cell fusion and morphology in Saccharomyces cerevisiae. J Cell Biol *143*, 375-389.

Prillinger, H., Schweigkofler, W., Breitenbach, M., Briza, P., Staudacher, E., Lopandic, K., Molnar, O., Weigang, F., Ibl, M., and Ellinger, A. (1997). Phytopathogenic filamentous (Ashbya, Eremothecium) and dimorphic fungi (Holleya, Nematospora) with needle-shaped ascospores as new members within the Saccharomycetaceae. Yeast *13*, 945-960.

Pringle, J. R., and Hartwell, L. H. (1981). The Saccharomyces cerevisiae cell cycle. In The Molecular Biology of the Yeast Saccharomyces: Life Cycle and Inheritance, Volume 1, pp. 97-142.

Queralt, E., Lehane, C., Novak, B., and Uhlmann, F. (2006). Downregulation of PP2A(Cdc55) phosphatase by separase initiates mitotic exit in budding yeast. Cell *125*, 719-732.

Queralt, E., and Uhlmann, F. (2008). Cdk-counteracting phosphatases unlock mitotic exit. Curr Opin Cell Biol *20*, 661-668.

Queralt, E., and Uhlmann, F. (2008). Separase cooperates with Zds1 and Zds2 to activate Cdc14 phosphatase in early anaphase. J Cell Biol *182*, 873-883.

Rice, P., Longden, I., and Bleasby, A. (2000). EMBOSS: the European Molecular Biology Open Software Suite. Trends Genet *16*, 276-277.

Rock, J. M., and Amon, A. (2009). The FEAR network. Curr Biol *19*, R1063-1068.

Roy, N., and Runge, K. W. (2000). Two paralogs involved in transcriptional silencing that antagonistically control yeast life span. Curr Biol *10*, 111-114.

Sambrook (2001). Molecular Cloning, a Laboratory Manual: Cold Spring Harbour Press).

Schindler, K., and Schultz, R. M. (2009). The CDC14A phosphatase regulates oocyte maturation in mouse. Cell Cycle *8*, 1090-1098.

Schmitz, H. P., Kaufmann, A., Kohli, M., Laissue, P. P., and Philippsen, P. (2006). From function to shape: a novel role of a formin in morphogenesis of the fungus Ashbya gossypii. Mol Biol Cell *17*, 130-145.

Schrader, N., Stelter, P., Flemming, D., Kunze, R., Hurt, E., and Vetter, I. R. (2008). Structural basis of the nic96 subcomplex organization in the nuclear pore channel. Mol Cell *29*, 46-55.

Seshan, A., Bardin, A. J., and Amon, A. (2002). Control of Lte1 localization by cell polarity determinants and Cdc14. Curr Biol *12*, 2098-2110.

Shirayama, M., Matsui, Y., Tanaka, K., and Toh-e, A. (1994). Isolation of a CDC25 family gene, MSI2/LTE1, as a multicopy suppressor of ira1. Yeast *10*, 451-461.

Shirayama, M., Matsui, Y., and Toh, E. A. (1994). The yeast TEM1 gene, which encodes a GTP-binding protein, is involved in termination of M phase. Mol Cell Biol *14*, 7476-7482.

Shou, W., Seol, J. H., Shevchenko, A., Baskerville, C., Moazed, D., Chen, Z. W., Jang, J., Shevchenko, A., Charbonneau, H., and Deshaies, R. J. (1999). Exit from mitosis is triggered by Tem1-dependent release of the protein phosphatase Cdc14 from nucleolar RENT complex. Cell *97*, 233-244.

Sikorski, R. S., and Hieter, P. (1989). A system of shuttle vectors and yeast host strains designed for efficient manipulation of DNA in Saccharomyces cerevisiae. Genetics *122*, 19-27.

Son, S., and Osmani, S. A. (2009). Analysis of all protein phosphatase genes in Aspergillus nidulans identifies a new mitotic regulator, fcp1. Eukaryot Cell *8*, 573-585.

Stahmann, K. P., Arst, H. N., Jr., Althofer, H., Revuelta, J. L., Monschau, N., Schlupen, C., Gatgens, C., Wiesenburg, A., and Schlosser, T. (2001). Riboflavin, overproduced during sporulation of Ashbya gossypii, protects its hyaline spores against ultraviolet light. Environ Microbiol *3*, 545-550.

Stahmann, K. P., Revuelta, J. L., and Seulberger, H. (2000). Three biotechnical processes using Ashbya gossypii, Candida famata, or Bacillus subtilis compete with chemical riboflavin production. Appl Microbiol Biotechnol *53*, 509-516.

Stark, M. J. (1996). Yeast protein serine/threonine phosphatases: multiple roles and diverse regulation. Yeast *12*, 1647-1675.

Stegmeier, F., Huang, J., Rahal, R., Zmolik, J., Moazed, D., and Amon, A. (2004). The replication fork block protein Fob1 functions as a negative regulator of the FEAR network. Curr Biol *14*, 467-480.

Stegmeier, F., Visintin, R., and Amon, A. (2002). Separase, polo kinase, the kinetochore protein Slk19, and Spo12 function in a network that controls Cdc14 localization during early anaphase. Cell *108*, 207-220.

Steiner, S., Wendland, J., Wright, M. C., and Philippsen, P. (1995). Homologous recombination as the main mechanism for DNA integration and cause of rearrangements in the filamentous ascomycete Ashbya gossypii. Genetics *140*, 973-987.

Stoepel, J., Ottey, M. A., Kurischko, C., Hieter, P., and Luca, F. C. (2005). The mitotic exit network Mob1p-Dbf2p kinase complex localizes to the nucleus and regulates passenger protein localization. Mol Biol Cell *16*, 5465-5479.

Straight, A. F., Marshall, W. F., Sedat, J. W., and Murray, A. W. (1997). Mitosis in living budding yeast: anaphase A but no metaphase plate. Science *277*, 574-578.

Straight, A. F., Shou, W., Dowd, G. J., Turck, C. W., Deshaies, R. J., Johnson, A. D., and Moazed, D. (1999). Net1, a Sir2-associated nucleolar protein required for rDNA silencing and nucleolar integrity. Cell *97*, 245-256.

Sullivan, M., Higuchi, T., Katis, V. L., and Uhlmann, F. (2004). Cdc14 phosphatase induces rDNA condensation and resolves cohesin-independent cohesion during budding yeast anaphase. Cell *117*, 471-482.

Sullivan, M., Lehane, C., and Uhlmann, F. (2001). Orchestrating anaphase and mitotic exit: separase cleavage and localization of Slk19. Nat Cell Biol *3*, 771-777.

Sullivan, M., and Uhlmann, F. (2003). A non-proteolytic function of separase links the onset of anaphase to mitotic exit. Nat Cell Biol *5*, 249-254.

Tollervey, D., Lehtonen, H., Carmo-Fonseca, M., and Hurt, E. C. (1991). The small nucleolar RNP protein NOP1 (fibrillarin) is required for pre-rRNA processing in yeast. Embo J *10*, 573-583.

Tomson, B. N., Rahal, R., Reiser, V., Monje-Casas, F., Mekhail, K., Moazed, D., and Amon, A. (2009). Regulation of Spo12 phosphorylation and its essential role in the FEAR network. Curr Biol *19*, 449-460.

Trautmann, S., and McCollum, D. (2002). Cell cycle: new functions for Cdc14 family phosphatases. Curr Biol *12*, R733-735.

Trautmann, S., Rajagopalan, S., and McCollum, D. (2004). The S. pombe Cdc14-like phosphatase Clp1p regulates chromosome biorientation and interacts with Aurora kinase. Dev Cell *7*, 755-762.

Trautmann, S., Wolfe, B. A., Jorgensen, P., Tyers, M., Gould, K. L., and McCollum, D. (2001). Fission yeast Clp1p phosphatase regulates G2/M transition and coordination of cytokinesis with cell cycle progression. Curr Biol *11*, 931-940.

Traverso, E. E., Baskerville, C., Liu, Y., Shou, W., James, P., Deshaies, R. J., and Charbonneau, H. (2001). Characterization of the Net1 cell cycle-dependent regulator of the Cdc14 phosphatase from budding yeast. J Biol Chem *276*, 21924-21931.

Visintin, C., Tomson, B. N., Rahal, R., Paulson, J., Cohen, M., Taunton, J., Amon, A., and Visintin, R. (2008). APC/C-Cdh1-mediated degradation of the Polo kinase Cdc5 promotes the return of Cdc14 into the nucleolus. Genes Dev *22*, 79-90.

Visintin, R., Craig, K., Hwang, E. S., Prinz, S., Tyers, M., and Amon, A. (1998). The phosphatase Cdc14 triggers mitotic exit by reversal of Cdk-dependent phosphorylation. Mol Cell *2*, 709-718.

Visintin, R., Hwang, E. S., and Amon, A. (1999). Cfi1 prevents premature exit from mitosis by anchoring Cdc14 phosphatase in the nucleolus. Nature *398*, 818-823.

Visintin, R., Stegmeier, F., and Amon, A. (2003). The role of the polo kinase Cdc5 in controlling Cdc14 localization. Mol Biol Cell *14*, 4486-4498.

Wendland, J., Ayad-Durieux, Y., Knechtle, P., Rebischung, C., and Philippsen, P. (2000). PCR-based gene targeting in the filamentous fungus Ashbya gossypii. Gene *242*, 381-391.

Wendland, J., and Philippsen, P. (2000). Determination of cell polarity in germinated spores and hyphal tips of the filamentous ascomycete Ashbya gossypii requires a rhoGAP homolog. J Cell Sci *113 (Pt 9)*, 1611-1621.

Wendland, J., and Walther, A. (2005). Ashbya gossypii: a model for fungal developmental biology. Nat Rev Microbiol *3*, 421-429.

Wright, M. C., and Philippsen, P. (1991). Replicative transformation of the filamentous fungus Ashbya gossypii with plasmids containing Saccharomyces cerevisiae ARS elements. Gene *109*, 99-105.

Yanisch-Perron, C., Vieira, J., and Messing, J. (1985). Improved M13 phage cloning vectors and host strains: nucleotide sequences of the M13mp18 and pUC19 vectors. Gene *33*, 103-119.

Yeh, E., Skibbens, R. V., Cheng, J. W., Salmon, E. D., and Bloom, K. (1995). Spindle dynamics and cell cycle regulation of dynein in the budding yeast, Saccharomyces cerevisiae. J Cell Biol *130*, 687-700.

Yoshida, S., Asakawa, K., and Toh-e, A. (2002). Mitotic exit network controls the localization of Cdc14 to the spindle pole body in Saccharomyces cerevisiae. Curr Biol *12*, 944-950.

Yoshida, S., Ichihashi, R., and Toh-e, A. (2003). Ras recruits mitotic exit regulator Lte1 to the bud cortex in budding yeast. J Cell Biol *161*, 889-897.

Yoshida, S., and Toh-e, A. (2001). Regulation of the localization of Dbf2 and mob1 during cell division of saccharomyces cerevisiae. Genes Genet Syst *76*, 141-147.

Zanelli, C. F., and Valentini, S. R. (2005). Pkc1 acts through Zds1 and Gic1 to suppress growth and cell polarity defects of a yeast eIF5A mutant. Genetics *171*, 1571-1581.

Zhong, Y., Wang, X., and Wang, T. (2008). [Recent advances in the production of heterologous proteins in filamentous fungi]. Sheng Wu Gong Cheng Xue Bao *24*, 531-540.

Zimniak, T., Stengl, K., Mechtler, K., and Westermann, S. (2009). Phosphoregulation of the budding yeast EB1 homologue Bim1p by Aurora/Ipl1p. J Cell Biol *186*, 379-391.

Abbreviations and glossary

aa: amino acids
Ag: *Ashbya gossypii*
AFM: *A. gossypii* full medium
AGD: *A. gossypii* genome database
ALF: *A. gossypii* low fluorescence medium
APC: anaphase-promoting complex, also known as "cyclosome"
ARS: autonomously replicating sequence
ASC: *A. gossypii* synthetic complete medium (Michael Köhli, doctoral thesis)
ascomycete: sac fungus
BASF: Badische Anilin- und Soda-Fabrik
bp: base pairs
Cdc: cell division cycle
Cdk: cyclin dependent kinase
cMT: cytoplasmic microtubules
D-Box / destruction box: amino acid motif required for APC dependent degradation
DNA: deoxyribonucleic acid
dSPB: daughter SPB
GAP: GTPase-activating protein
GEF: guanine nucleotide exchange factor
GFP: green fluorescent protein
G protein: guanine nucleotide-binding protein
EM: electron microscopy
EMBOSS: european molecular biology open software suite
FEAR: cdc fourteen early anaphase release
hypha: filamentous fungal cell
ID: identity (of amino acid sequence)
IF: immunofluorescence
kb: kilo-base pair
mCherry: monomeric Cherry
MCS: multiple cloning site
MEN: mitotic exit network
mSPB: mother SPB
MTOC: microtubule organizing center
MT: microtubules
mycelium: network of branching hyphae
N: sample size
N/A: not available
NES: nuclear export signal
NLS: nuclear localization signal
nucleolus: substructure of nucleus and site of rRNA transcription
ohnolog: homolog separated by a whole genome duplicaton event
o/n: over night
ORF: open reading frame
ortholog: homolog separated by a speciation event
paralog: homolog separated by a gene duplication event
PCR: polymerase chain reaction
PERL: practical extraction and report language
RENT: regulator of nucleolar silencing and telophase exit
RNA: ribonucleic acid
rRNA: ribosomal RNA
RT: room temperature
SAC: spindle assembly checkpoint
Sc: *Saccharomyces cerevisiae*
SD: standard deviation
SGD: *Saccharomyces cerevisiae* genome datbase
SIN: septation initiation network
Sp: *Schizosaccharomyces pombe*
SPB: spindle pole body
SPOC: spindle positioning checkpoint
synteny: conserved gene order and orientation
TL: time-lapse
ts: temperature sensitive
wt: wild-type
yEGFP: yeast-enhanced GFP
YFP: yellow fluorescent protein
YNB: yeast nitrogen base

ACKNOWLEDGEMENTS

Acknowledgements

I would like to thank Peter Philippsen for all his efforts during my PhD years. His constant support, positive attitude, generosity, interest and scientific input have made the time I have spent in his lab very enjoyable and fruitful.

Special thanks to the members of my thesis committee, Anne Spang and Frank Uhlmann for their thoughts, opinions and contributions to this work.

Thanks to Sandrine and Peter for proof-reading.

Thanks to all present and former members of the Philippsen group for providing such a nice working environment and helping out with everything, from fetching happy-meals to donating AFM plates, giving advice or just joking around.

Thanks also to fellow PhD students from other labs, such as Tommy for being such a chilled-out flat-mate, or Andy and Reto, for granting me admission to their exclusive coffee breaks.

Thanks to Leo, Kühni, Gio and Dominique for generating significant distraction outside of Basel.

Thanks to my whole family for their support over the years and for all the relaxing weekends.

Special thanks to Nathalie Fabienne Manac'h for the many years of adventures (and many more to come). Thanks also for all the support, not to mention the exquisite dining during the final weeks of writing.

CURRICULUM VITAE

Curriculum vitae

Mark Robert Finlayson

Born on February 11, 1981
in Wanganui, New Zealand

Education:

2001	Matura type C (Mathematics), Kantonsschule, Solothurn
2005	B.Sc. (in Biology) Major in Molecular Biology University of Basel
2006	M.Sc. (in Molecular Biology) Major in Cell Biology University of Basel
2007-2010	PhD project "Investigation of FEAR and MEN pathway homologs in multinucleate cells" University of Basel Supervision: Peter Philippsen Thesis committee: Prof. Anne Spang Prof. Frank Uhlmann

Contact:

Muespacherstrasse 37
4055 Basel
Switzerland
Mark.Finlayson@gmail.com

Activities:

Conference: Computational Cell Biology, 2008, Hinxton, UK, poster: "Exit from mitosis in multinucleate cells".

Meeting: European Meeting on Yeast and Filamentous Fungi, 2008, Université Louis Pasteur, Strasbourg, France, poster: "Exit from mitosis in multinucleate cells".

Meeting: Systems Biology of a Filamentous Yeast, 2008, Biozentrum, University of Basel, Switzerland, talk: "Exit from mitosis in multinucleate cells"

Meeting: Yeast Genetics and Molecular Biology, 2008, Toronto, ON, Canada, poster: "Evolution of cellular networks: Exit form mitosis in multinucleate hyphae".

Conference: Cell Growth & Proliferation, 2009, Colby College, Waterville, ME, USA, Poster: "Driven by FEAR. Exit from mitosis in multinucleate hyphae".

Publication: Lang, C., Grava, S., Finlayson, M., Trimble, R., Philippsen, P., and Jaspersen, S. L. (2010). Structural mutants of the spindle pole body cause distinct alteration of cytoplasmic microtubules and nuclear dynamics in multinucleated hyphae. Mol Biol Cell 21, 753-766.

Publication: Finlayson, M. R., Helfer-Hungerbühler, A.K., Philippsen, P. (2011) Regulation of exit from mitosis in multinucleate *A. gossypii* cells relies on a minimal network of genes. Accepted for publication in Mol Biol Cell.